United States Naval Postgraduate School

THESIS

SOME CHARACTERISTICS OF TEMPERATURE MICROSTRUCTURE IN THE OCEAN

by

Peyton Marshall Magruder, Jr.

April 1970

Some Characteristics of Temperature Microstructure in the Ocean

by

Peyton Marshall Magruder, Jr.
Lieutenant Commander, United States Navy
B.S., United States Naval Academy, 1962

Submitted in partial fulfillment of the
requirements for the degree of

MASTER OF SCIENCE IN OCEANOGRAPHY

from the

NAVAL POSTGRADUATE SCHOOL
April 1970

Author Peyton Marshall Magruder, Jr.

Approved by: Harvey H. Demmon
Thesis Advisor

Noël Boston
First Reader

Chairman, Department of Oceanography

R. F. Rinehart
Academic Dean

ABSTRACT

The background of microstructure and its effect on sound propagation is reviewed. The expendable bathythermograph (XBT) system and current digitizing procedures are evaluated to determine their adequacy in investigating vertical thermal microstructure. Several methods of microthermal analysis are proposed. Temperature gradient versus depth plots are used to analyze data from several ocean regions - Atlantic Coastal, Andaman Sea, Eastern North Pacific, and the northern boundary of the Gulf Stream. Analysis of these data suggest a water mass dependence of the thermal microstructure. The significance of the small-scale structure to Naval operations is discussed.

TABLE OF CONTENTS

I. SIGNIFICANCE OF MICROTHERMAL STRUCTURE

Naval interest in the thermal structure of the ocean is presently centered on gross features such as sea surface temperature, mixed layer depth, thermocline gradient, and depth to the bottom of the thermocline. Some attention has been given, especially in the Canadian Navy, to the transients in the mixed layer [Tully, 1964] and their possible association with internal waves. The above gross features are used primarily as a means of classifying thermal structure.

Technological developments have led to measurements which indicate the thermal structure is made-up of layers of varying thickness; from less than a centimeter to tens of meters [Stommel and Federov, 1967; Osborn, 1969; for example].

Of the variables affecting sound velocity in the ocean, temperature has the greatest effect. The presence of variations in temperature, or temperature gradient, causes sound velocity fluctuations to occur. Research on the effects of the thermal layers on sound in the ocean show that further investigation in theory and experiment is required. Small scale sound velocity variations cause irregular bending of sound rays. The microstructure can affect attenuation, forward and backward scattering, reverberation, reflection, and refraction which can converge or diverge the energy in a sound beam [Meyer and Romberg, 1963]. The physical features of the microthermal structure must be adequately described before their effects upon acoustic propagation can be fully understood.

The purpose of this thesis is to review the present knowledge concerning microstructure as measured by expendable bathythermographs (XBT), to evaluate the capability of the XBT in measuring microthermal structure, to develop a scheme of quantitatively examining the microthermal structure, and to test this scheme on real data.

II. REVIEW OF PRESENT KNOWLEDGE

A. MICROTHERMAL STRUCTURE IN THE OCEAN

Prior to 1937, vertical thermal structure was measured at discrete points using reversing thermometers. This method provided a point-to-point analysis of the vertical structure at one location. Even using point-to-point measurements, it was clear that the temperature variability decreased with depth in most regions. In fact, the most common analysis of the temperature and salinity data, T-S correlation, usually ignored the upper 100 meters or so. However, this same analysis showed that in many ocean regions, in deep water, (e.g., below 1000 to 2000 m), the variability was on the order of the instrument error [Sverdrup, Johnson and Flemming, 1942]. This result was not unexpected because the gradients in the deep ocean became smaller. The discrete measurements of the Nansen cast are not suitable for studying small scale variability.

The development of the mechanical bathythermograph (MBT) by Spilhaus [1938] provided the first convenient means of measuring a continuous profile of temperature. The mechanical bathythermograph was widely used during World War II. A large number of bathythermograms with double traces, which could not be explained as instrument errors, were discovered [Urick and Searfoss, 1948]. The double traces indicated that small-scale horizontal and/or vertical temperature variations occurred between the lowering and raising of the MBT. Urick and Searfoss [1949] recognized that this small-scale microstructure could be significant to sound propagation, depending on the size and shape of the inhomogeneity.

Horizontal microthermal structure was measured by Holder in 1944 using a thermopile mounted on a submarine. He detected horizontal temperature differences of 0.02F over distances of about 10 m [Smith, 1967]. Measurements of these horizontal temperature variations were also made by Urick and Searfoss [1948, 1949] in July of 1948 near Key West, Florida. With a thermocouple mounted on the conning tower and, later, its bow, a submarine proceeded at a constant speed and depth, while the probe measured the water temperature to a resolution of 0.003C.

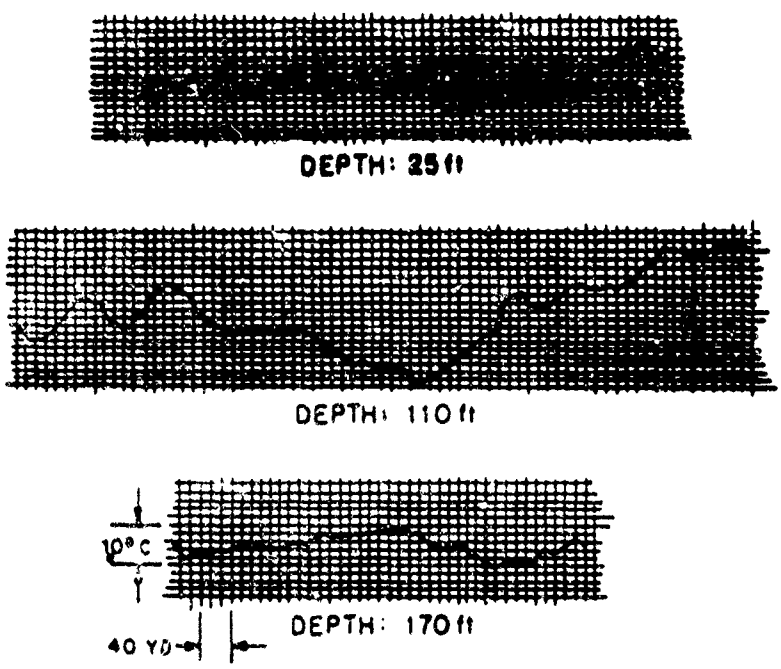

Figure 1. Microthermal Variations at Various Depths [Urick and Searfoss, 1948].

Urick and Searfoss [1949] calculated the peak-to-peak root-mean-square (rms) variation for peaks in excess of 20 percent of the total

variation in a record calling this the root-mean-square maximum (rmsm). A significant difference between the value of rmsm in the mixed layer and in the thermocline was observed. In the mixed layer a mean rmsm value of 0.013C was observed. In the thermocline, the mean value was 0.450C. The rmsm increased with depth in the mixed layer and decreased with depth in the thermocline. Applying Taylor's hypothesis, the mean horizontal thermal "patch size" was found to vary from 5 to 30 m in the mixed layer and from 30 to 200 m in the thermocline region [Urick and Searfoss, 1949].

Liebermann [1951] mounted a sensitive platinum-resistance thermometer and a thermocouple on the periscope of a submarine. The platinum-resistance element could resolve spatial temperature variations on the order of 10 cm in horizontal distances as the submarine proceeded at a constant speed of a few meters per second at a fixed depth (Figure 2). To characterize the temperature fluctuations, he used the autocorrelation function. "Patch size" was defined as the distance of the microthermal structure, within which the temperature variations maintained coherence.

The function is given by:

$$R(\rho) = \int_0^\infty [T(x) \cdot T(x+\rho_0)]\, dx. \tag{1}$$

His results could be fit equally well by an exponential,

$$R(\rho) = e^{-\rho/a} \tag{2}$$

or the Gaussian,

$$R(\rho) = e^{-(\rho/a)^2} \tag{3}$$

where:

$T(x)$ = temperatute at some point x;

$T(x+\rho_0)$ = temperature at another point displaced a distance ρ_0 from x;

ρ = autocorrelation distance;

$\langle\bar{\rho}\rangle = a$ = "patch size".

Whereas, the exponential function fitted the data points and decayed rapidly as ρ increased (Figure 2), it did not have a zero slope at the origin, thus, the exponential function was not appropriate for very small correlation distance (e.g., a few cm or less) because of heat conductivity in sea water. He proposed the Gaussian function to correct this difficulty, reasoning that thermal conductivity would prevent any discontinuity in the temperature field [Liebermann, 1951].

Liebermann assumed that the thermal microstructure represented a cloud of spheres with a Rayleigh distribution having a mean size value of the correlation distance and therefore yielding

$$R(\rho) = R(a) = e^{-1}. \tag{4}$$

Using this definition, the mean size of the inhomogeneities, a, was found to equal 60 cm in the ocean (Figure 2).

Piip [1961] investigated the sound velocity microstructure in the sound channel off Bermuda with a NBS velocimeter. It was noted that a number of thin steps remained over periods of hours, some oscillating 30 m in depth in a three-hour period. At the same station and same depth, sound velocity changes of one m/sec in a few hours were common and "nearly the rule". The sound velocity axis was observed to change 150 m in depth and 3.5 m/sec over a three-month period. Pipp showed that the base of the main thermocline (about 1000 to 1300 m) exhibited

relatively large and rapid changes in sound velocity in an inhomogeneous region in a constant state of fluctuation.

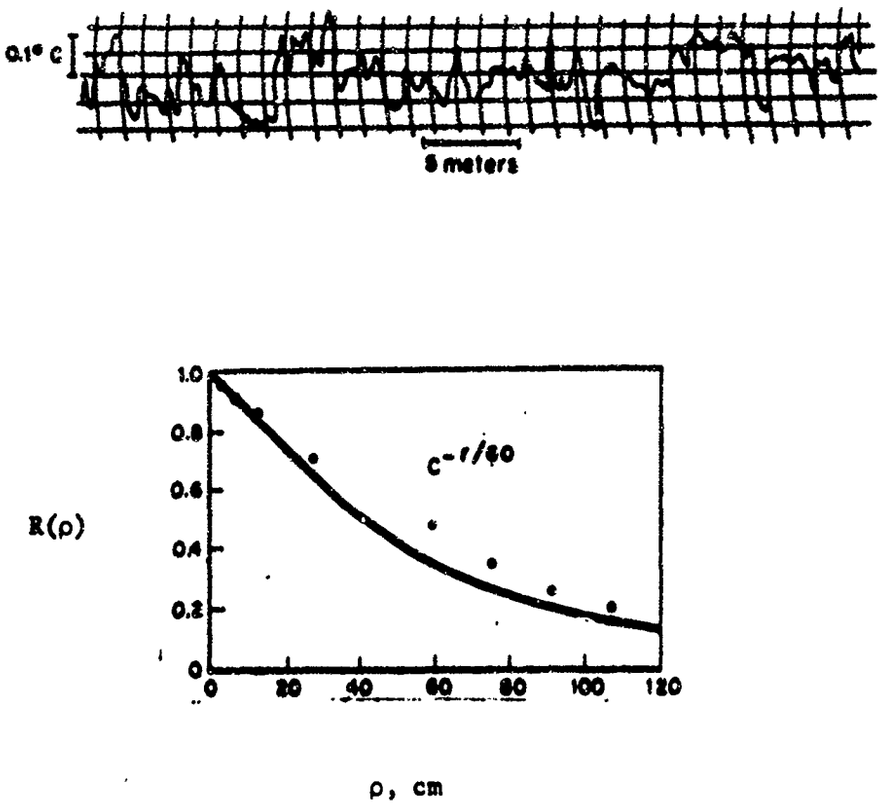

Figure 2. Temperature Fluctuations and Associated Correlation Function (After Liebermann)

Small-scale temperature and salinity structure was measured with a salinity, temperature, and depth recorder (STD) by Stommel and Federov [1967] near Timor and Mindinao during July of 1965. Their measurements revealed that the vertical microstructure actually consisted of very thin high-gradient layers. The thin layers were separated by thicker layers of nearly homogeneous (isothermal or isohaline) water, i.e., step-like in appearance on their STD traces. By following a discrete

feature from one cast to the next, homogeneous layers were found to be continuous from two to 20 km horizontally and to range in thickness from two to 40 m (Figure 3). A boot-like feature was found at the bottom of the mixed layer (Figure 4). At a depth of 200 to 300 m, the mean thermal gradient was about 0.040C/m. In the thin steps, the gradient was less than 0.003C/m, and in the homogeneous steps, the thermal gradient was greater than 0.350C/m. Stommel and Federov concluded that the ocean consisted of nearly homogeneous layers separated by steps with extremely high thermal gradients.

Tate and Howe [1968], in the summer of 1966 in the Northwestern Atlantic, used an STD to look at the thermocline stratification in the Mediterranean Water intrusion at a depth of 1280 to 1500 m. They found layering with steps varying on the order of 0.17 to 0.35C in temperature, from 0.02 to 0.055 o/oo in salinity, and from thickness of 15 to 30 m (Figure 5). A step's average temperature change of 0.25C produced a σ_t change of -0.044, while the average salinity step of 0.044 o/oo produced a σ_t change of +0.039. The resulting change of σ_t (-0.005) gave a slightly stable layer system in a situation which was clearly one of opposing salinity and temperature density gradients.

Cooper and Stommel [1968], using an STD, found the main thermocline in the Sargasso Sea to consist of regular salinity and temperature steps of homogeneous layers three to five meters thick, separated by transitional layers 10 to 15 meters thick, with temperature changes of 0.30 to 0.50C and salinity changes of 0.04 to 0.10 o/oo (Figure 6). The horizontal extent of these steps was between 400 to 1000 meters. The main thermocline contained up to 100 steps on each cast.

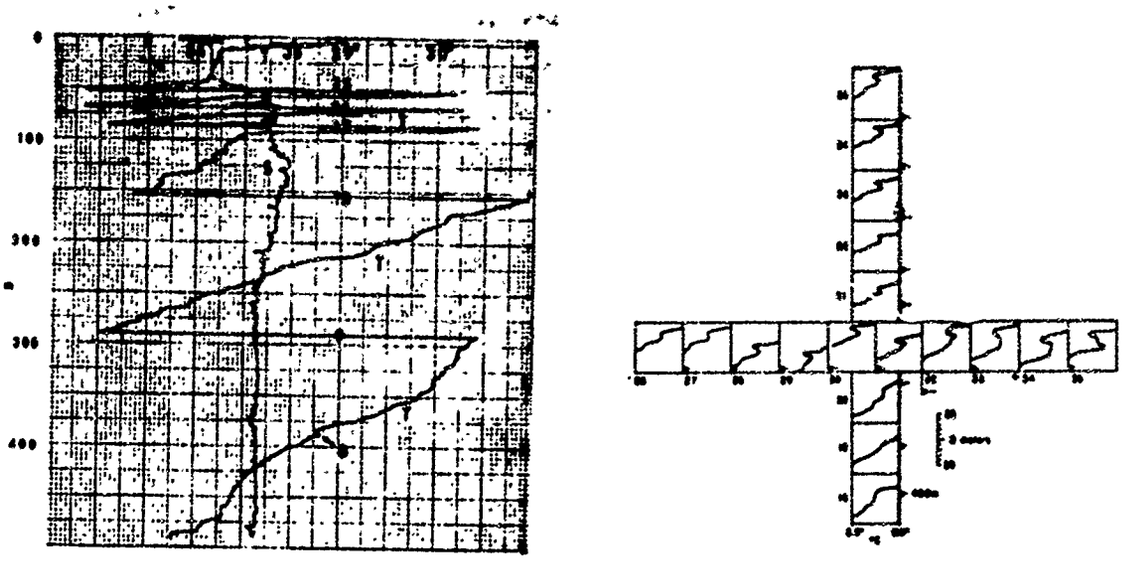

a. b.

Figure 3.a. Photographic copy of actual STD trace (not retouched) of station 21 off Mindinao. Depth scale is 500 m, each small division being 5 m. The salinity curve, labeled S, has the smallest division being 0.05 o/oo. The temperature, labeled T, has a smallest division of 0.05C. The lamina B is so labeled. Because the pens cannot both traverse the same path mechanically, the temperature curve is offset downward by 5 m and always reads 5 m too deep. The salinity scale is not offset in depth. Uniform corrections for salinity of -0.9 o/oo and temperature of 0.07C have not been applied.

Figure 3.b. A composite chart-graph for lamina B off Mindinao. Each square is 0.05C wide (8.5 to 9.0C) and 50 m high. The small arrow indicates a depth of 400 m in each square. Numbers in the lower left hand corners are the station numbers. The distances from stations 18 to 25 and 26 to 35 are about 10 nm. For lamina B, the large geographical extent of this small lamina is self-evident.

[Stommel and Federov, 1967]

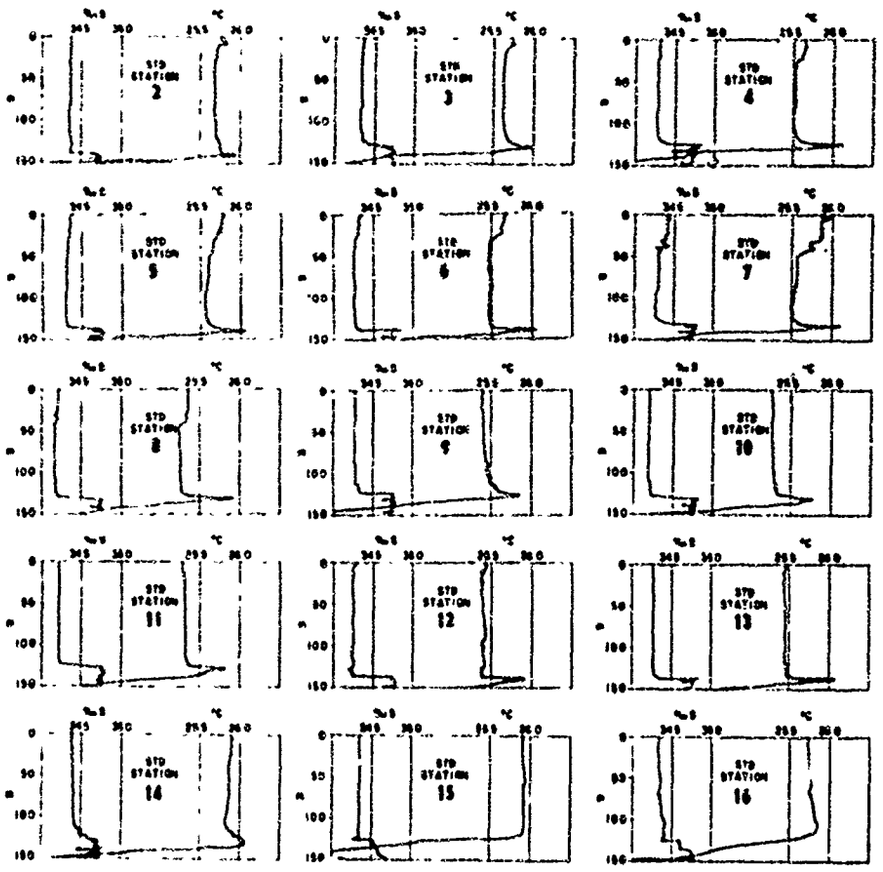

Figure 4. From the soundings in the mixed layer off Timor, gross differences in the properties in different locations are self-evident. There is considerable variation in vertical structure but each sounding shows a nearly homogeneous region near the surface (station 13) but some stations (like 7) have shallow irregular layers overlying the mixed layer.

[Stommel and Federov, 1967]

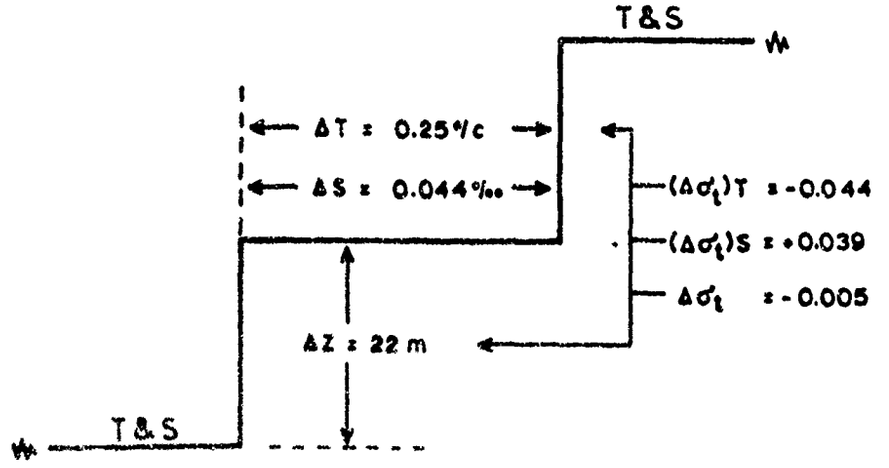

Figure 5 A typical step in Mediterranean Water [Tait and Howe, 1968].

Woods [1968, 1968a] investigated the microstructure in the summer thermocline off Malta using a temperature-gradient meter for obtaining the thermal gradient between two thermistors set 50, 25 or 10 cm apart on a vertical staff. The resolution of the thermal gradient was within 0.01C per thermistor separation distance. An additional thermistor recorded temperature. Woods plotted profiles of the thermal gradient and temperature versus depth (Figures 7, 8 and 9). Using time-lapse photography, Woods obtained pictures of streaks left in the wakes of free-dropping dye pellets for shear measurements. A dye-packet array tied between moored, submerged floats injecting dye into selected levels of the thermocline, indicated that the thermocline was divided into layers a few meters thick. These layers were characterized by weak thermal gradients, less than 0.001C/m, and by turbulence with a mean velocity of less than one mm/sec. The layers were separated by sheets only centimeters thick. (Sometimes, he detected sheets up to a meter thick but they appeared as aggragates of the 10 cm thick sheets.) The sheets were characterized by strong thermal gradients up to 0.05C/cm and little or no turbulence. Mature sheets contained thin laminar-flow zones in their centers. Neighboring layers had dissimilar properties indicating different salinities, velocities, and turbidities. This suggested different trajectories and a very slow exchange of properties across the intervening sheets. If turbulence was small, flux exchange was small; therefore, the exchange had to rely on molecular processes, which were very slow indeed.

Individual layers were followed horizontally for distances up to 72 km by soundings from high-speed launches. Layers were identified on

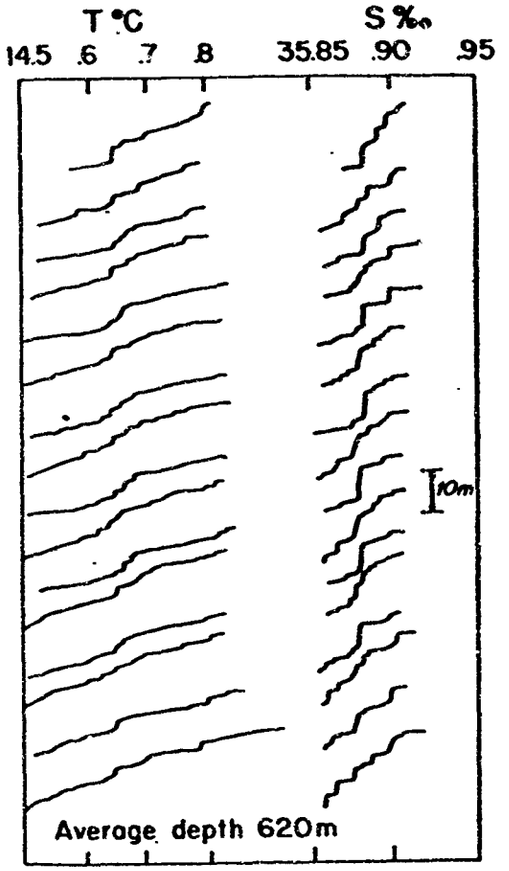

Figure 6. Steps in the Saragasso Sea made by taking several temperature and salinity soundings in rapid succession across a single "homogeneous" step [Cooper and Stommel, 1968].

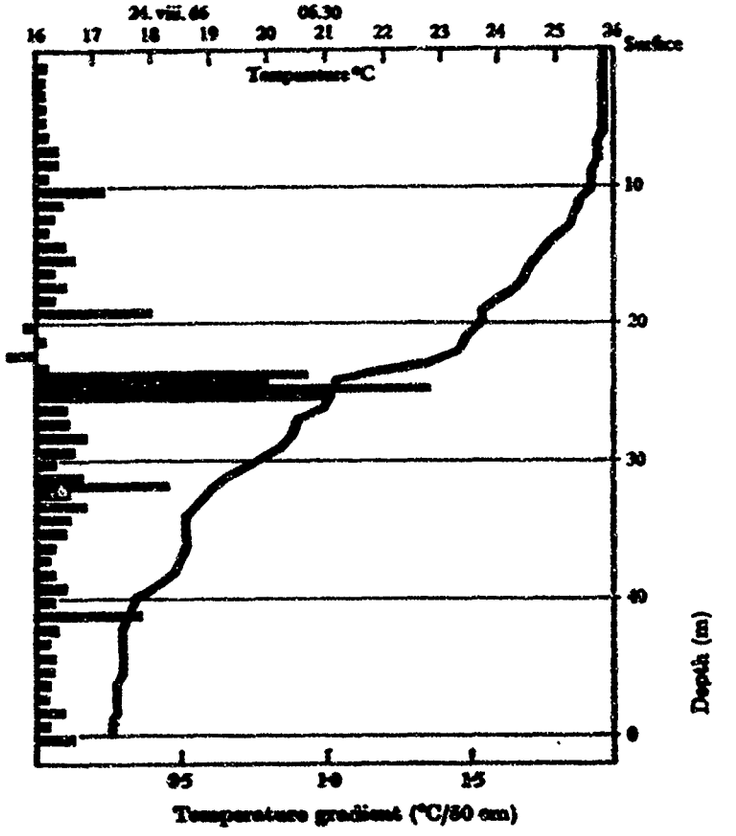

Figure 7. A typical temperature-depth and temperature gradient-depth values obtained by Woods with a 50 cm thermistor spacing [Woods, 1968].

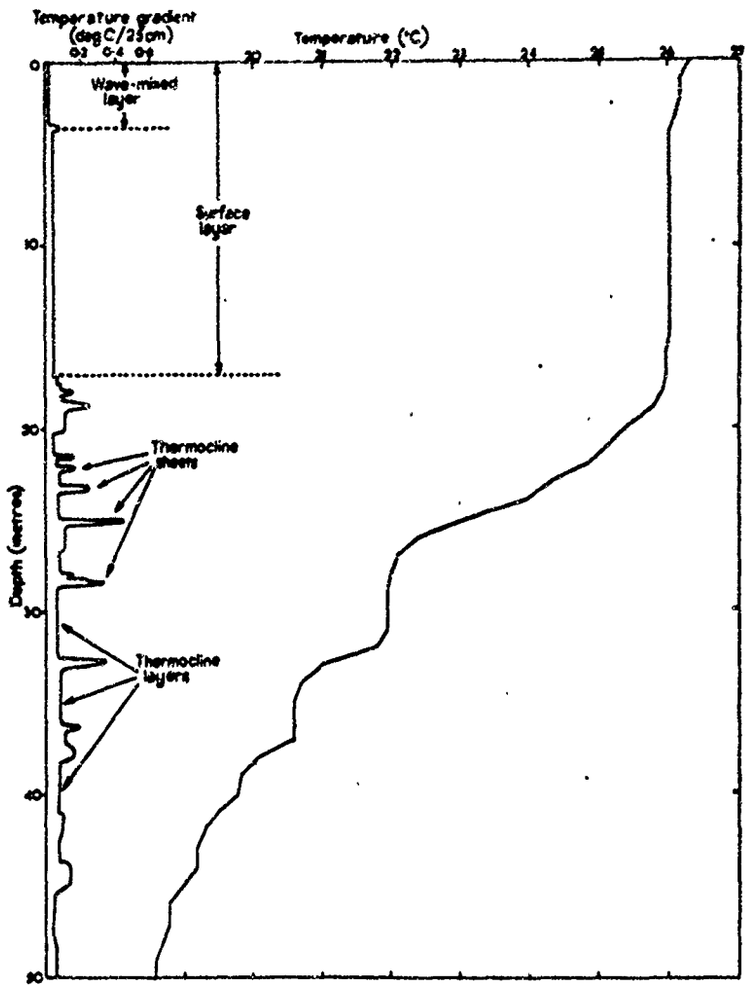

Figure 8. Temperature and Temperature-Gradient Soundings for Maltese Waters, 14 September 1967 [Woods, 1968a].

Temperature 0918-0919 local time, (i.e., GMT + 1).

Temperature gradient 1132-1145 local time.

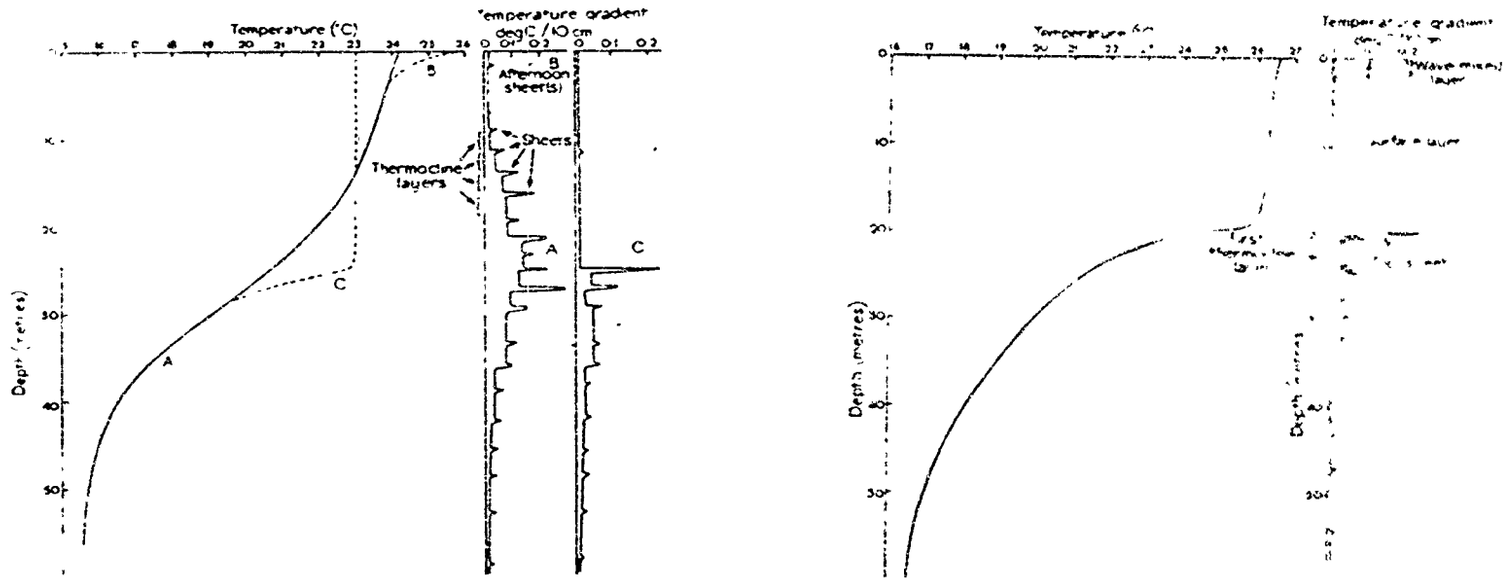

Figure 9. Idealized Temperature and Temperature-Gradient Profiles for Maltese Waters in Early July and Late August [Woods, 1968a].

Early July

A Calm weather (morning).
B 'Afternoon effect' (surface warming without wave-mixing).
C Mixed surface-layer following an extended period of rough seas.

Late August

Moderate seas.

successive soundings for many hours, thus confirming the results of Stommel and Federov.

The dye experiments showed that in a thermocline sheet there was a central laminar-flow region only a few centimeters thick. Dye was spread in this region by internal waves to form a "broad carpet of color". This colored sheet made it possible to photograph the internal waves as they crossed it. Wave-lengths between 5 and 10 m were dominant and appeared in long, coherent trains, each associated with a single sheet. They had heights up to 1.0 m, a phase speed of 2.5 cm/sec and periods of about 5 min. These waves only affected a single sheet, being much shorter than the long internal waves which move the entire thermocline.

A sheet was defined as stable when it appeared smooth everywhere; this indicated laminar flow. When a wave passed over a sheet, shear had its greatest effects at the crest and trough. Wave shear and drift shear interacted either cancelling or reinforcing each other causing a sheet to become unstable and patchy.

Wavelets, about 75 cm in length, caused banding to appear parallel to the crests and troughs. These wavelets generally formed, grew, and broke in a period of less than two minutes. Upon breaking in classical fashion, a second smaller breaker was generally thrown forward. The wavelets had a maximum height of about 20 cm. After breaking, a turbulence region remained for about 5 minutes, and the scar in the sheet remained for several hours. These scars were a common feature in thermocline sheets. The thinnest sheet observed to become unstable had a thickness of 3 cm; the thickest was 30 cm. The great majority were between 8 and 15 cm.

Transient thermoclines [Tully, 1964] which occur sporadically between the surface and the top of the thermocline were considered as further examples of sheets. Woods divides the thermocline into a half-dozen or so layers of low shear and moderate thermal gradient separated by thin liminar flow sheets of intense shear and thermal gradient. He discussed the important aspect of heat transfer through such a layered ocean. He suggested that the molecular heat transfer through the high gradient stable layers was negligible, but that heat transfer does take place through the turbulent scars from one layer to another as an effect of the breaking of the internal waves.

The use of the Ramsey SVTP (sound velocity, temperature, and pressure) probe provides a digital output of these parameters. This instrument has an accuracy of $\pm$ 0.01C and $\pm$ 0.25 percent of depth with a precision of $\pm$ 0.08 m/sec in sound velocity [Lovett, 1968]. In view of the plus-or-minus-one count for electronic counters, small-scale features, i.e., less than $\pm$ 0.01C and $\pm$ 1 m in depth, are ambiguous. Lovett [1968] discussed the thermal gradients determined with this instrument (Figure 10). The 10 m depth increments he used eliminated some microstructure; however, using 5 m increments introduced random readout errors.

Ingham [1968] used an STD probe to investigate the mixed layer in tropical waters. The vertical salinity and temperature structures forming the "isothermal" and "isohaline" layers were generally analogous in the near-surface layers. The difference in the depths of these two layers exceeded 7.5 m in 45 percent of the casts and 17.5 m in 31 percent as shown by Figure 11 [Ingham, 1968]. Microstructure effects on sound velocity in the near-surface layers would depend on salinity in some ocean regions.

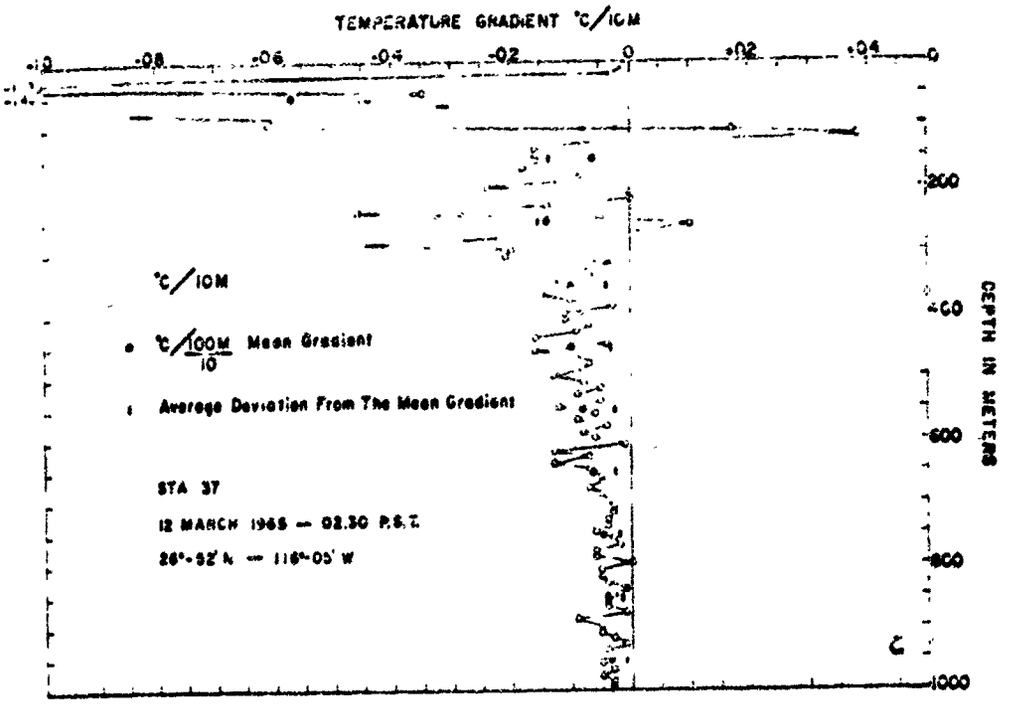

Figure 10. **Temperature Gradient per 10 m, Mean Gradient per 100 m, and Average Deviation from Mean versus Depth from Ramsey Probe Data [Lovett, 1968].**

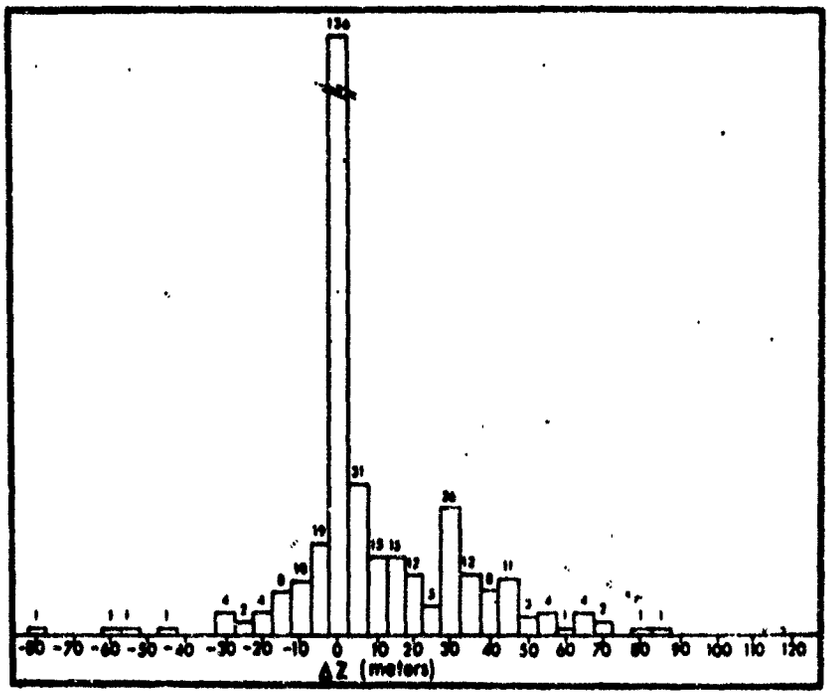

Figure 11. **Histogram of Depth Differences ΔZ of the Isothermal and Isohaline Layer Depths [Ingham, 1968].**

Pingree [1969] using an STD, recorded analogue signals on tape. He made fine-scale plots of salinity and temperature. In particular, he investigated the stability of the deep water, i.e., about 500 to 2000 m (Figure 12).

Osborn [1969] using a free-falling temperature gradient meter obtained excellent profiles of temperature gradient (Figure 13). Off San Diego, the horizontal extent of the layers was greater than 750 meters in the seasonal thermocline, but only a few hundred meters at depths greater than 400 meters. He noted the layers were, in fact, made up of even finer layers with a thickness of only a few centimeters. His average sheet was about one meter thick.

Recent work by Neshbya, Neal, and Denner [1969] using the expendable bathythermograph manufactured by General Motors Defense Laboratories, obtained records of temperature steps (Figures 14, 15 and 16). While on Ice Station T-3 in the Arctic (near 84-38N, 128-22W), they lowered XBT probes by hand. The Ice Station results are the first XBT microstructure records without ship motion.

B. APPLICATIONS

Urick and Searfoss [1949] calculated theoretically that a sound ray would be bent through an angle of only 3.7 sec by the average inhomogeneity in the mixed layer but as much as 2.1 min of arc in the thermocline.

Sheehy [1950] measured sonar signal fluctuation as functions of depth and range. He found the coefficient of variation, defined as the standard deviation of the amplitudes expressed as a percentage of the mean amplitude, varied as the square root of range and did not appear to be a function of depth.

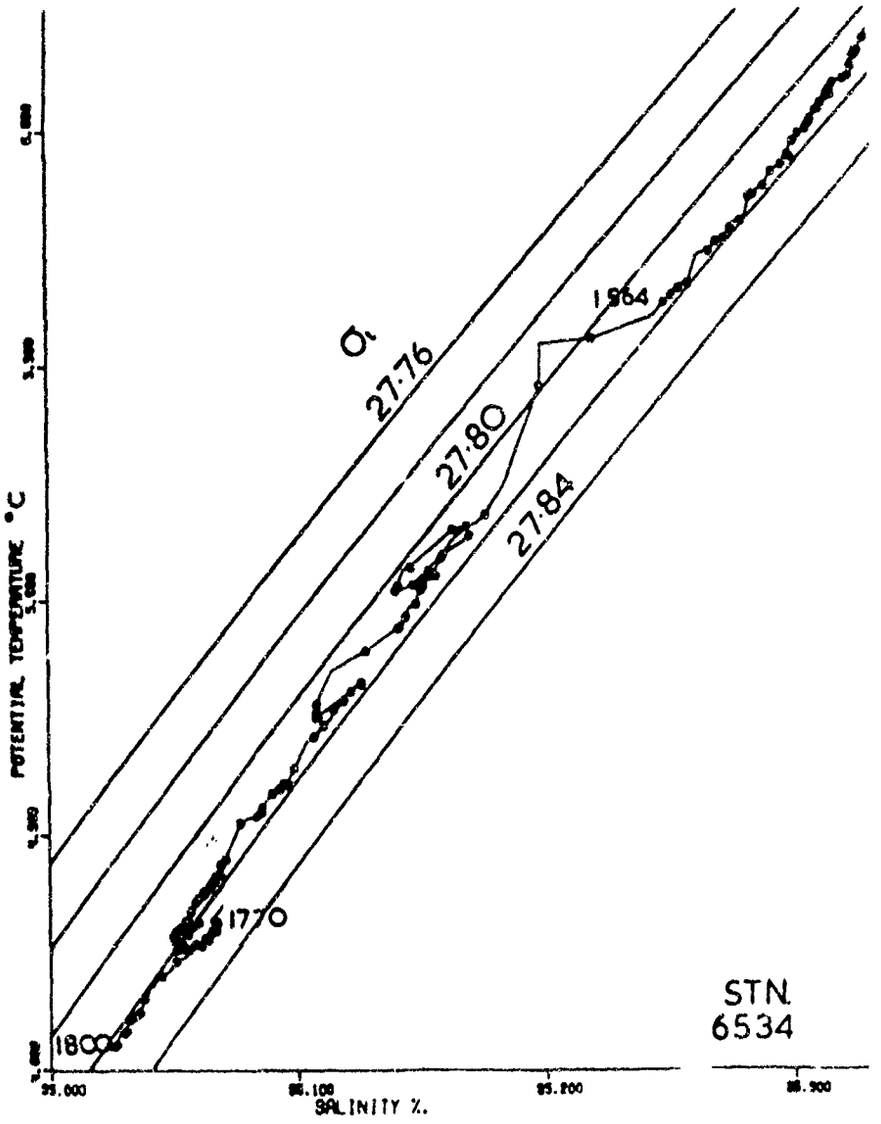

Figure 12. T-S Curve from 1500 to 1800 m with a Value Every Meter. Circles Represent Increments of 2 m in Depth [Pingree, 1969].

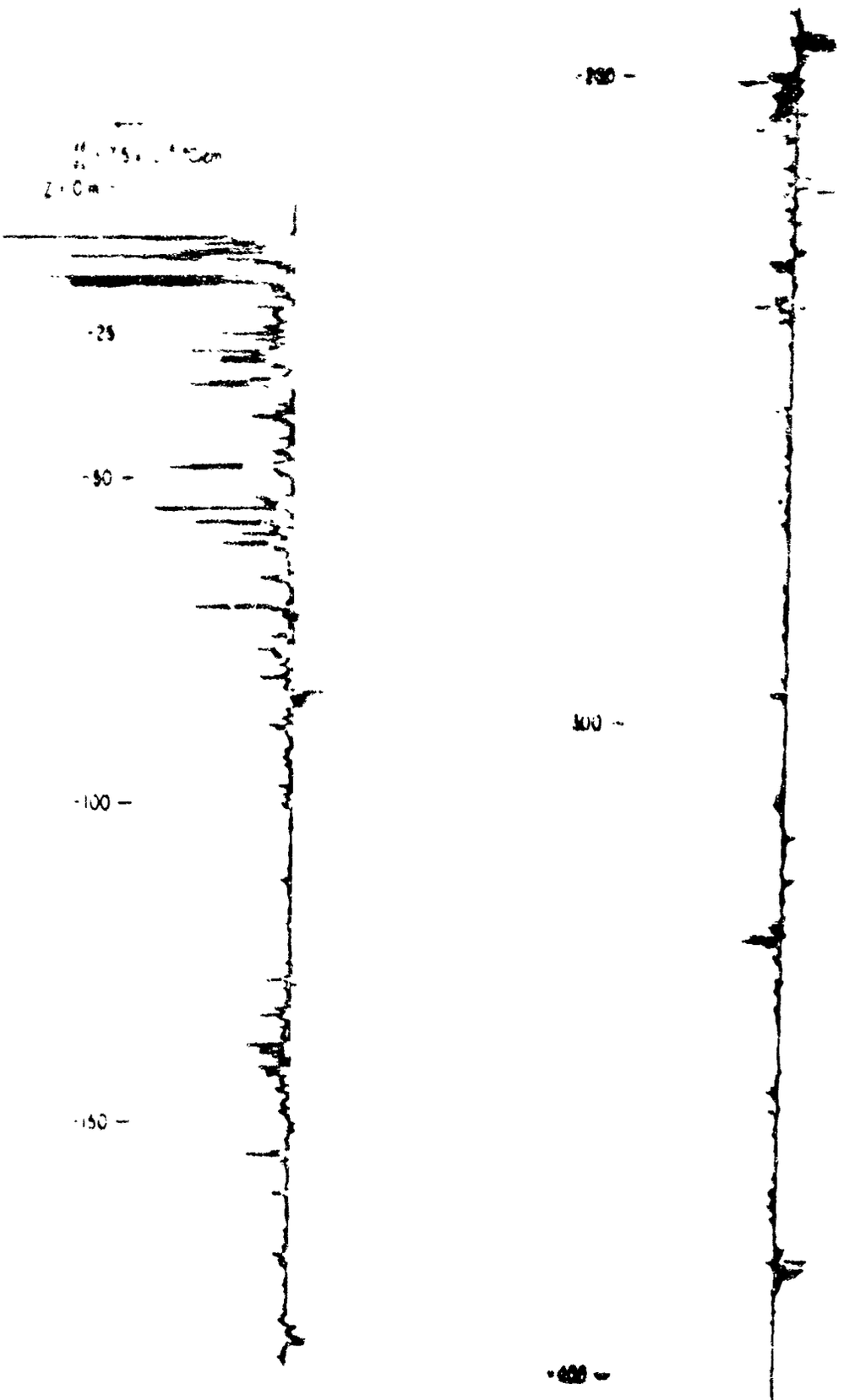

Figure 13 Temperature Gradient-Depth Values [Osborn, 1969].

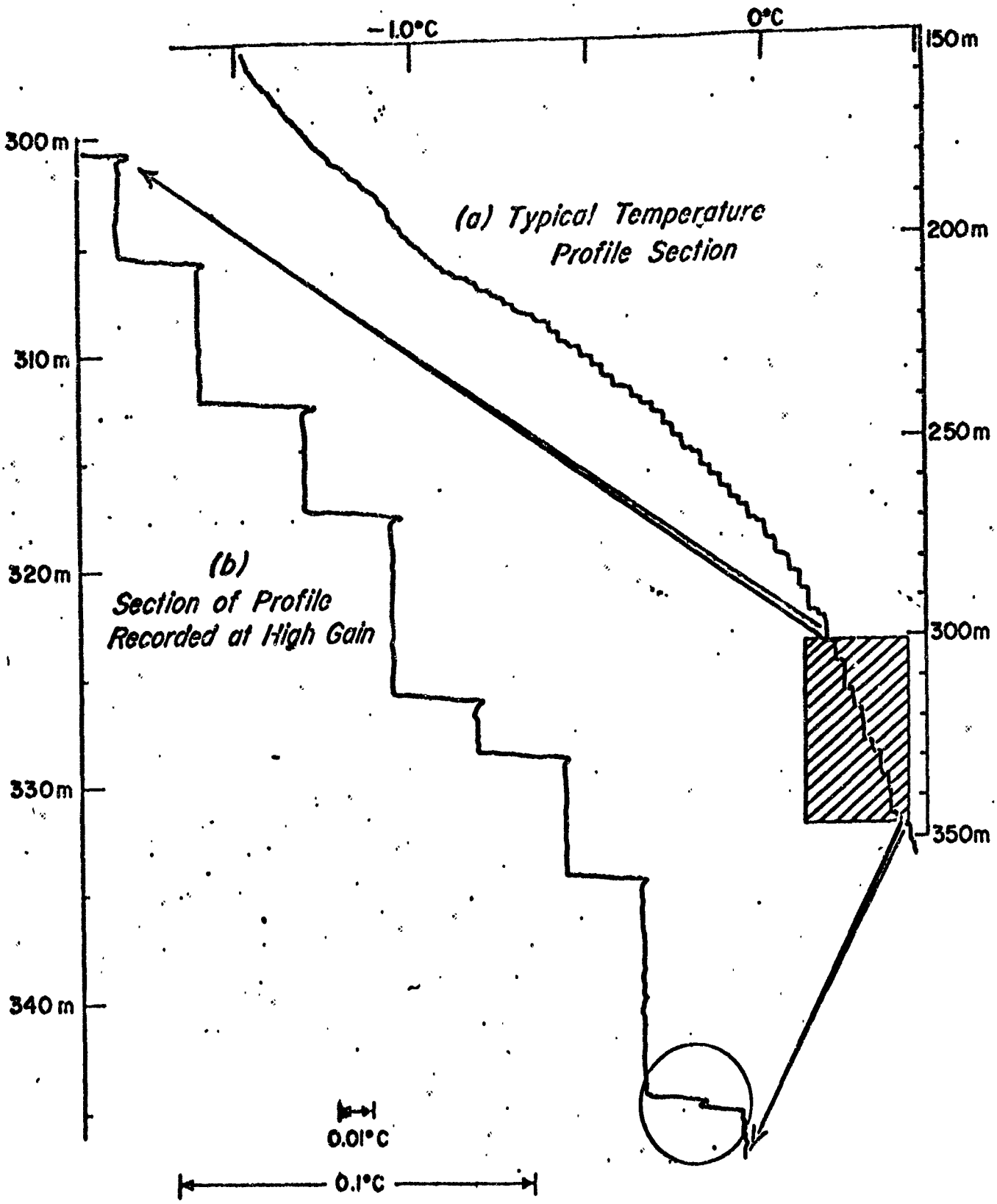

Figure 14. Vertical Profile of Temperature Under Ice Station T-3 (84-38N, 128-22W) 19 March 1969. [Nashbya, Neal and Denner, 1969].

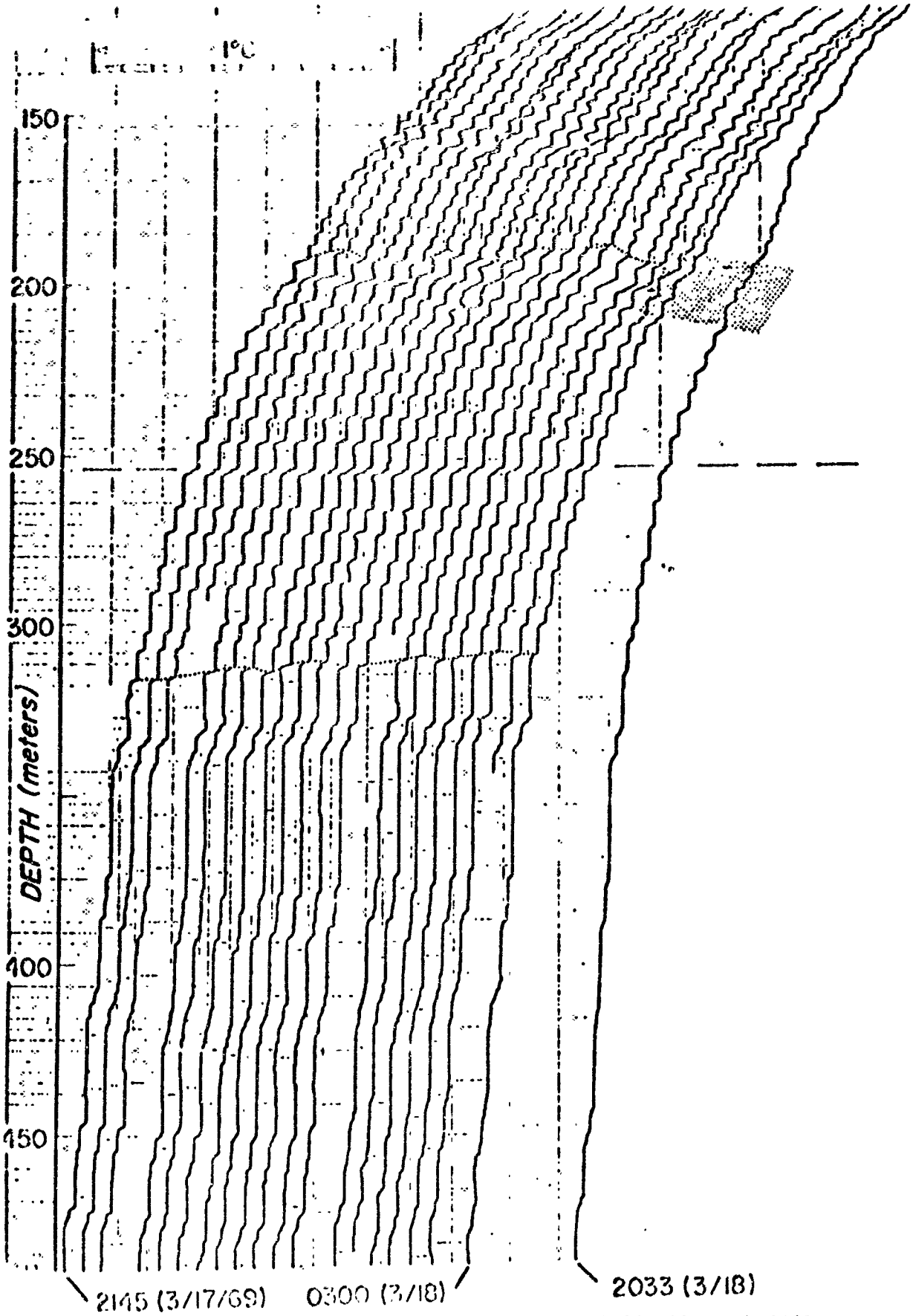

Figure 15. Time Series from 2145Z 17 March to 2033Z 18 March 1969. [Neshbya, Neal and Denner, 1969].

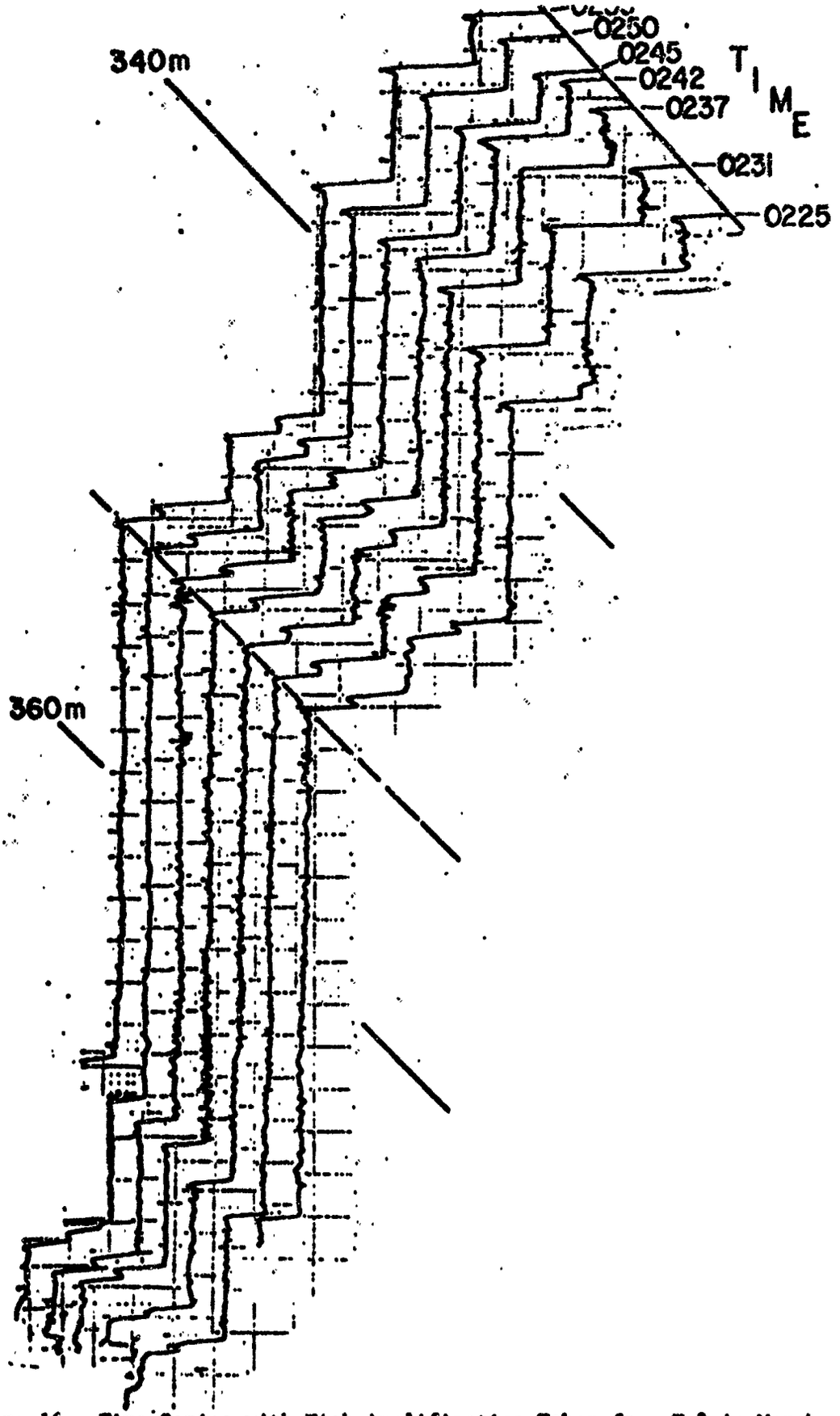

Figure 16. Time Series with High Amplification Taken from T-3 in March 1969. Temperature increases from right to left. [Meshbya, Neal and Denner, 1969].

Liebermann [1951] described the influence of the microstructure on acoustic propagation He wrote the sharpness of temperature boundaries determines influence of the microstructure on acoustic propagation. When temperature changes occur within a distance of less than one acousti wavelength, the temperature boundaries may reflect sound energy depending upon the size and shape of the "patch" The temperature microstructure may reflect, refract, scatter, or focus acoustic waves, The microthermal structure was considered to be made up of randomly sized "spheres", spaced randomly throughout the medium, with a scattering cross section dependent upon the autocorrelation of the temperature inhomogeneities, R (ρ). Comparing derived scattering cross section with actual scattering in the ocean (i.e., volume reverberation), Liebermann concluded the observed reverberation was higher than one would expect from thermal inhomogeneities He attributed volume reverberation to biological scatters.

Liebermann found that refraction effects of the inhomogeneities resulted in warping of the wave fronts, and caused the wave front to be a complex surface exhibiting both convergence and divergence. The temporal motion of the inhomogeneities resulted in sound "scintillation" at the receiver

Mintzer [1953] found Sheehy's coefficient of variation to be dependent upon the three-halves power of the range rather than the one-half power of range.

Skudrzyk [1957] discussed the focusing and defocusing effect within the focusing range r_0 given by $r_0 = ka^2$ where a is the "patch" radius and k is the acoustic wavenumber At ranges greater than r_0, in the interference range, phase interference results (Figures 17 and 18).

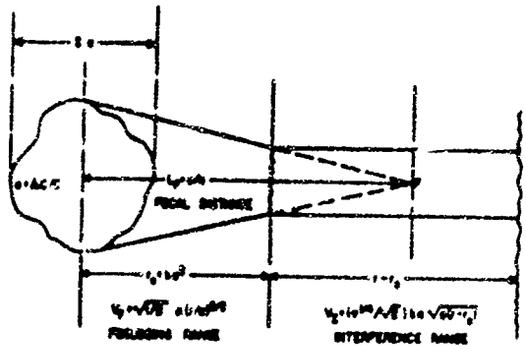

Figure 17. Illustration of the Various Types of Acoustic Scattering Due to a Thermal Patch in the Sea [Whitemarsh, Skudrzyk and Urick, 1957].

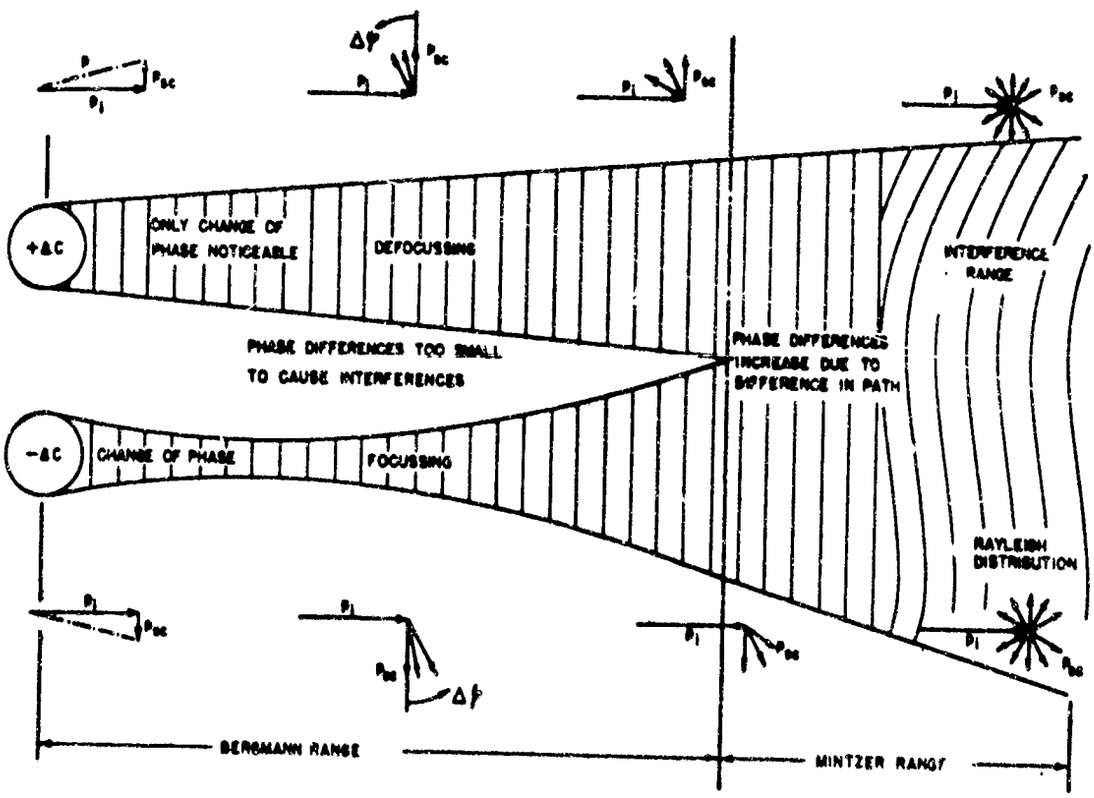

Figure 18. The Phase Angle Between the Incident and the Scattered Pressure and the Physical Nature of the Scattering as a Function of the Range [Skudrzyk, 1957].

Using this concept, Skudrzyk (Figure 19) shows the focusing range r_0 as a function of frequency and patch size. (For example, a 50 kHz frequency sonar has a focusing range of 75 meters, if the patch size is assumed to be 60 centimeters.) For finding patch size, Skrudzyk used the Urick-Searfoss [1948] data to show patch size was twice the depth (Figure 20). Further, Skudrzyk started theoretical investigation with spheroidal patches, which he found to have a considerably stronger focusing effect than the spherical patches.

Whitemarsh, Skudrzyk, and Urick [1957] did additional work with the spheriodal theory. The correlation functions previously used were discussed. It was concluded that the present correlation functions were not suitable and either had to be replaced or redefined. The authors argued if the temperature microstructure was produced by turbulent motion in the sea, then the Kolmogorov Law for statistical equilibrium must hold. This, they show, was in excellent agreement with their data. Lending support to continued studies such as are presented in this thesis, their final conclusion states that the

> "... greatest gap seems to lie in the microthermal statistics of the ocean. If these were known better than they are now, apparently the amplitude statistics of the fluctuations of sound transmitted through the sea could be predicted roughly, but with some assurance."[1]

Works by Peterson [1965], Barakus [1968] and DiNapoli [1969] have considered the normal mode approach to the interference range solution for the temperature inhomogeneities and have also investigated the effects of internal waves on sound in stratified mediums.

---

[1] Whitemarsh, D. C., Skudrzyk, E., and Urick, R. J., "Forward Scattering of Sound in the Sea and Its Correlation with the Temperature Microstructure," J. Acous. Soc. Am., v. 29, p. 1141, October 1957.

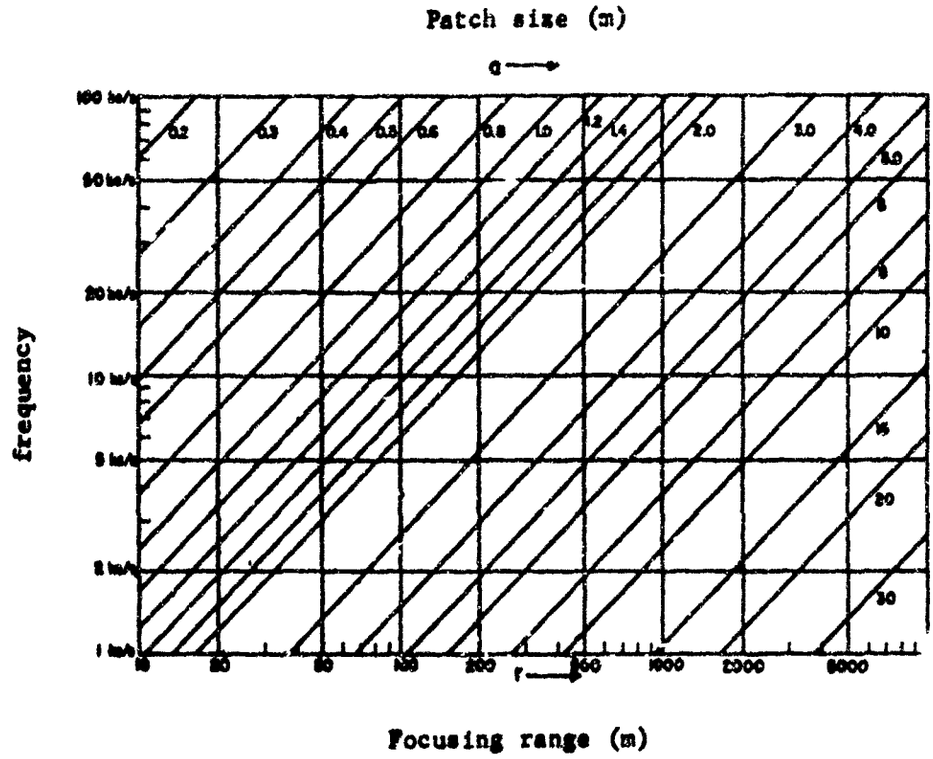

Figure 19. Focusing Range (meters) as a Function of Frequency and Patch Size (meters) [Skudrzky, 1957].

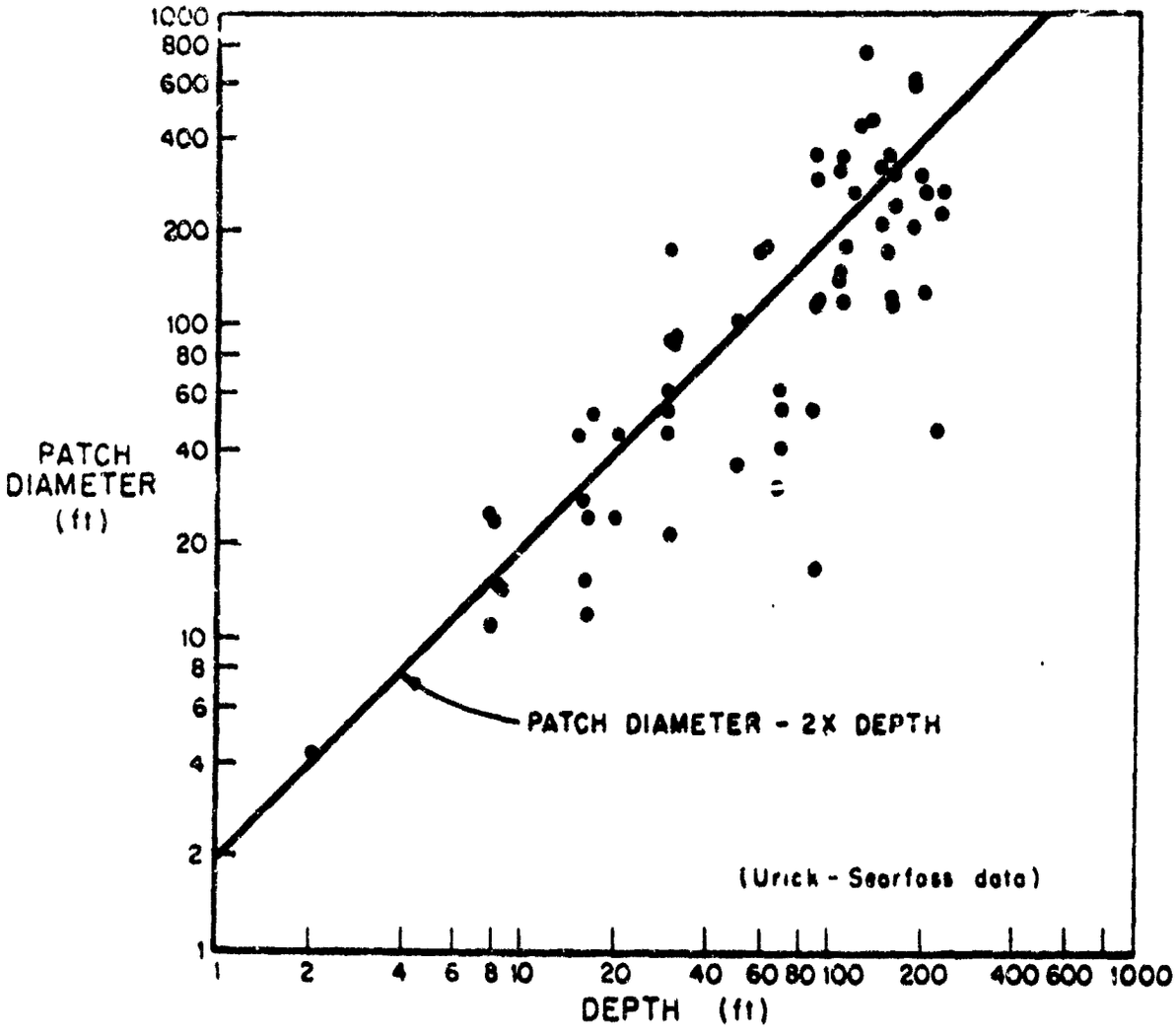

Figure 20. Patch Diameter Versus Depth [after Skudrzyk, 1957].

C. INADEQUACIES OF THE PRESENT THEORY

Since the thermal microstructure is not related simply to the gross thermal features measured on MBTs, there is presently no easy way to predict, on a day-to-day basis, the effects of microthermal structure on the propagation of sound in the sea. The theories, so far, have developed in two classes.

The first theories [Liebermann, 1951; Mintzer, 1953, 1953a, 1954; and Skudrzyk, 1957] concerned spherical and, more recently, spheriodal shaped inhomogeneities throughout the ocean. Part A above has discussed the present knowledge of microstructure showing that the long thin sheets and layers do exist as microthermal structure. These first acoustical theories do not apply to what is now described as the microstructure of the ocean.

The theoretical treatment by Whitemarsh, Skudrzyk and Urick [1957], considering speriodal patches and Kolomogorov's turbulence theories, could not find any real theoretical explanation of what happens in the sea when sound passes through an inhomogeneity. The investigations using normal modes have not produced any practical operational results.

Lee [1961] using ray path theory, demonstrated the effect of a typical sinusiodal internal wave o sound intensity in a three-layered model. For the medium with an internal wave, intensity variations up to 22 db were found in distances of less than one internal wavelength, as shown by Figures 21 and 22. In contrast, the same medium, without an internal wave, produced a 5 db variation, including a 2.5 db spreading loss, over the same distance.

Another study investigation the effects of sound velocity microstructure was conducted by FNWC [Wolff, Tatro and Megehee, 1967]. A

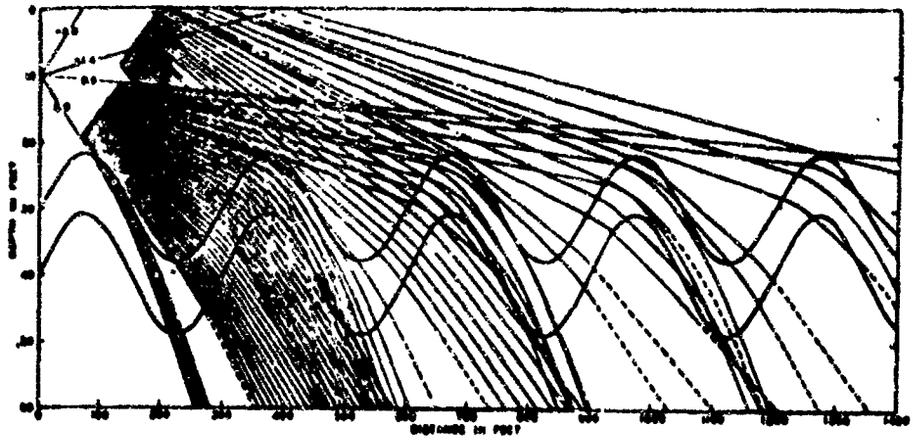

Figure 21. Diagram of Sound Rays through a Medium Which has an Internal Wave on the Thermocline [Lee, 1961].

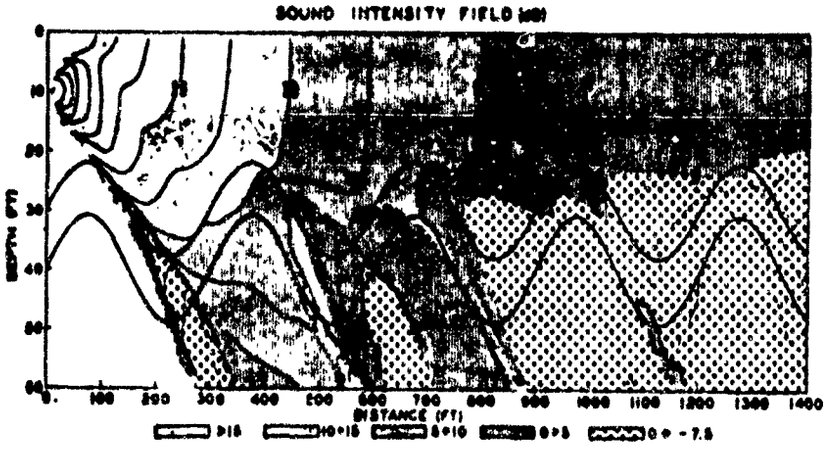

Figure 22. Sound Level in the Medium with an Internal Wave on the Thermocline. The db reference level is that corresponding to a sound level of 60 db at 1 foot from the directional source (X equals 0, Z equals 10 ft) along the horizontal. The field is contoured at intervals of 2.5 db [Lee, 1961].

sophisticated ray-tracing program [Ayers, Wolff, Carstensen and Ayers, 1966] was used for the analysis. Three complete ray trace runs were made to the first convergence zone using 120, 54, and 20 digitized sound velocity points from one SVTP trace containing sound velocity microstructure. The 120-point sound velocity profile preserved all the "wiggles" or microstructure, the 54-point profile used values at every 50 meter of depth, and the 20-point profile used the standard oceanographic depth values for sound velocity (Figure 23). The range to the first convergence zone agreed within 150 yards for all three cases. Based on the ray trace runs only, it was concluded the sound velocity microstructure was "essentially self-cancelling" and did not affect the convergence zone parameters [Wolff, Tatro, and Maghee, 1967]. Propagation loss and reverberation effects were not reported.

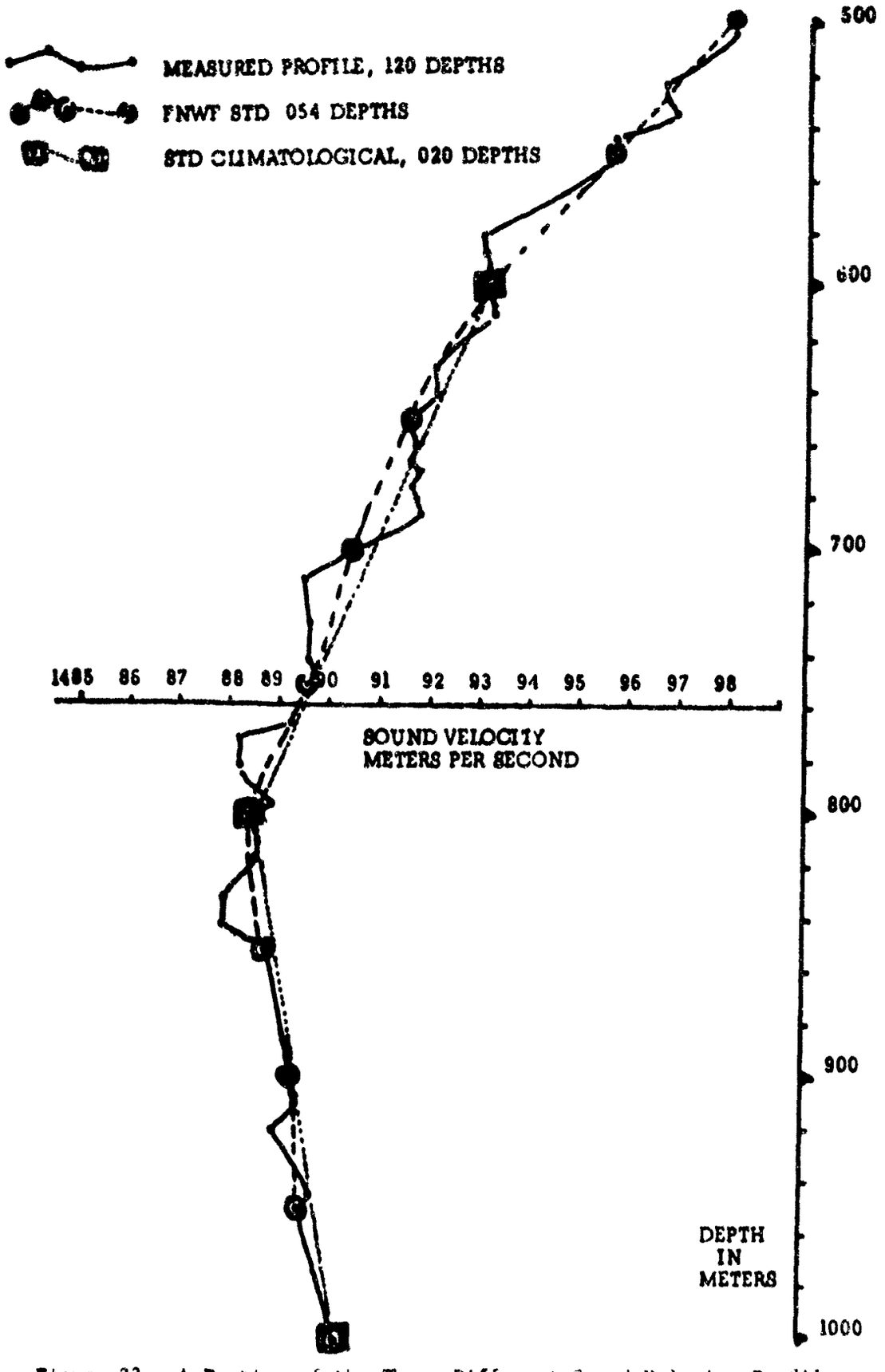

Figure 23. A Portion of the Three Different Sound Velocity Profiles Used by FNWC for Ray Tracing [after Wolff, et al.].

III. MEASURING MICROTHERMAL STRUCTURE

A. THE BATHYTHERMOGRAPH

1. Mechanical Bathythermograph

At the present time temperature is the most readily observed variable in the upper few hundred meters of the ocean. A major contributor to this situation is a singularly successful oceanographic instrument known as the mechanical bathythermograph or MBT. Subsequent to its introduction by Rossby and Montgomery [1934] and perfection by Spilhaus [1938], the MBT has become one of the basic instruments of almost all oceanographic agencies because of its simplicity of operation, reliability and relatively low cost. The result has been that a large number of bathythermograms have been collected.

Researchers during World War II, using the MBT, observed microthermal structure on their traces. No theory had been formulated which took into account the effects caused by microthermal structure on underwater sound transmission. It was recognized, however, that temperature microstructure must be considered in any explanation of observed underwater sound transmission [National Defense Research Committee, 1946].

2. The Expendable Bathythermograph

a. Capabilities

Presently the U. S. Navy is using the XBT system manufactured by the Sippican Corporation of Marion, Massachusetts. This system consists of an expendable shipboard cannister and probe, shipboard launcher, and a strip chart recorder. Data so obtained are submitted to FNWC and were used in this thesis.

The original Bureau of Ships' specifications [Denner, 1966] for an XBT system are given in Table I.

TABLE I

Temperature range	28F to 96F
Temperature accuracy	± 0.4F
Depth range	0 to 1000 ft
Depth accuracy	± 2% or 15 ft, whichever is greater
Ship's speed when launching	± 63% of a temperature step after 3 ft depth change

The expendable Sippican probe currently used has a thermistor sensor in its nose. The probe is connected electrically to the recorder by two conductor wires which pay out from both the probe and the canister. The canister in the launcher is connected to the recorder by a cable. There are no splices in the wire. The probe's weight is a critical factor in determining its fall-rate. The Sippican system was found to be within ± 3 gms both with and without its internal copper wire. (The deviation was from 0.3% to 0.64% of the total weight of the probe.) The observed average fall-velocity of the probe was 20.3 ± 0.2 ft/sec. A probe, with its internal wire, had an average terminal velocity of 19.9 ± 0.7 ft/sec. Terminal velocity was reached at 18.0 ± 0.5 ft [Gouzie, Sanders and Littlehale, 1966].

The present XBT strip chart recorder is a Mark 2A model using pressure sensitive paper for recording the thermal profile. The paper moves vertically on the recorder at a rate of 3.25 in/min. In one minute, the XBT, falling at 20 ft/sec, will have reached a depth of 1200 ft. Thus, 1200 ft will be recorded on 3.25 inches of chart paper, or 0.0027 of an inch of chart paper is used for every foot of fall.

The chart paper records horizontally from 28F to 96F in 7.0 inches, or about 0.103 of an inch of chart paper per 1.0F. Table II shows the resolution capabilities of the paper using different recording intervals.

TABLE II

Chart Spacing (inches)	Resolution Temperature (F)	Depth (ft)
0.01	0.0971	3.690
0.005	0.0476	1.045
0.001	0.0097	.369

The response time for the thermistor is 110 milliseconds nominal and 130 milliseconds maximum [Choate, 1970 and Demeo, 1968]. A time constant-temperature change plot shows that 98.2 percent of a temperature change has been recorded in 10.4 feet of fall, 83 percent recorded in 5.2 feet of fall, 68 percent in two feet of fall and 35 percent in one foot of fall (Figure 24).

The thermistor, because of its finite size, has thermal inertia which causes it to act as a low pass filter. As a result, fine structure is lost or at best smoothed out. The original trace could be reconstructed if the filtering characteristics (of both phase and amplitude) of the thermistor were known. These could be obtained experimentally.

b. Data Handling

Present procedures for handling XBT data are indicated by the log sheets which accompany the XBT's in the shipping container. First, a BATHY or BAXBT message is required to be submitted to the appropriate addressee using a PRIORITY precedence message [National

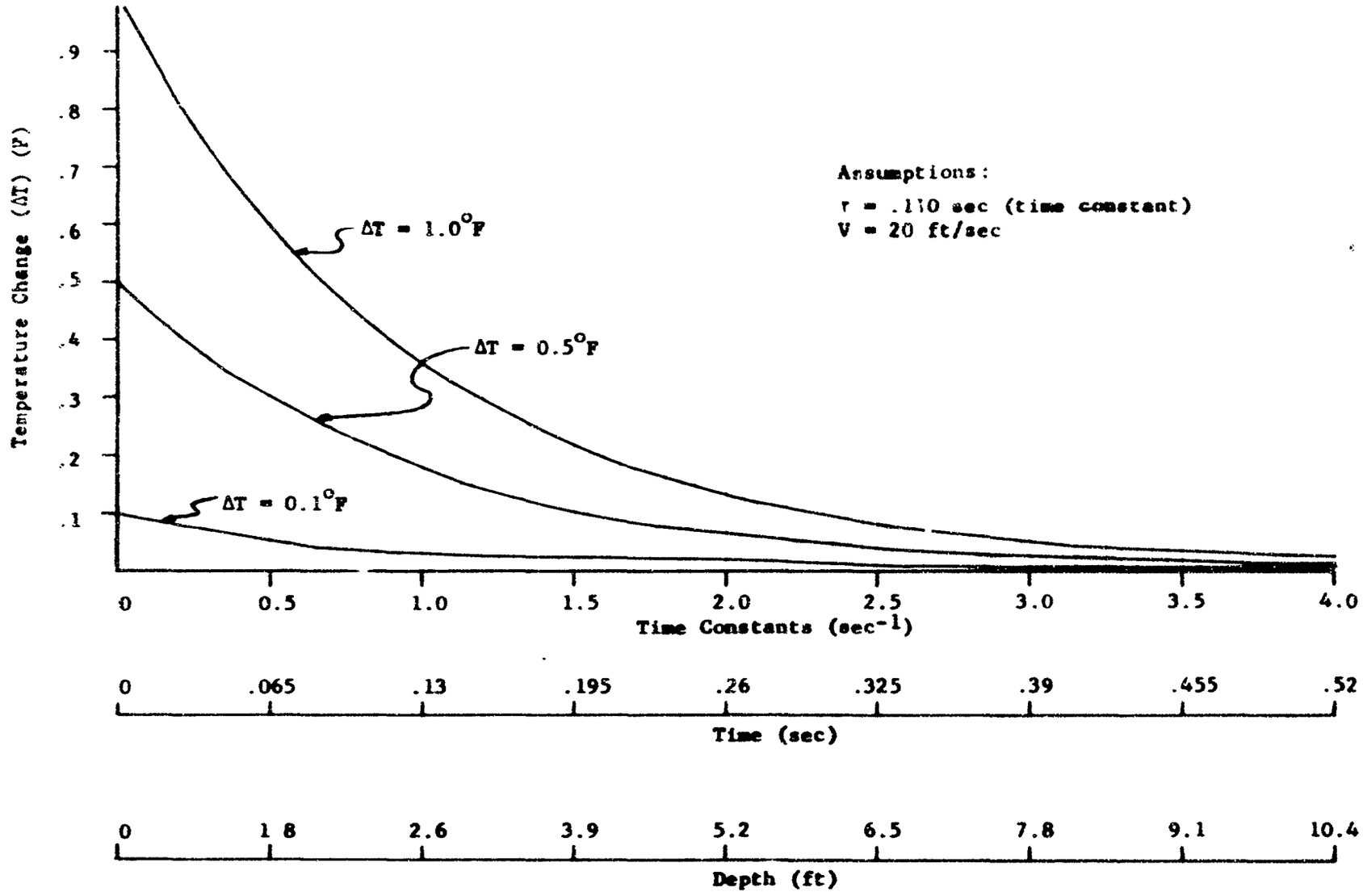

Figure 24. Temperature Change as Functions of Time, Time Constants, and Depth for Various Temperature Steps.

Oceanographic Data Center, 1968, 1968a]. Upon receipt of the BATHY or BAXBT message the receiving agency uses this as synoptic data for subjective ocean forecasts in his locality. The BATHY or BAXBT is forwarded through the Naval Environmental Data Network to FNWC in Monterey. FNWC uses the message reports to update its ocean fields for objective forecasting in various oceanographic and meteorological products.

Upon completion of a cruise the ship which took the XBT cast mails the original trace and log sheet to FNWC for digitizing. The original XBT trace is digitized for use by FNWC, and, when requested, the results of the digitizing are provided to the XBT submitting activity. Upon completion of digitizing, the original XBT traces are forwarded to the National Oceanographic Data Center (NODC) for storage in their archives. NODC also receives a copy of the digital data on tape.

Present procedures at FNWC use DIGITBT and several other specialized XBT data handling programs. New XBT digitized data are stacked on the XBT Master File (presently at a rate of about 500 traces per week).

B. OTHER SENSORS

Sensors for measuring microthermal structure, other than those discussed elsewhere in this thesis, are numerous.

From a fixed platform, like the NEL Oceanographic Tower, thermistor strings and arrays are used. Bottom devices, such as thermistors, attached to the shore or a tower by a wire, have been employed to give continuous temperature records.

From submarines, thermopiles, thermocouples, thermistors, platinum resistance thermometers, and thin film thermometers have been employed. Almost any oceanographic electronic or mechanical thermometer could be used on a submarine.

C. DIGITIZING PROCEDURES

At the present time, all XBT traces are submitted to Fleet Numerical Weather Central (FNWC) in Monterey, California, the only digitizing center for these strip chart analogue traces [National Oceanographic Data Center, 1968, 1968a; and Bauer, 1969].

At the Point Pinos Annex of FNWC, two Calma Model 480 flat-bed digital recorders are used to digitize XBT traces in 0.01 inch increments. These digital recorders are operated in a mode which makes the recorded intervals dependent on the tracing speed. The Calma output recorded on digital magnetic tape containing binary mode characters at a density of 556 bits per inch (BPI) with even parity and variable length records.

FNWC program DIGITBT, written by Lieutenant N. L. Perkins, USN, in FORTRAN IV for FNWC's CDC 6500 computer, is used currently for the reduction of data from XBT traces. FNWC tape input, tape output, and some other subroutines of DIGITBT are written in COMPASS language. In order to analyze microthermal structure, DIGITBT was extensively modified. The new program, referred to as MICROXBT, is included as Appendix A. The basic procedures for DIGITBT and MICROXBT programs are the same.

DIGITBT and MICROXBT programs both convert the X and Y measurements of the digitizer into depth (X) versus temperature (Y) values.

Corrections are made for nonlinearities produced by the XBT recorder in both the depth and temperature directions. All shipboard XBT recorders are assumed to produce error-free traces. The 62.0F temperature line drawn on the trace when the probe is loaded is used as a baseline for digitizing. No correction is made if this baseline temperature line is not the same as the 62.0F line printed on the trace paper. An eye-interpolated value of the XBT-drawn baseline temperature on the printed temperature grid is noted as a part of the identification record.

The rigid procedures for digitizing require that exactly one identification (ID) record and two digitized trace records for each XBT be recorded on the tape. The ID record information contains the data (day, month, year); time (hour and minute); latitude and longitude (degree, minute, hemisphere); baseline temperature (to nearest 0.1C or 0.1F depending on the grid type); printed-grid type; and maximum depth for the probe (coded as 15 for 1500 ft XBT or 25 for the 2500 ft XBT). Each trace record contains pairs of increments (ΔX, ΔY) read from the baseline to the true surface temperature, a point "flag" and then pairs of values (ΔX, ΔY) along the trace to a cut-off depth. Each trace is digitized twice. The complete procedure is described by Bauer [1969].

To process digitized XBT data using the DIGITBT program, the two trace records are compared point-by-point in a deviation test. If the X and Y paired values (i.e., depth and temperature) differ by more than 0.035 inches, DIGITBT rejects the whole XBT record and the XBT trace must be completely re-digitized. If the XBT record passes the deviation test,

Temperature units are converted from digitized inches to F by a temperature table and from F to C by formula. These depth and temperature tables were constructed to account for the nonlinearities between the recorder and the actual trace. Values of depth are rounded to the nearest m and temperature to the nearest 0.01C in DIGITBT. MICROXBT has eliminated the ft to m and F to C conversions. Depths are rounded to the nearest 0.1 ft and temperature to the nearest 0.001F.

After the conversion from ft to the nearest m, DIGITBT removes, for a second time, any of the rounded-off values which are nonlinear between two neighboring points. If depth values appear as duplicates, one value is omitted in the output listing. In MICROXBT, there are no duplicate values because 0.1 ft in depth is well beyond the hundredth of an inch digitizing capability of the digitizer. Thus, by reading depths in tenths of a ft and temperature in thousandths of a degree F, MICROXBT looses no values from duplicate depths, and the possibility of introducing false linearities is reduced considerably. For these reasons, MICROXBT gives a much finer digitized record than DIGITBT.

The DIGITBT output tape is written in binary for the CDC 6500; the MICROXBT output tape is written for the IBM 360/67 at the Naval Postgraduate School (NPS). Appendix C contains the job control cards (JCL) required for using a CDC 6500 output tape from MICROXBT with external BCD at a density of 556 BPI as in input to a separate microthermal analysis program at NPS.

IV. MODELS FOR EXAMINING MICROTHERMAL STRUCTURE

All models and methods used in this thesis required the output tape from MICROXBT to be used as a direct input on the seven channel tape unit. The XBT ID record information was read first and if the recorded XBT was from a desired geographical region the data (depth and temperature) were analyzed for microthermal structure at NPS.

A "best" value for the temperature structure was found by using the depth inflection points from MICROXBT. For this "best" array, temperature was linearily interpolated to a value for every foot of depth. The mixed layer depth (MLD) was determined, using inflection points from MICROXBT, as that depth immediately above the depth where the temperature was 2.0F different from that at the surface [Naval Weather Service, 1967].

Several microstructure models were tried in order to perform an objective analysis of the oceanic microthermal structure. The use of a numerical temperature derivative model was found to give the most satisfactory presentation of the microthermal structure.

A. DERIVATIVE MODEL

1. Mathematical Model

The most significant feature of the thermal structure is the thermal gradient defined as the derivative of the temperature with respect to depth (dT/dZ). By plotting the gradient versus depth (Z), the thermal structure of the water column is emphasized. Furthermore, a parameter such as the thermal gradient is related to stability, entrophy generation, turbulent heat transport, and the Brunt-Väisälä frequency [Ref. 19].

2. Experimental Methods

There are two methods for experimentally determining the thermal gradient presently in use.

a. Electronic

A resistance thermometer in an electronic bridge passing through water produces a signal which is proportional to temperature as a function of time. By differentiating this signal with respect to time (which is analogous to differentiating with respect to distance), the values of gradient versus distance the probe travels are found.

This method was successfully employed by Grant, Moillet and Vogel [1968], in the horizontal direction for temperature and turbulence measurements. A thin-film resistance thermometer, mounted on the bow of a submarine, measured temperature versus horizontal distance traveled. The time derivative was taken to produce a direct plot of dT/dX, the horizontal thermal gradients.

Osborn [1969] used a thermistor, capacitively coupled to two differentiating amplifiers, to measure the vertical temperature gradient with his free-falling gradiometers. His resulting output (Figure 13) shows a gradient versus depth record for the North Pacific off the San Diego Trough.

b. Two-probe System

Temperature gradients may be found by using two vertically spaced thermistors. The temperature difference is a measure of the mean gradient between them. Such a gradient-meter was used by Woods [1968, 1968a] who obtained gradient at various depths (Figures 7, 8, and 9). This method is limited to the resolving power of the thermistors and is a function of thermistor spacing.

3. Numerical

The numerical method is based on the derivative, dT/dZ, for the gradient but uses the finite difference approximation. The derivative of the temperature at any depth $T(Z_i)$ with respect to depth Z is defined as:

$$\frac{dT}{dZ} = \lim_{Z_i \to Z} \frac{T(Z_i) - T(Z)}{Z_i - Z} \tag{5}$$

which can be shown to equal:

$$\frac{dT}{dZ} = \lim_{\Delta Z \to 0} \frac{\Delta T}{\Delta Z} = \lim_{\Delta Z \to 0} \frac{T(Z + \Delta Z) - T(Z)}{\Delta Z}. \tag{6}$$

For this thesis, $\Delta Z = 1$ foot, which yields the finite difference approximation for the vertical temperature derivative:

$$\frac{dT}{dZ} \approx \Delta T. \tag{7}$$

B. MISCELLANEOUS METHODS

1. Statistical Bias and Variance

For this method, a standard or smooth curve was required. Several standard curves were investigated. The variance and bias were calculated between the standard and the "best" curves. The standard was found by computing the temperature values for a series of specified depths.

The first standard curve investigated used MLD and the FNWC significant levels (surface, 100, 200, 300, 400, 600, 800, and 1200 ft). The temperature values were found using the "best" temperature values at those depths. Next, an array of temperature values was found at foot increments by linear interpolation between the temperature values at the significant levels or the MLD. This was designated the FNWC significant

level curve. Calculations of bias and variance did not reveal any correlation with the microthermal structure easily visible on the XBT trace.

The second standard curve investigated used the temperatures at the standard oceanographic station depths (surface, 10, 20, 30, 50, 70, 100, 150, 200, 250, 300, 400, 500, and 800 m). Since these depths are metric, a linear interpolation was done between the two neighboring values on the "best" curve. Values of temperature for every foot were found by linear interpolations between the standard depth temperature values. Again, no significant correlation was found.

The third standard curve used these standard depth temperature values but used these standard depth values as an input to the LGINTP subroutine [Denner, 1969]. This subroutine uses the four standard depth points neighboring the depth in question to make an "average" curve from an upward and downward parabolic interpolation and a linear interpolation. This scheme produces a smoothing of points on the curve. This technique is usually used for interpolating standard depth oceanographic data [Rattray, 1965]. These values, after computing the bias and variance, again gave no correlation with the microthermal structure.

The LGINTP subroutine was not used with the FNWC significant level values for smoothing since the FNWC fields assume linear interpolation.

Other standards considered, but not investigated, included a Gaussian standard, using the technique for approximating the temperature structure proposed by Grosfils [1968] and an exponential standard.

2. Gradient Distribution Method

For investigating the temperature structure, the "best" temperature data were separated into the FNWC significant levels. For each

significant level, the temperature change from one depth to the next were calculated and then sorted in numerical ascending order with the IBM subroutine SHSORT. With these values of temperature change per foot or gradient (F/ft), the temperature structure was now characterized by the individual thermal gradient values and a total temperature change ΔT. Because of the range of temperature values in the thermocline, this region of the XBT trace was chosen for developing this method.

The capabilities of the XBT indicate a gradient interval of 0.02 F/ft is easily obtained with a high degree of confidence [Arthur D. Little, 1966]. Using 0.02 F/ft for the class interval, the frequency distribution of gradients was plotted for various XBT traces by significant levels. As expected, the greatest range in gradient values usually occurred in the significant level just below the mixed layer where the range of temperature values ΔT was the greatest.

This method appears to give a good indication of the variability of the thermal structure in the depth intervals investigated. Several examples of the different types of gradient distributions, using histograms and a cumulative frequency diagram, are shown in Figures 25 through 31. The actual analyzed XBT is also shown on the left of each figure. Looking at data off San Diego, the first three gradient distribution diagrams (Figures 25, 26 and 27) show fairly similar cumulative frequency distributions. The next two (Figures 28 and 29) show nearly identical distributions for water inside the Gulf Stream. The next two gradient distributions (Figures 30 and 31) show water in the Gulf Stream's frontal region. These last two distributions are not identical for many reasons, but mainly because the positive gradient region in the second example is below the [illegible] foot interval shown in the gradient

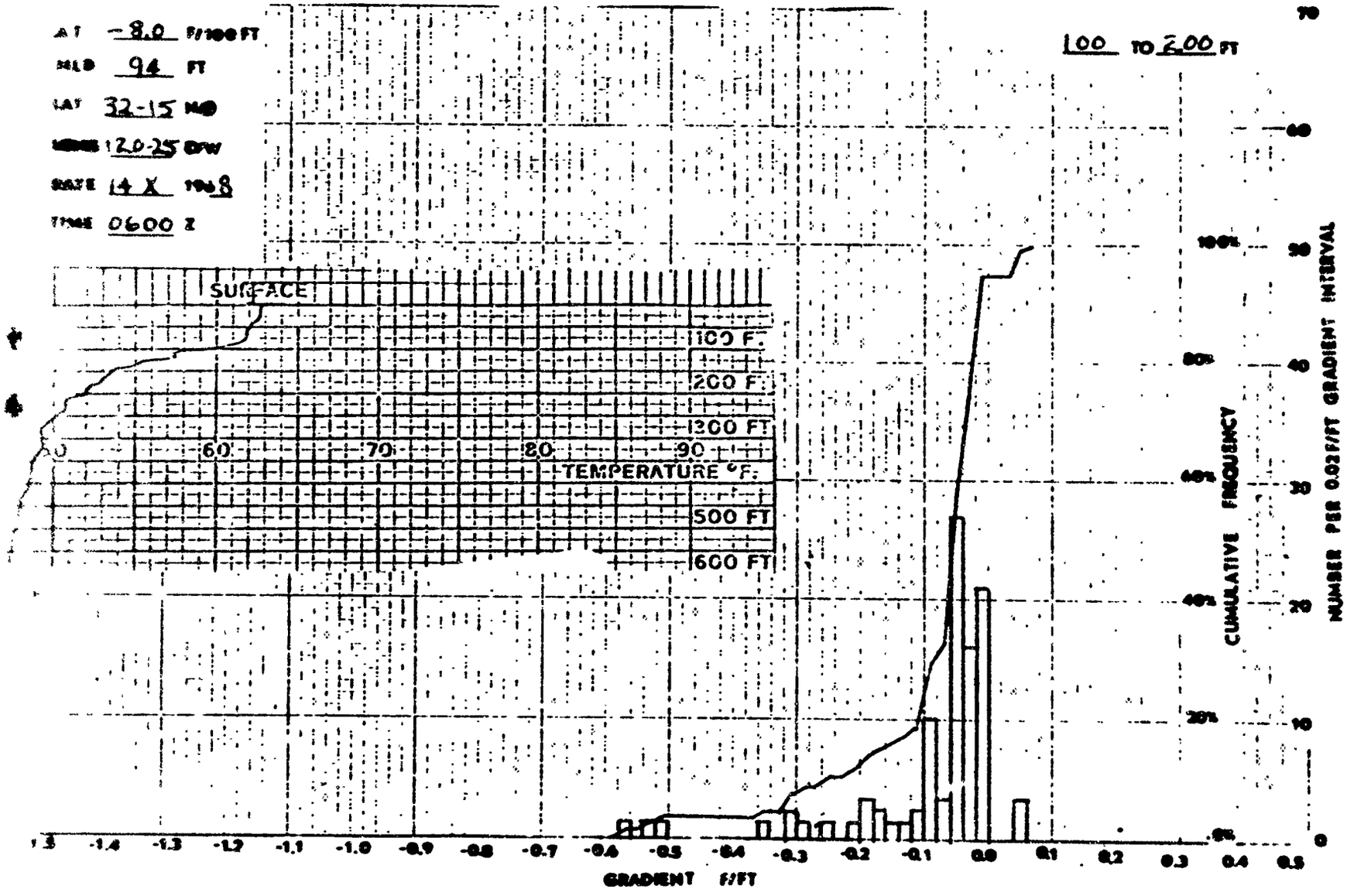

Figure 25. Gradient Distribution for the 100 to 200 Foot Interval for a Location 100 nm West of San Diego.

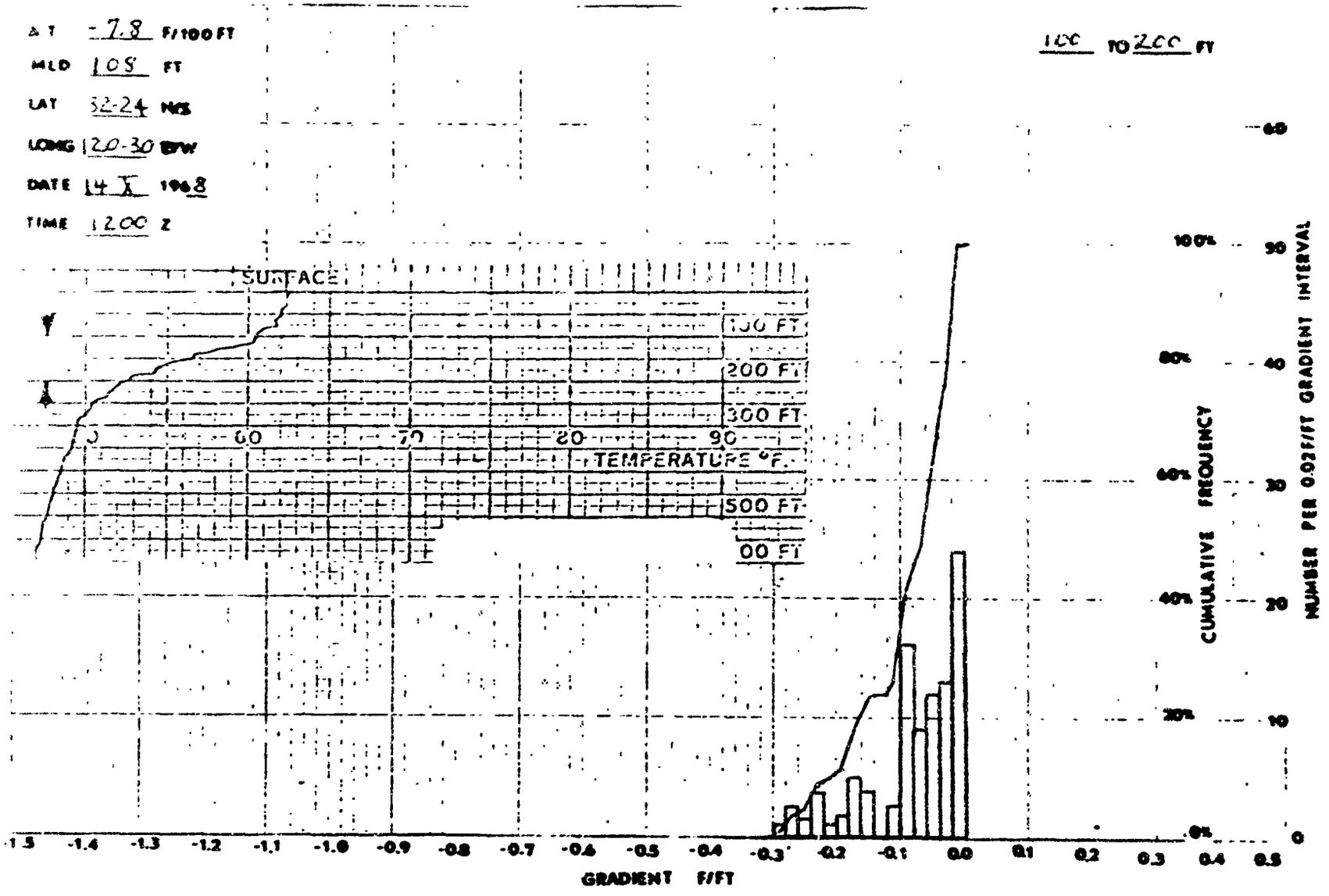

Figure 26. Gradient Distribution for the 100 to 200 Foot Interval for a Location 100 nm west of San Diego.

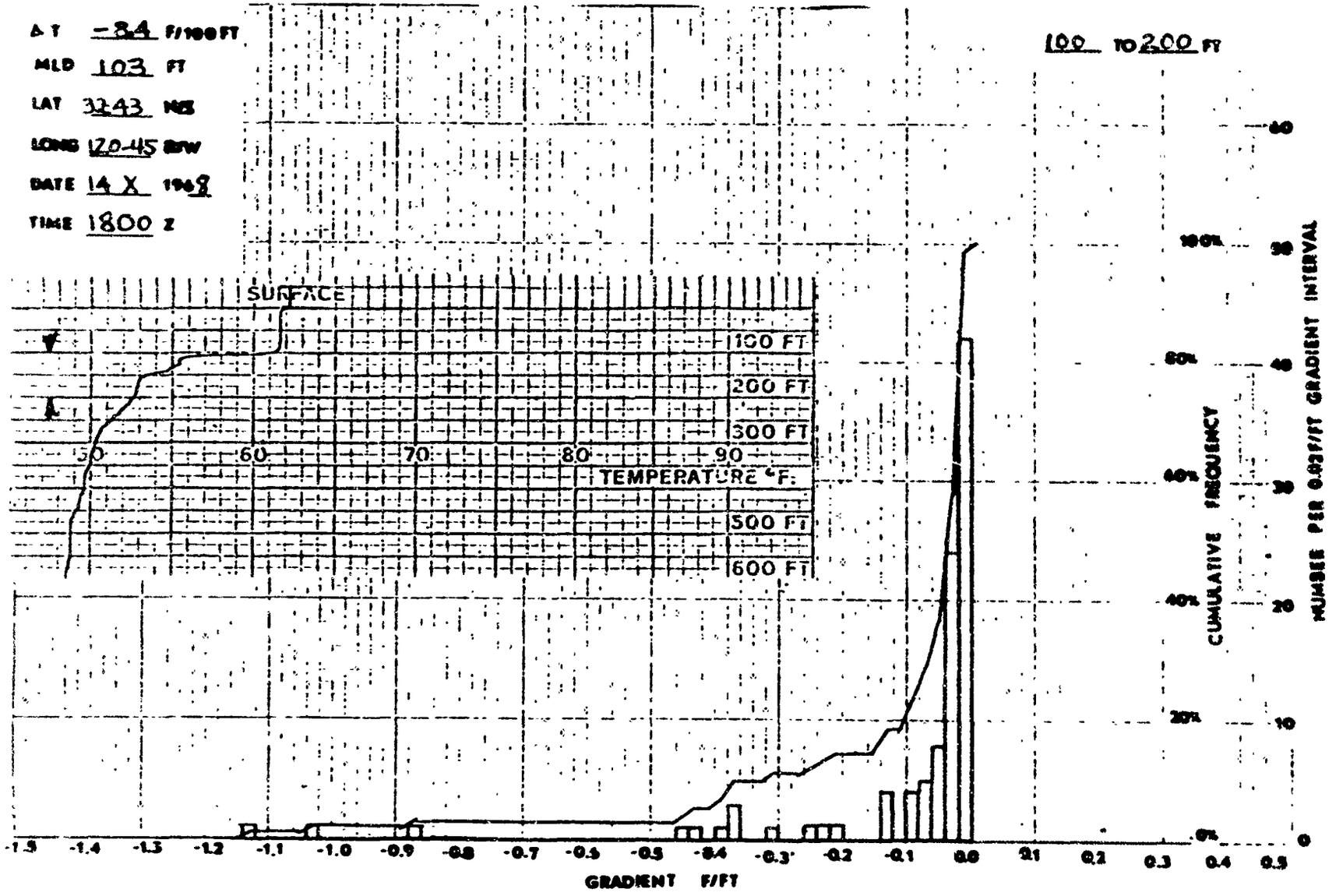

Figure 27. Gradient Distribution for the 100 to 200 Foot Interval for a Location 100 nm west of San Diego.

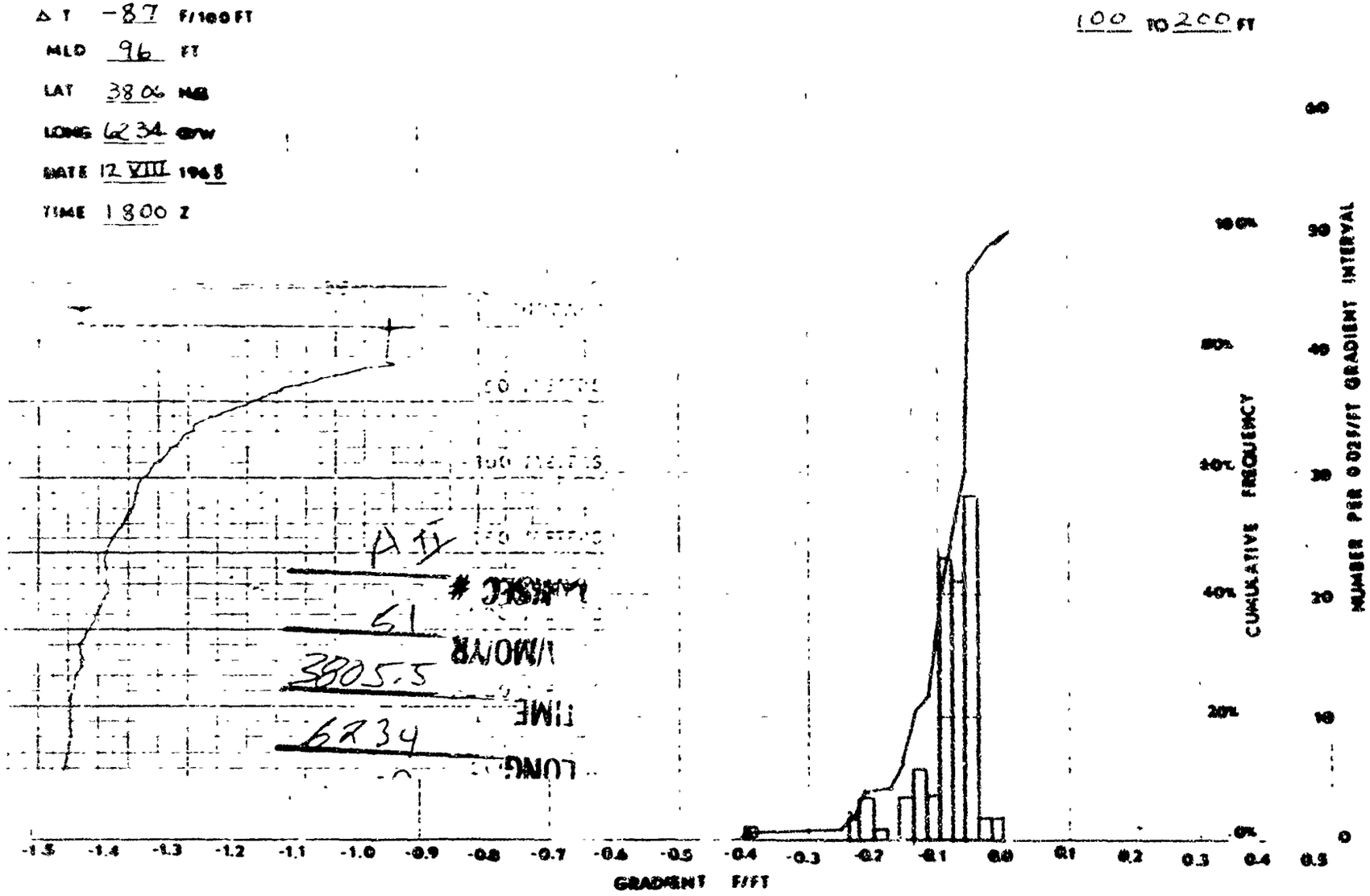

Figure 28. Gradient Distribution for the 100 to 200 Foot Interval for Water Inside the Gulf Stream.

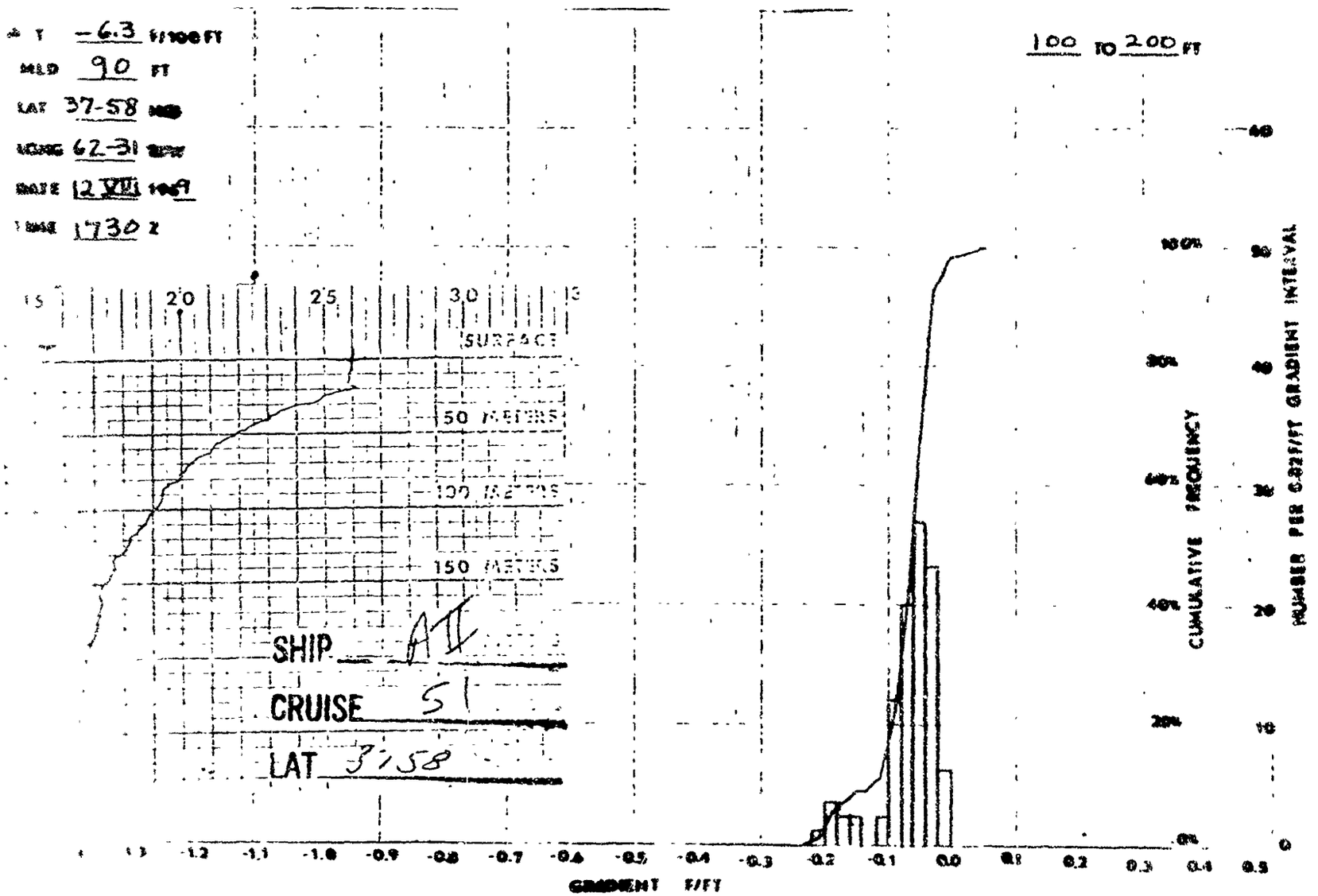

Gradient Distribution for the 100 to 200 Foot Interval for Water Inside the Gulf Stream.

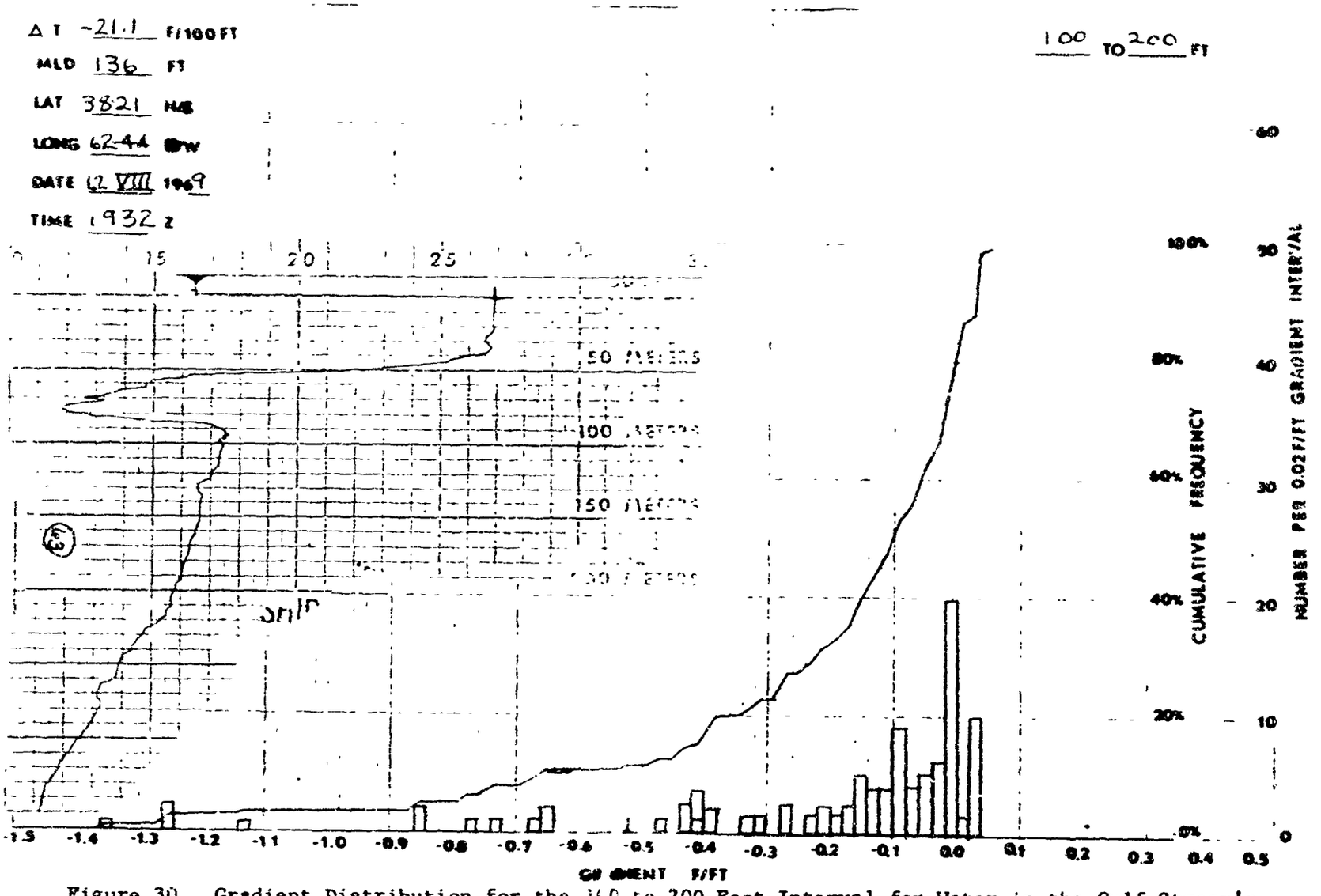

Figure 30. Gradient Distribution for the 100 to 200 Foot Interval for Water in the Gulf Stream's North Wall.

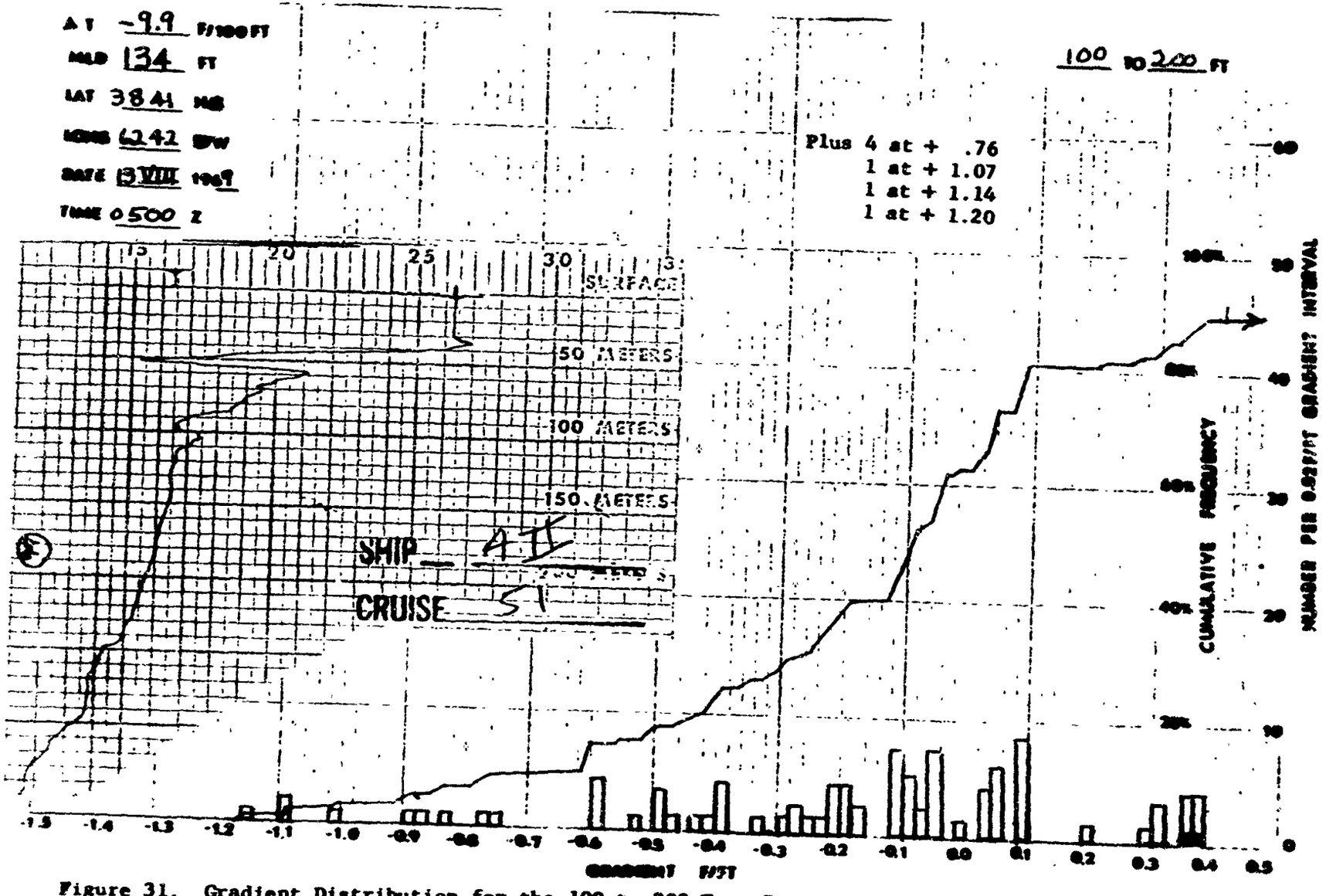

Figure 31. Gradient Distribution for the 100 to 200 Foot Interval for Water in the Gulf Stream's North Wall.

distribution plot. These results indicate that the small scale structure may be water mass related. However, this could not be fully examined in the time alloted for this thesis but is recommended for further investigation.

V. APPLICATION OF NUMERICAL DERIVATIVE MODEL

This chapter describes the application of the numerical derivative model or method (NDM) to several cases of real and assumed data.

A. BASIC CASES

Graphs are used to show the features of the NDM. For each station, temperature versus depth (T-Z) and temperature gradient versus depth (G-Z) plots were drawn by a CalComp plotter using the computer program with the DRAW subroutine in Appendix B. The scales are constant for all plots. The grid squares were drawn for 100-ft depth increments from the surface to a depth of 900 ft. On the T-Z plots (reporduced digitized XBT data), temperature was scaled at 10F per grid line. On the G-Z plots, the gradient was scaled to 0.1F/ft per grid interval, with the axis offset so that two-thirds of the plot was allocated to negative gradients. This scaling was chosen so that each hundredth of an inch, the resolving power of the CalComp plotter, represented one foot of depth and 0.01F of temperature or 0.001F/ft of temperature gradient. The plots included here have been reduced in size, but the relative proportions remain the same.

1. Linear Gradients

For a temperature distribution with linear thermal gradients, the G-Z plot is characterized by steps indicating a constant gradient during a temperature change. For this thesis the strength of a gradient is defined as the absolute value of the gradient (in F/ft units) and is described as strong when greater than 0.3F/ft or weak when less than 0.05F/ft. The term signed strength is defined as the true gradient

value and will thus distinguish absolute and true gradient values. The magnitude of a gradient is defined as the vertical extent of the gradient measured in feet. The product of magnitude and signed strength gives the total temperature change for the extent of the gradient.

a. Layer Structure

Figure 32 shows a two-layer temperature structure model with a T-Z plot on the left and a G-Z plot on the right. The strength of the upper layer is 0.05F/ft with a magnitude of 200 ft. The lower layer is weaker (0.02F/ft compared to 0.05F/ft) than the upper step but the magnitude is greater (600 ft to 200 ft).

For the multi-layered model (Figure 33) several linear gradient steps are shown. In the gradient region between 70 and 90 ft, the gradient is strong and goes off scale (Figure 33b).

b. Step Structure

A step structure is characterized by thin strong gradient regions The model (Figure 34) shows clearly that the four steps between 60 and 100 ft are stronger than any other steps shown. These four steps also have the smallest magnitude (five ft) in the figure. The steps at 200, 300, and 400 ft all have the same strength but increase in magnitude with depth.

The features of the T-Z trace (Figure 34a) are easily described by the G-Z model. The product of signed strength and magnitude gives the total temperature change from the surface temperature to a given depth for a step-structure temperature profile. The temperature at any depth could then be found if the sea surface temperature was known. Thus, with magnitude, signed strength and sea surface temperature, any layered or stepped thermal profile could be reconstructed.

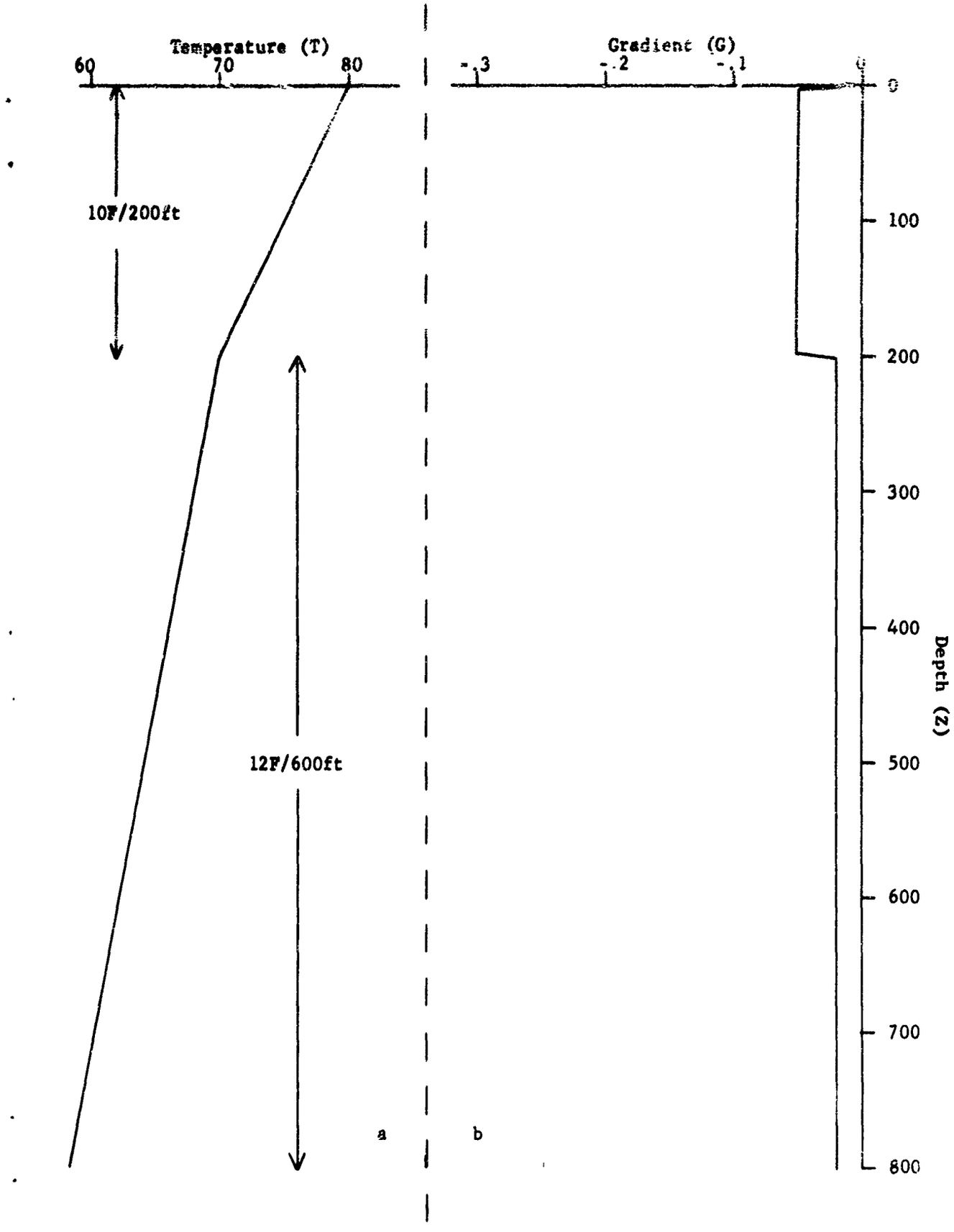

Figure 32. Two-Layer Model.

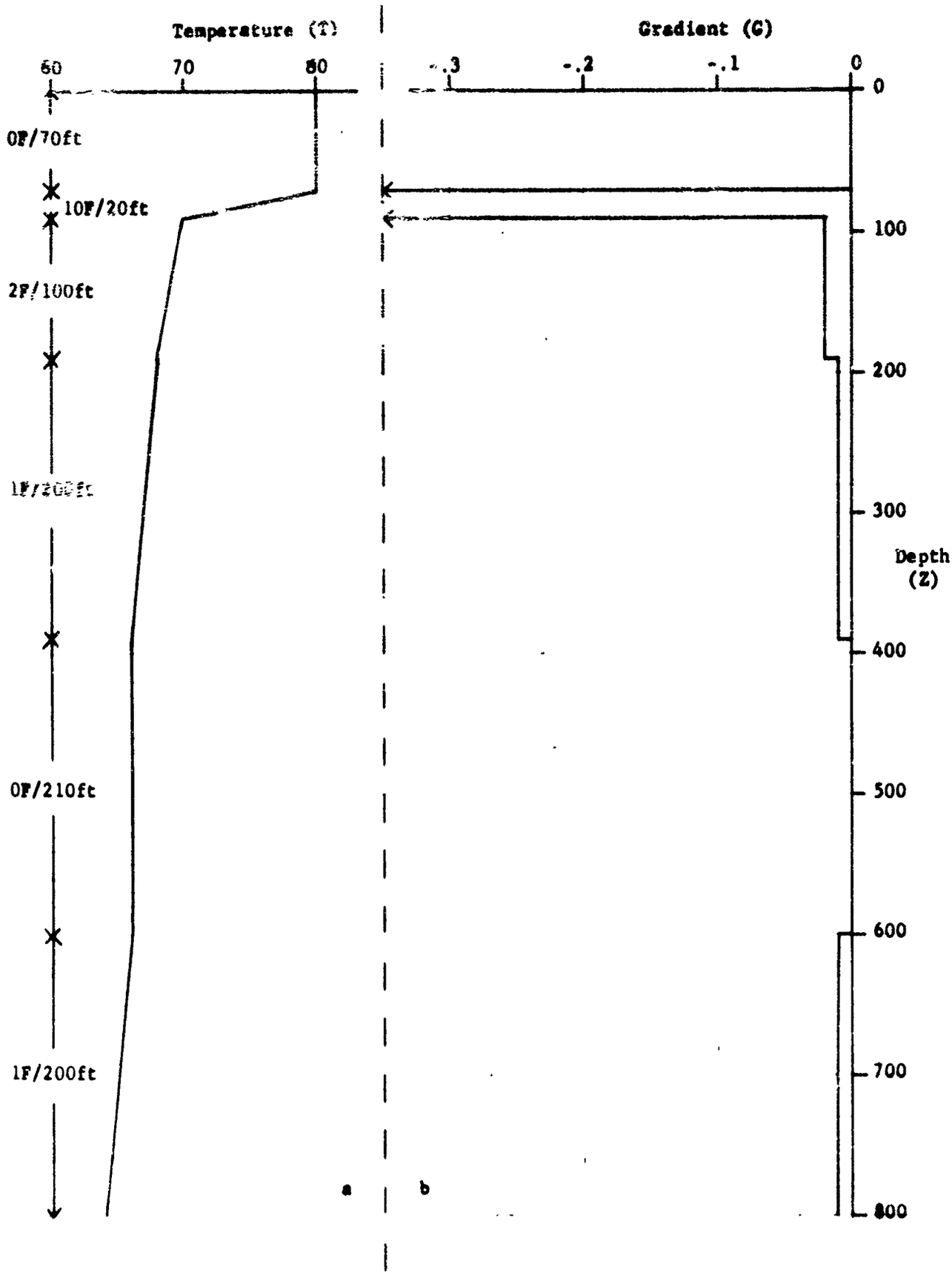

Figure 33. Multilayer Model.

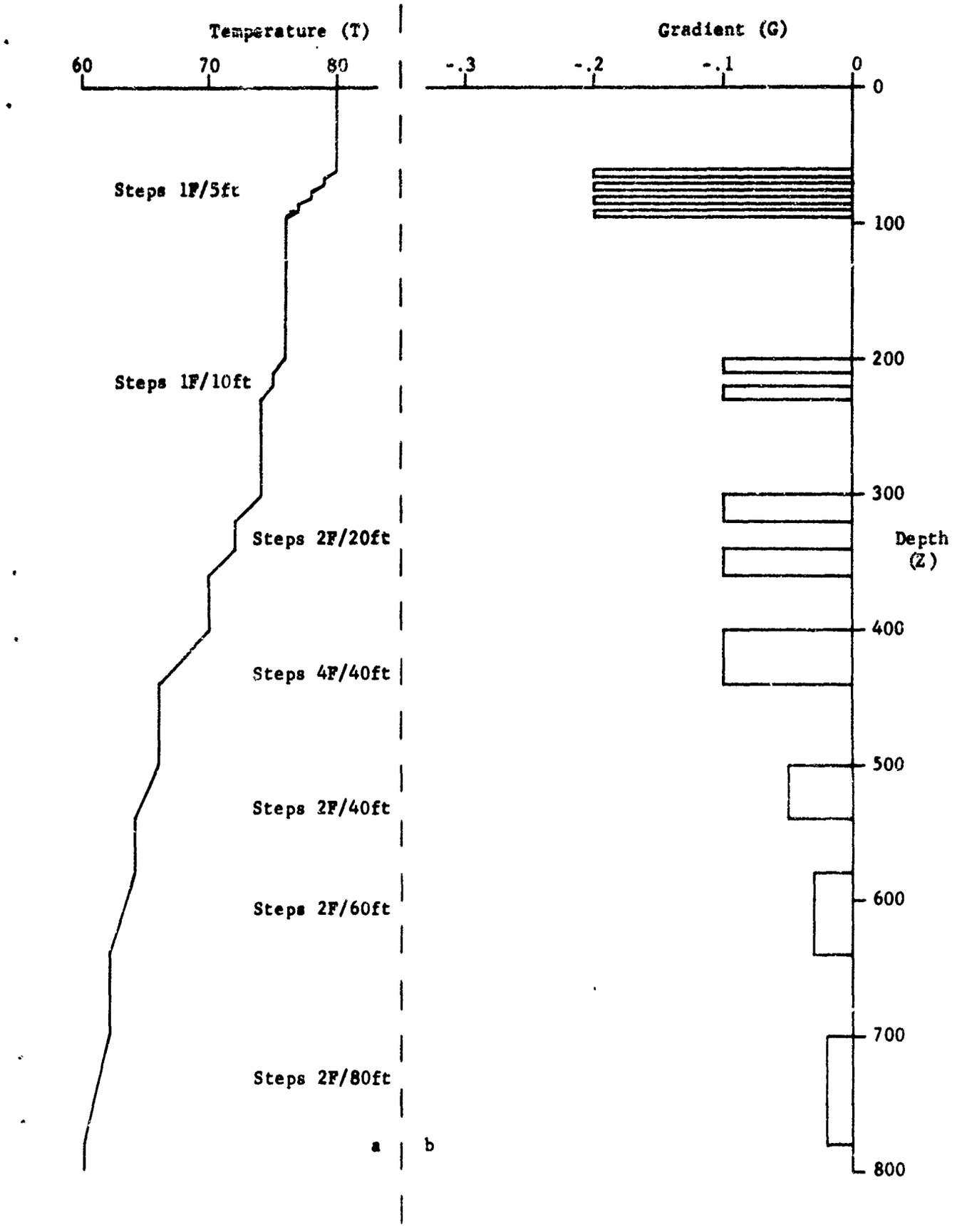

Figure 34. Step Structure Model.

2. Continuous Curving Gradients

Since finite values are used for both depth and temperature, a truly continuous curve cannot be drawn. The spacing by the CalComp plotter of every hundredth of an inch can cause variations of this size. Computed values of depth, temperature and temperature gradient were provided as inputs to a CalComp plotter at every hundredth of an inch to create a quasi-continuous curve, at least to a resolution of the plotter. It is this quasi-continuous field which accounts for the 0.01 inch steps encountered in curves drawn by the plotter for any truly continuous curve. This effect is also present whenever the plotter is drawing any line not directly in the X or Y axis directions. Accordingly, any steps shown of this size could be considered as possible adjustments made by the plotter or data to adjust to the hundredth of an inch grid.

Two examples of continuous gradients are given to show the resulting distributions of gradient with respect to depth.

a. Gaussian

An example of a Gaussian profile (Figure 35) shows a normal distribution of temperature with depth for the function, like

$$T(Z) = 80 - \frac{20}{\sqrt{2\pi}} \int_{-\infty}^{Z} e^{-\frac{1}{2}x^2} dx \qquad (8)$$

where: x = a dummy variable

80 = sea surface temperature.

The G-Z curve highlights the changes in the T-Z curve. The increase in gradient strength is very clear, reaching a maximum 200 feet, whereas the inflection point of the T-Z plot is difficult to find by visual inspection. The summation of signed strength values at every foot of

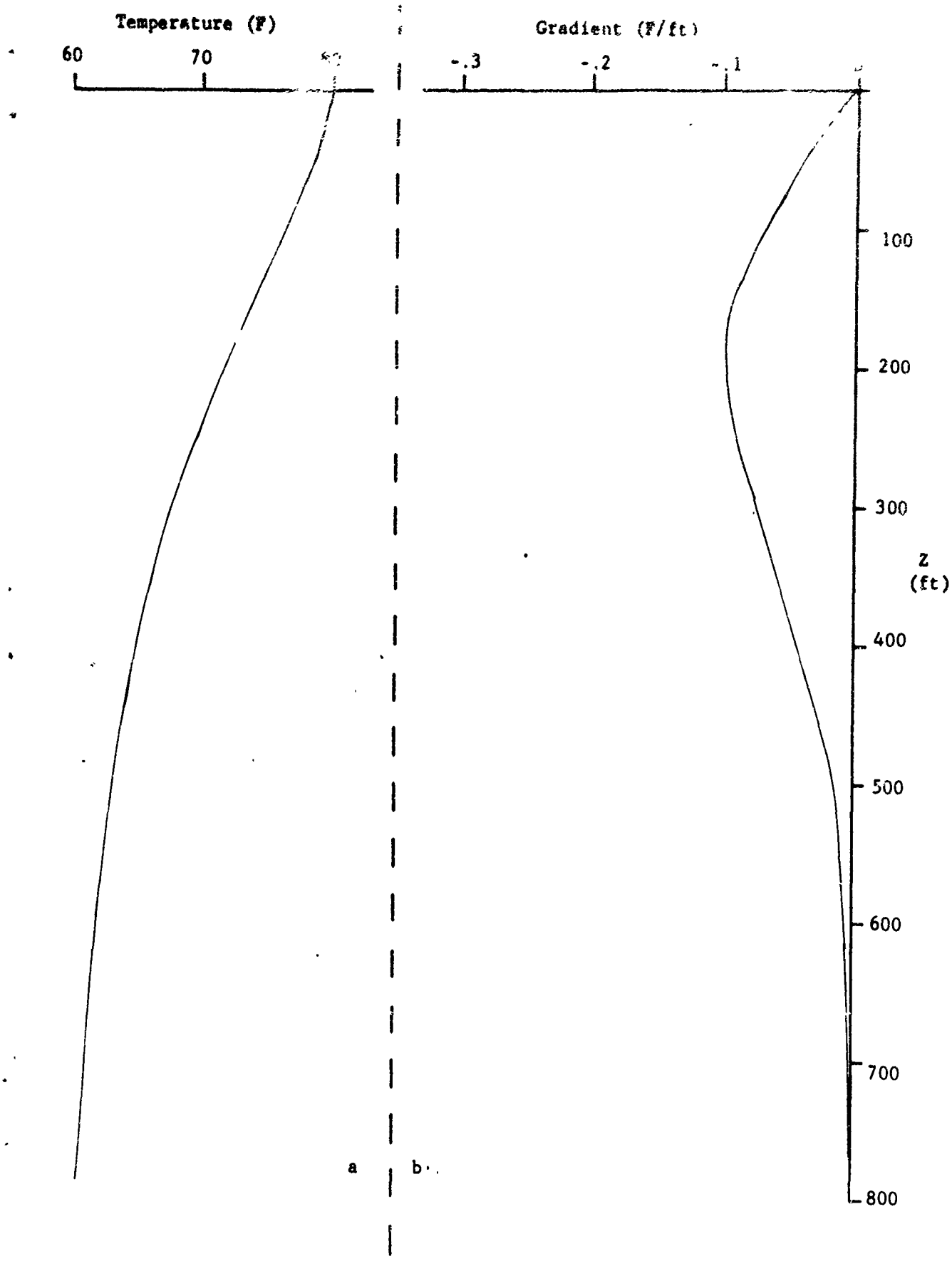

Figure 35. Gaussian Model.

depth from the surface down gives a total temperature change which is analogous to the product of magnitude and signed strength with all magnitudes set equal to one. With this summation and a given sea surface temperature (SST), a continuous temperature profile can be reconstructed.

b. Exponential

Using an exponential expression for the temperature distribution

$$T(Z) = 60 - 20e^{-\pi Z/1000} \tag{9}$$

where:

$$60 = SST,$$

the T-Z (Figure 36a) and G-Z curves (Figure 36b) appear as compliments of each other. The derivative of T(Z) with respect to Z gives:

$$\frac{dT(Z)}{dZ} = \frac{\pi e}{50}^{-\pi Z/1000} \tag{10}$$

which is the equation of the G-Z plot.

3 Superpositions

In the example of layers superimposed on an exponential model (Figure 37), the conditions for the exponential (9) hold for the depth intervals: surface to 40 ft, 220 to 340 ft and 460 to 800 ft, with various layers at the remaining depths. Isothermal layers exist below the weak surface exponential gradient layer and also in the 140 to 180 ft depth layer. From the T-Z plot, the layers at 340 and 400 ft are not as evident as they are in the G-Z plot.

4. Inversions

A model with two inversions and several linear steps (Figure 38) shows the positive gradient regions clearly. The second deeper inversion is clearly a weak gradient, but it is still discernible in Figure 38b.

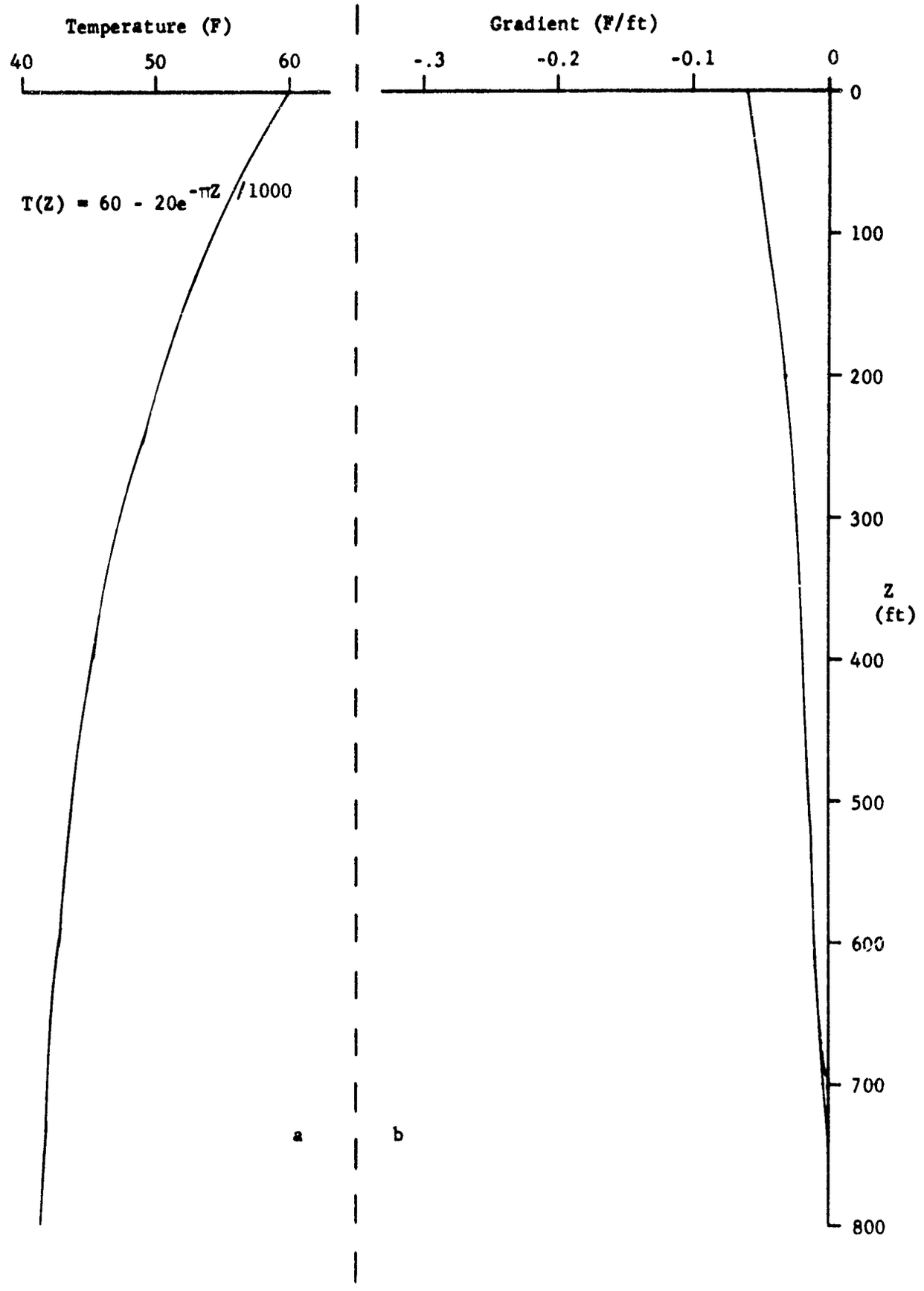

Figure 36. Exponential Model.

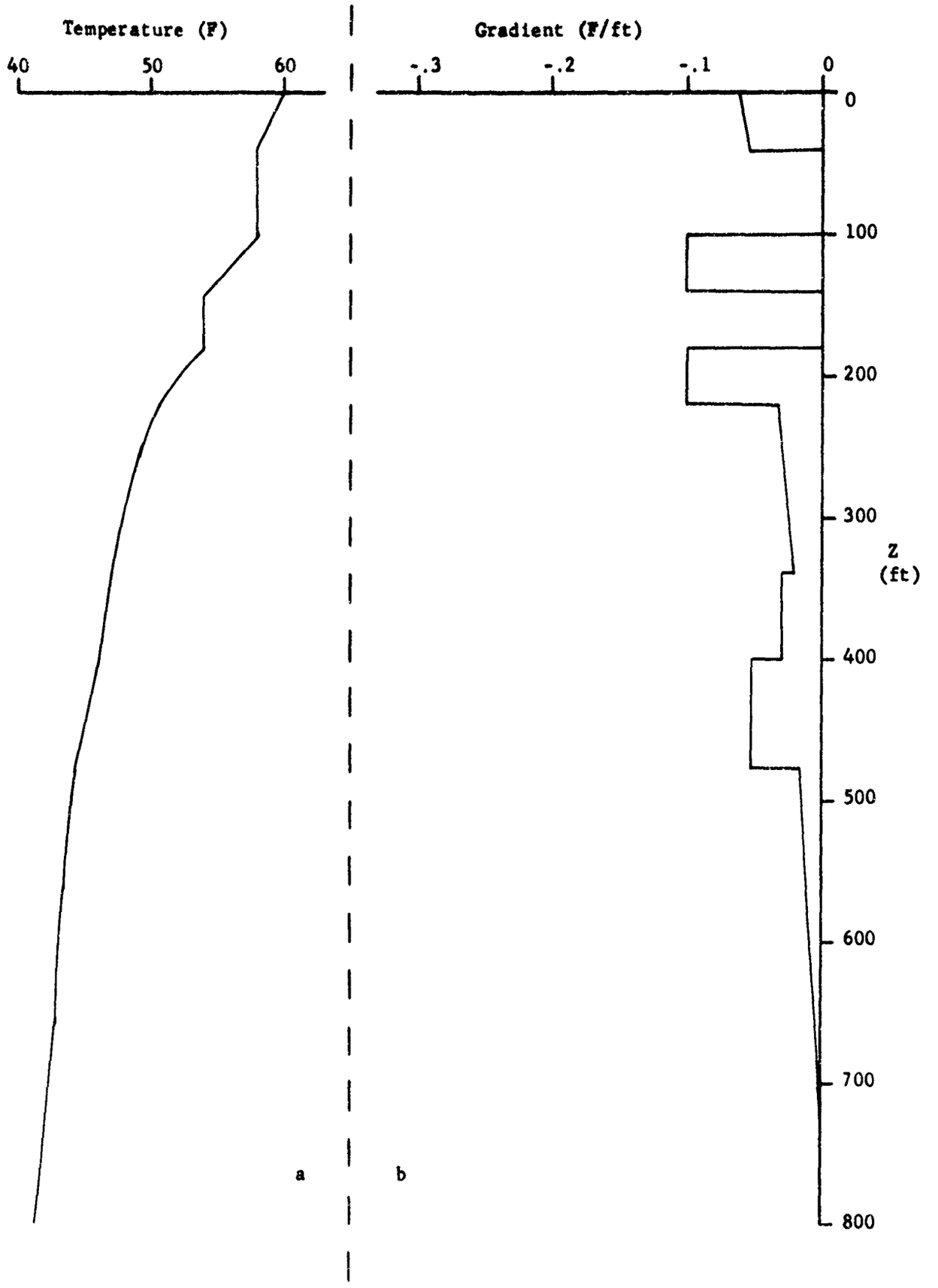

Figure 37. Exponential Model with Layers Superimposed.

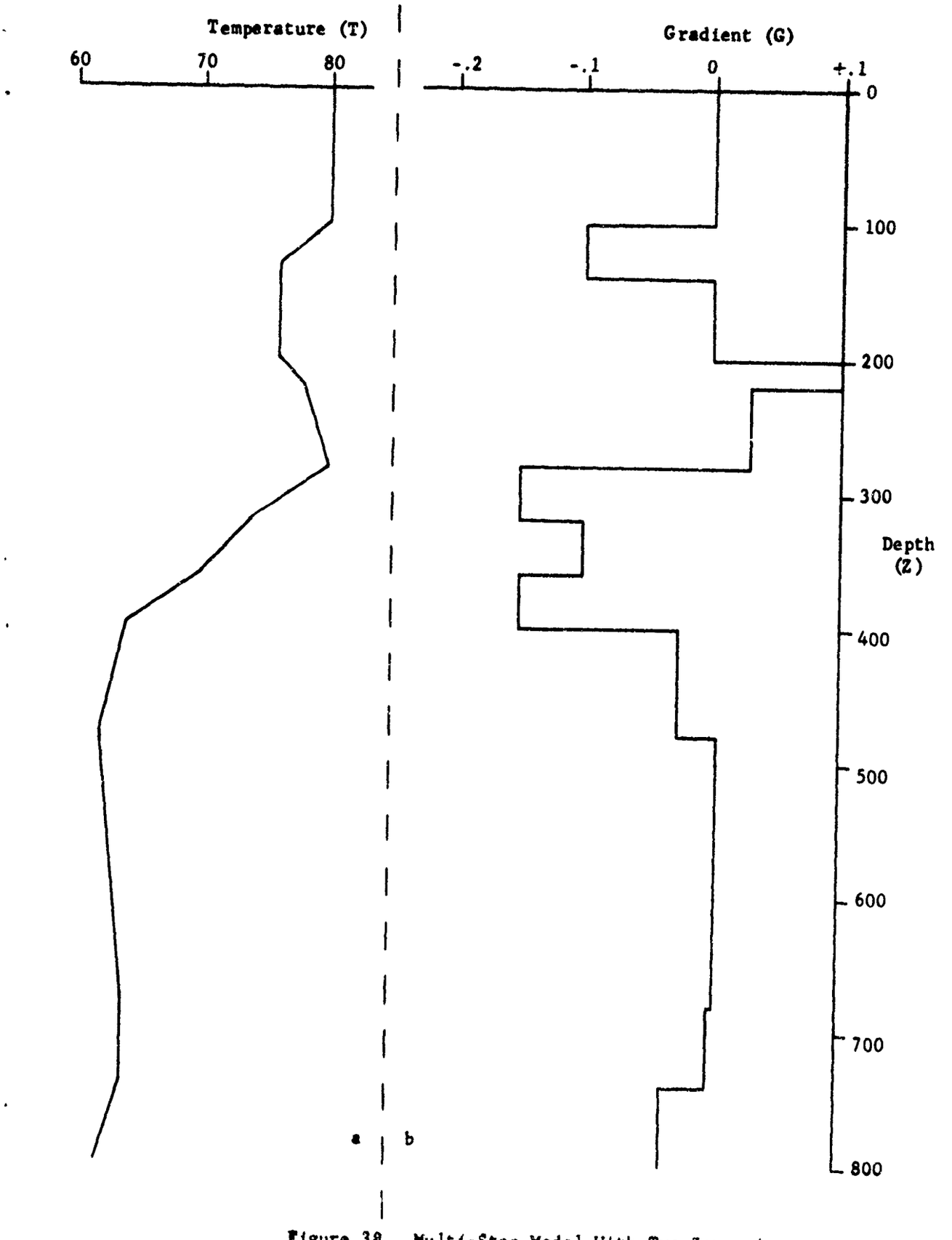

Figure 38. Multi-Step Model With Two Inversions

With inversions, summing the signed strength values for each foot gives the temperature change from the surface and adding this value to SST yields the actual temperature at any depth.

B. OBSERVATIONAL CASES

Several different oceanic regions were selected to establish features of this model. The oceanic regions explored were along the Atlantic Coast, in the Andaman Sea, Eastern North Pacific, and the Gulf Stream.

1. Atlantic Coastal Region

Stations in Massachusetts Bay occupied during December 1969 were used. The stations were within a radius of 13 miles. Water depths were between 280 and 420 feet. Lack of strong gradients in all seven traces shows that the water was probably well mixed (Figures 39 through 42). A positively signed strength in the upper 300 feet was common in the traces. Inversions (Figure 40) are quite clear in both the T-Z and G-Z plots. A portion of the actual XBT trace is shown for three of the stations. In these three cases, there is excellent visible correlation between the actual XBT trace and the reconstituted T-Z plots which shows that MICROXBT can resolve very small temperature features. In no case was there an isothermal layer greater than 140 feet thick.

2. Andaman Sea

In the Andaman Sea, near the Straits of Maalacca, a series of 15 XBT stations from the 18 to 20 July 1969 period were used. The stations were within a radius of 12 miles. Water depths varied between 290 and 380 feet. This oceanic region could be considered somewhat similar to the Atlantic Coastal region above.

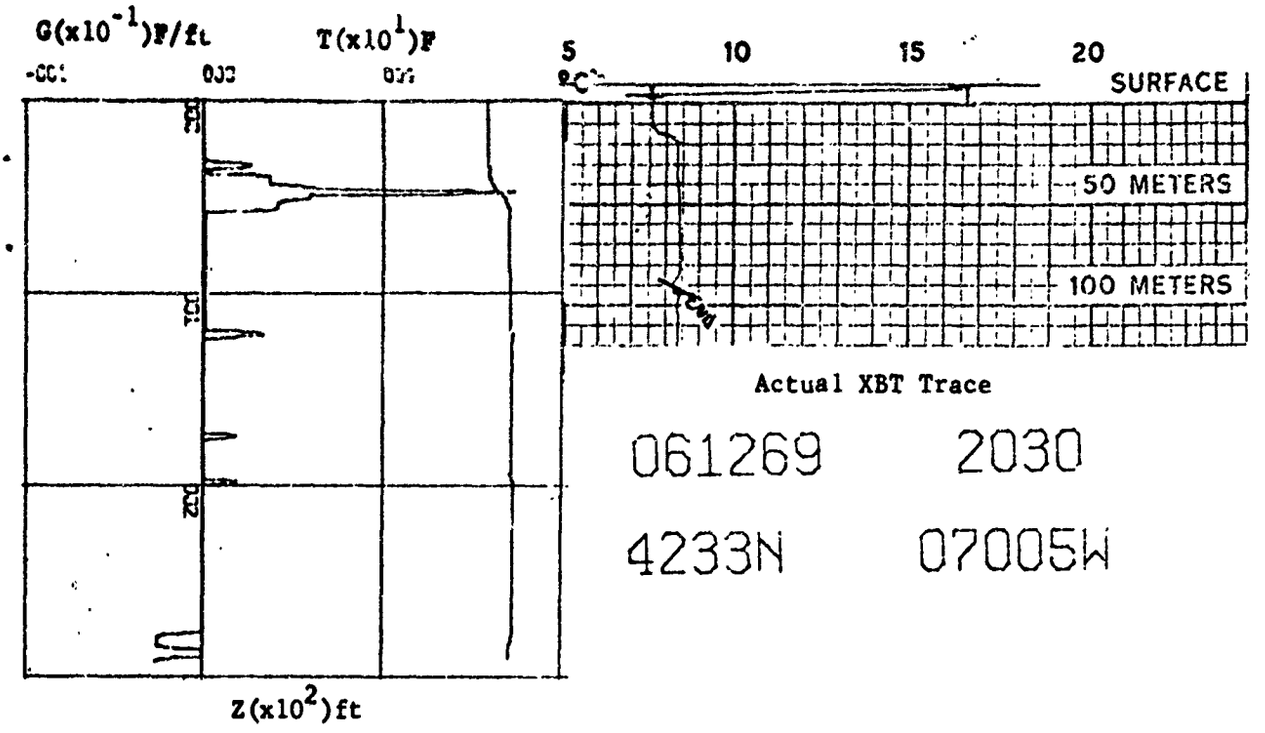

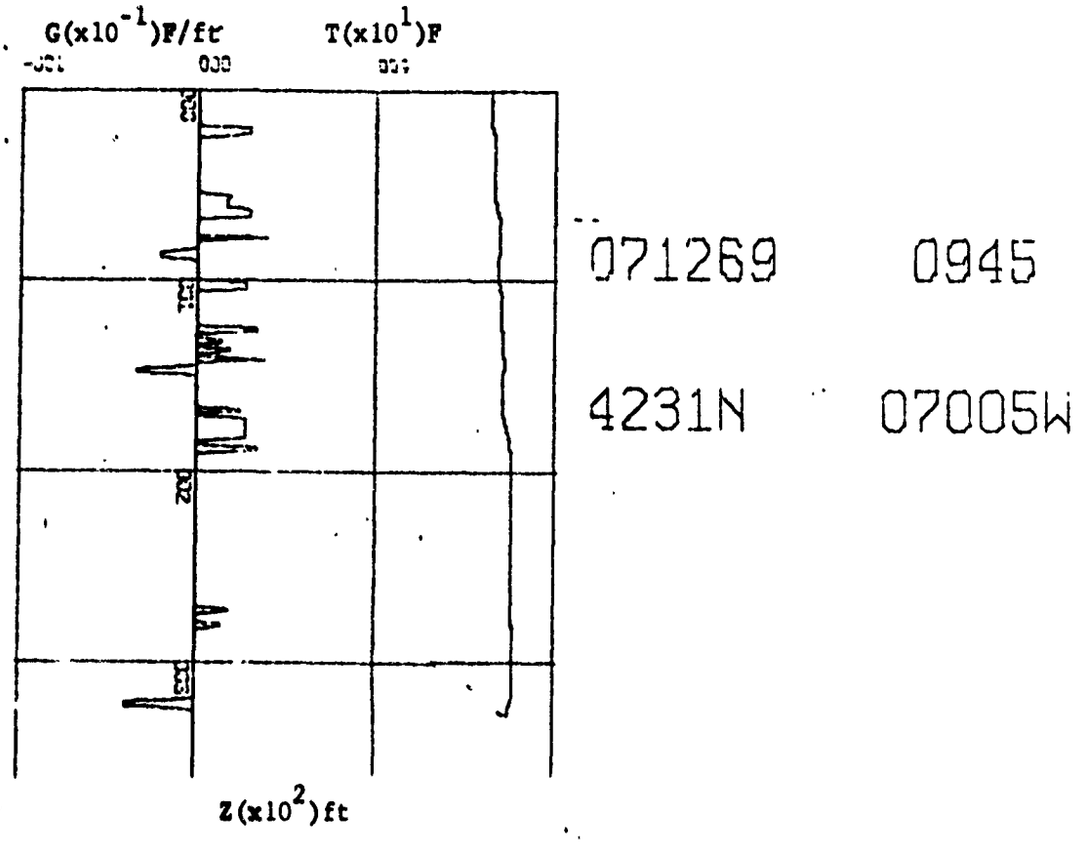

Figure 39. T-Z and G-Z Plots for Atlantic Coastal Region 6 and 7 December 1969.

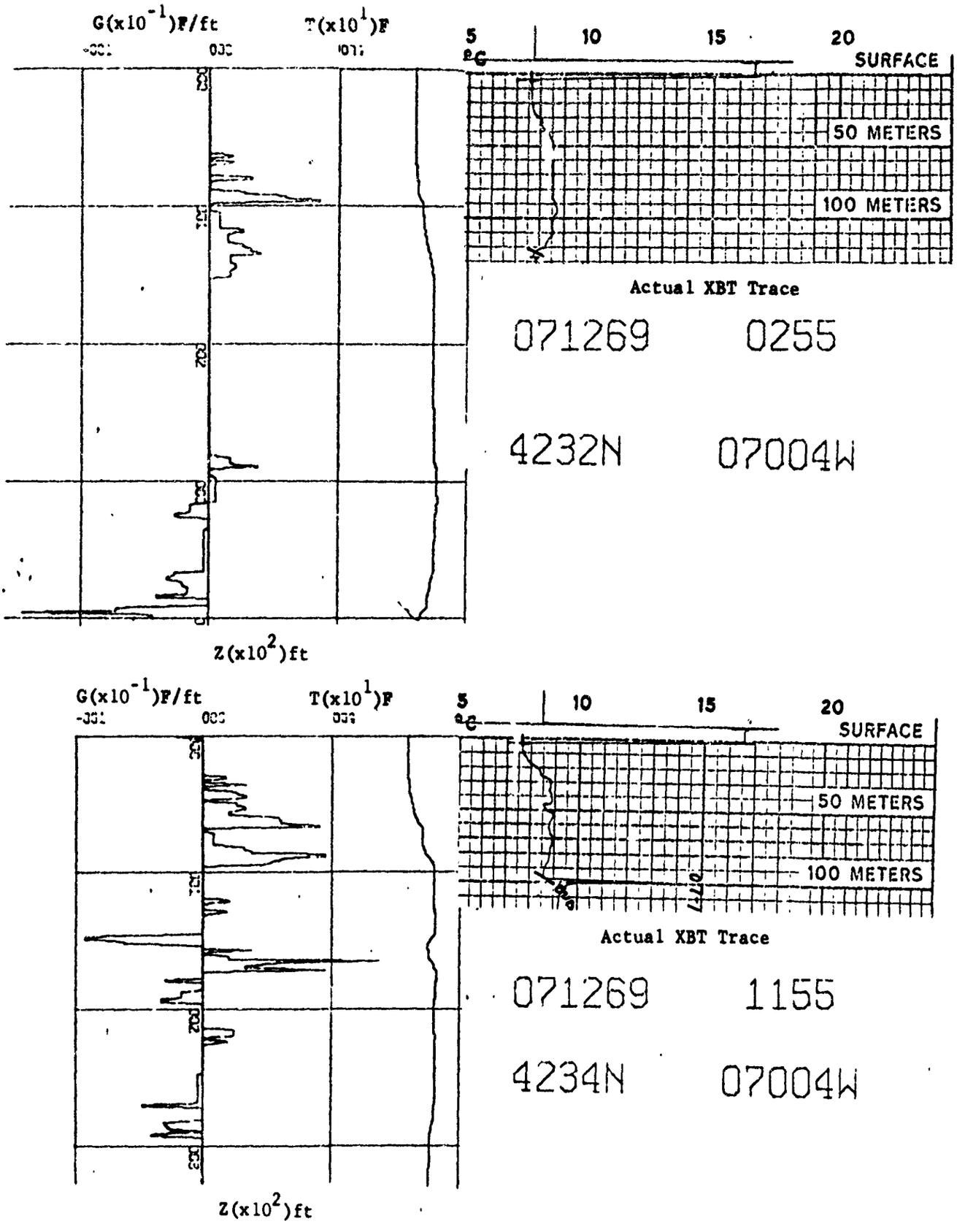

Figure 40. T-Z and G-Z Plots for Atlantic Coastal Region 7 December 1969.

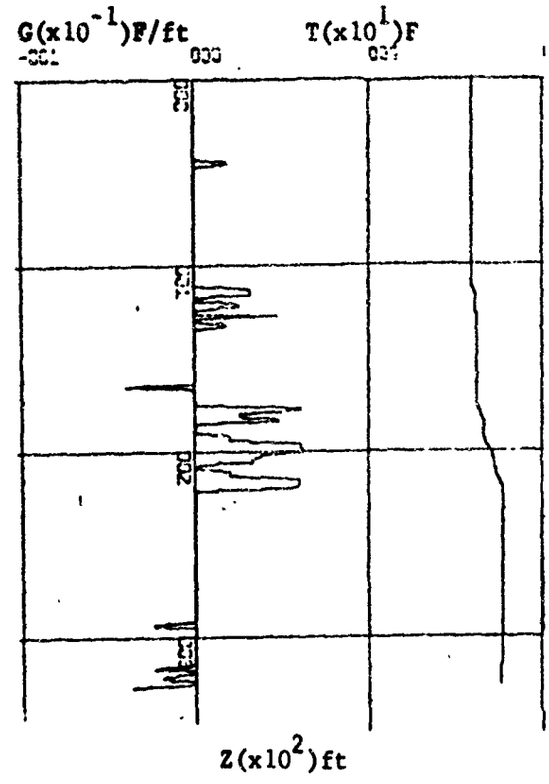

091269 1500

.4255N 07003W

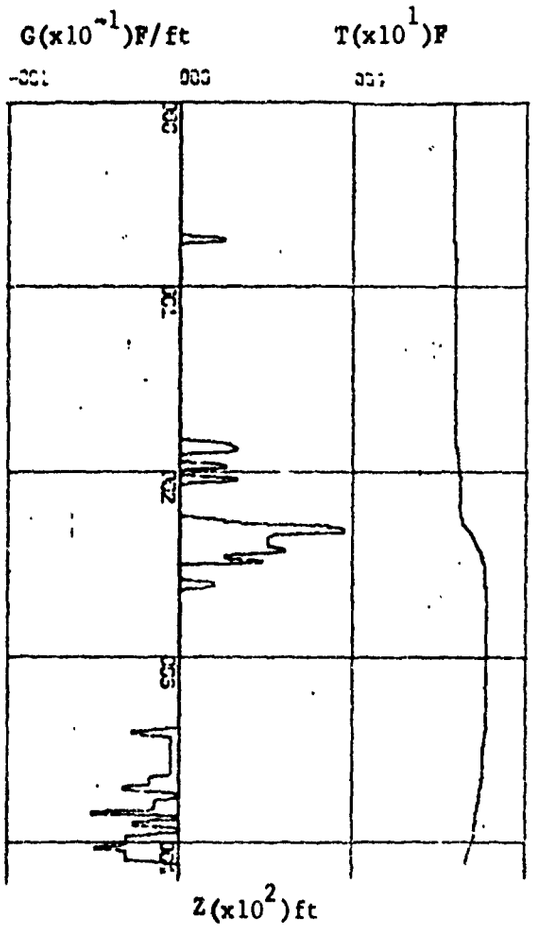

101269 1925

4252N 07004W

Figure 41. T-Z and G-Z Plots for Atlantic Coastal Region 9 and 10 December 1969.

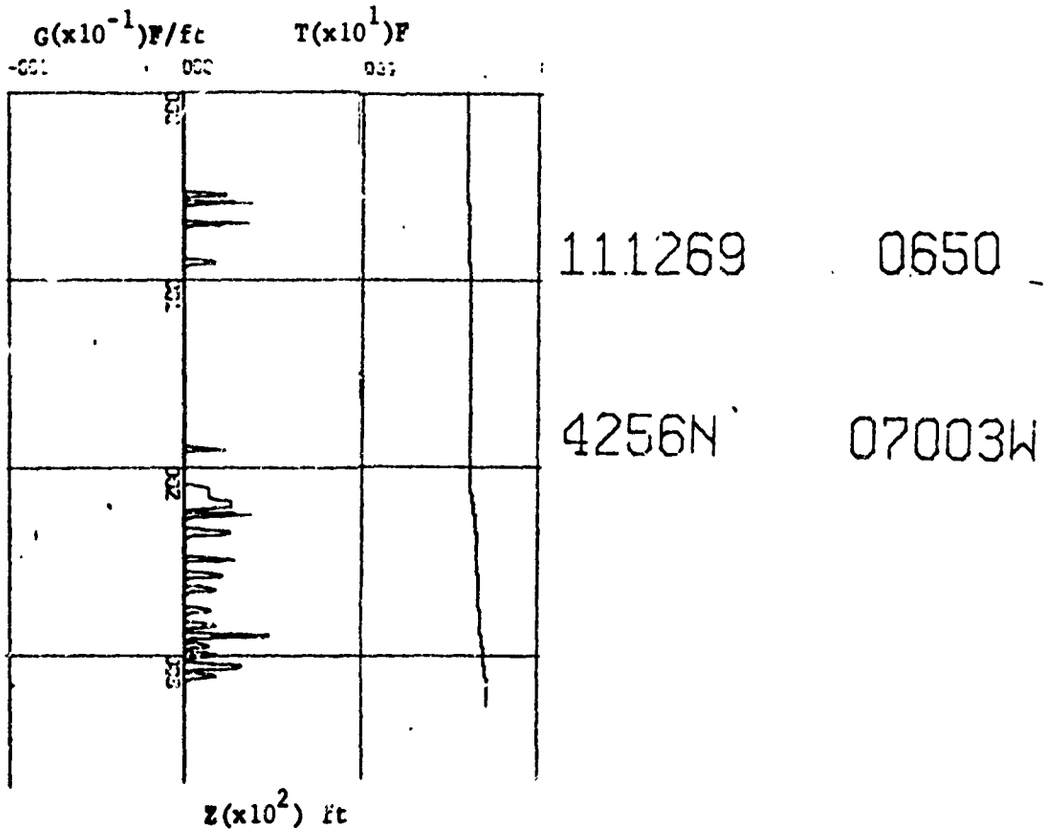

Figure 42. T-Z and G-Z Plots for Atlantic Coastal Region 11 December 1969.

The T-Z plots (Figures 43 through 50) contain a mixed layer to 200 or more feet except for one observation at 1200Z on the 19th (Figure 48b). The mixed layer transients are marked with spikes in the G-Z plots. Figure 50 shows transients with the greatest magnitude in the upper 100 feet. The seasonal thermocline is characterized by two steps (Figure 44, for example). The G-Z plots in most cases show this second step, averaging at a depth about 300 feet, with good resolution. Some strong gradients are found in the 200 to 300 feet depth region in every G-Z plot except in Figure 48b. This figure appears to indicate flow over a hump or have erroneous depth values. The fall-rate of the XBT probe, appearing erroneously in the T-Z plot, indicates a possible malfunction of the probe or the recorder for this one cast.

3. Pacific Oceanic Region

A series of XBT traces, taken over a week period in October 1968, in the deep waters (over 100 nm off the West Coast near San Diego, California) were used for this observation. A composite T-Z plot of the actual XBT temperature-depth traces is shown in Figure 51. This region is sub-tropical oceanic [Tully, 1964]. Plots of T-Z and G-Z (Figures 52 through 65) are presented from the surface to 900 feet. The seasonal thermocline is evident in all plots. The strong thermocline is clearly shown. Some transients are notable. Few inversion layers were present, and, generally, they were found only in the near-surface layer. The G-Z plot is characterized by strong gradients in the seasonal thermocline and by weak gradients in the main thermocline, each separate layer separated by isothermal waters from one to forty feet thick.

The mixed layer contained numerous temperature fluctuations in most cases. Some inversions, in particular the one at 0600Z on 14 October

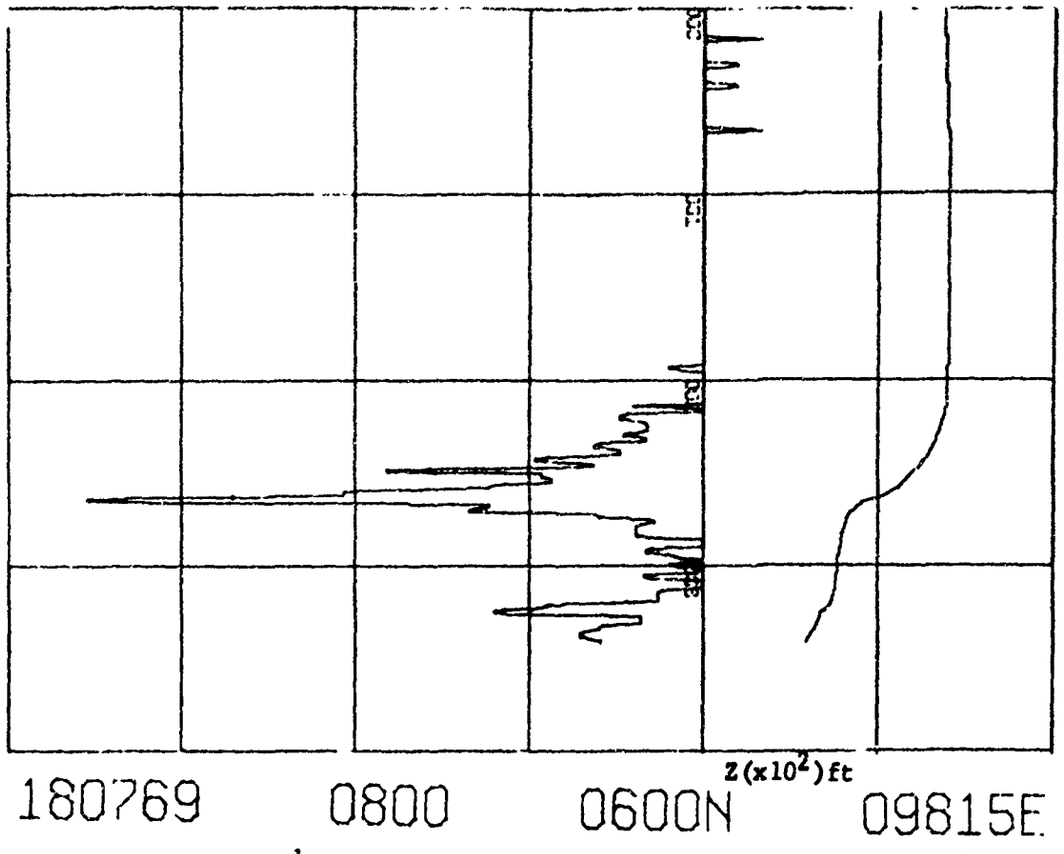

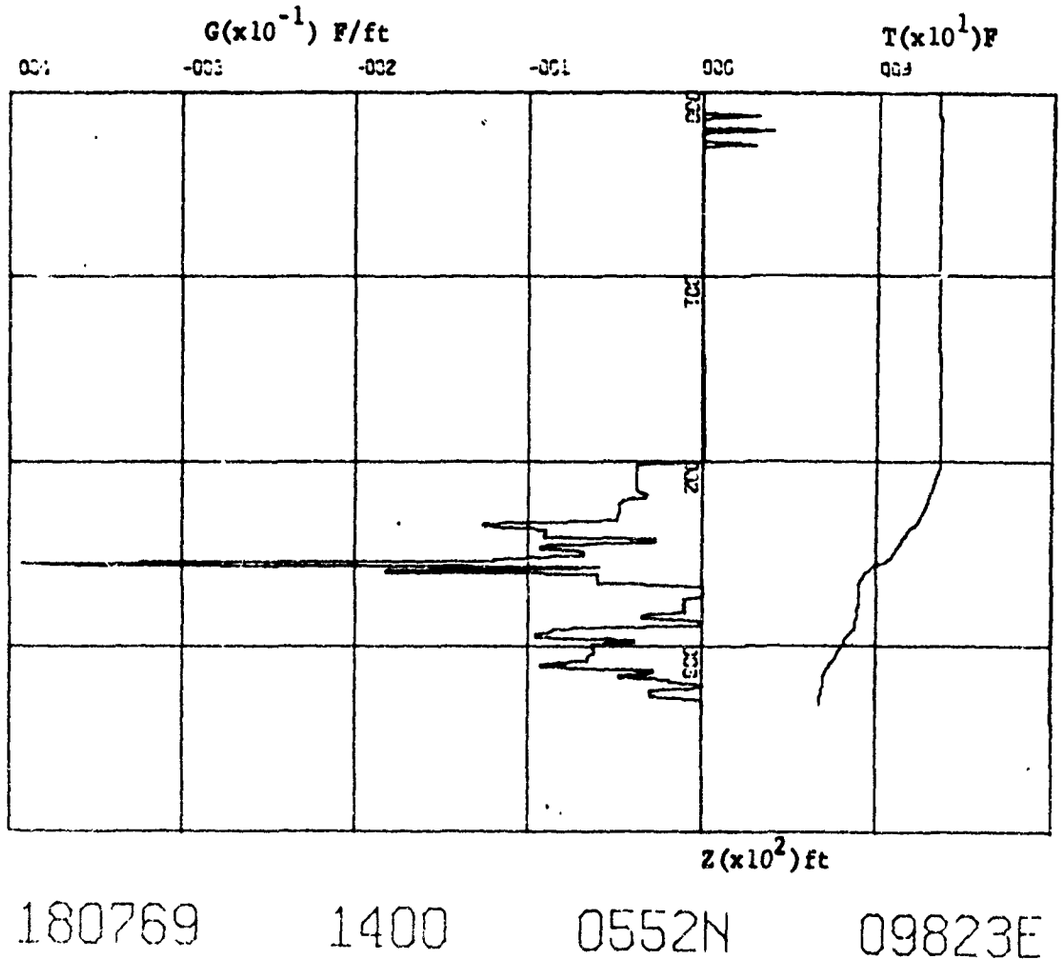

Figure 43. T-Z and G-Z Plots for Andaman Sea Region for 18 July 1969.

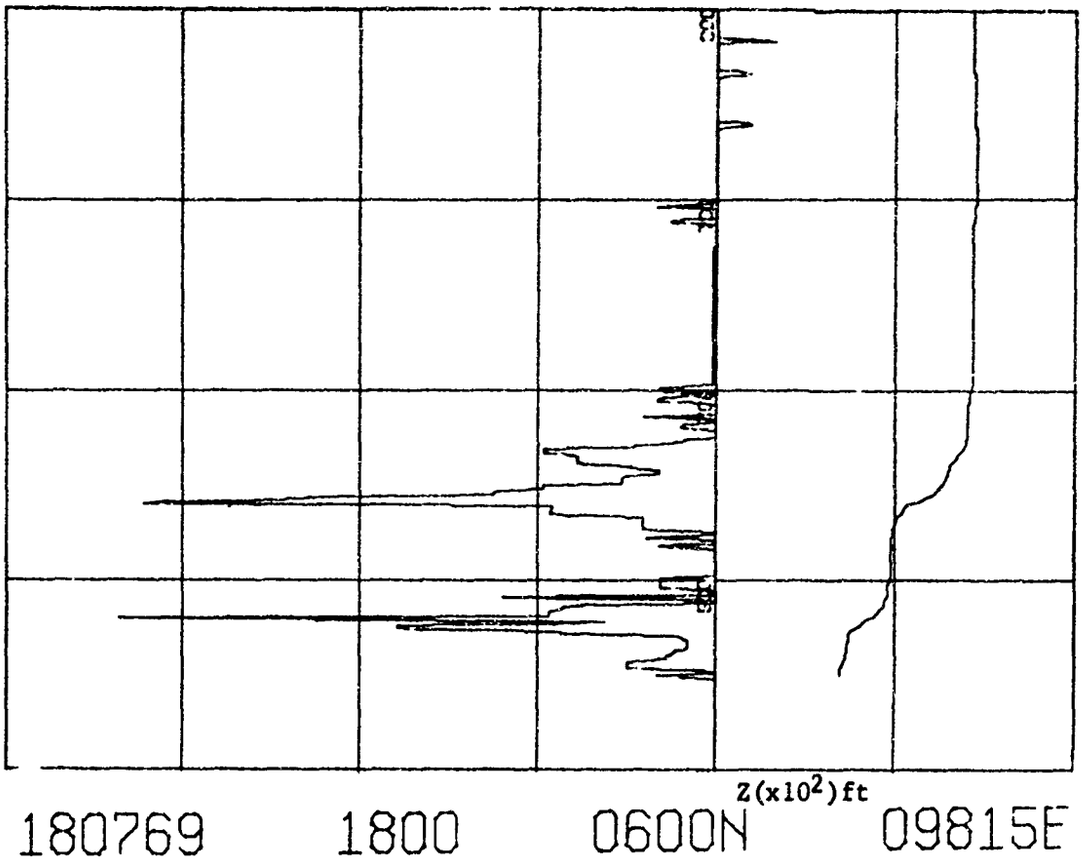

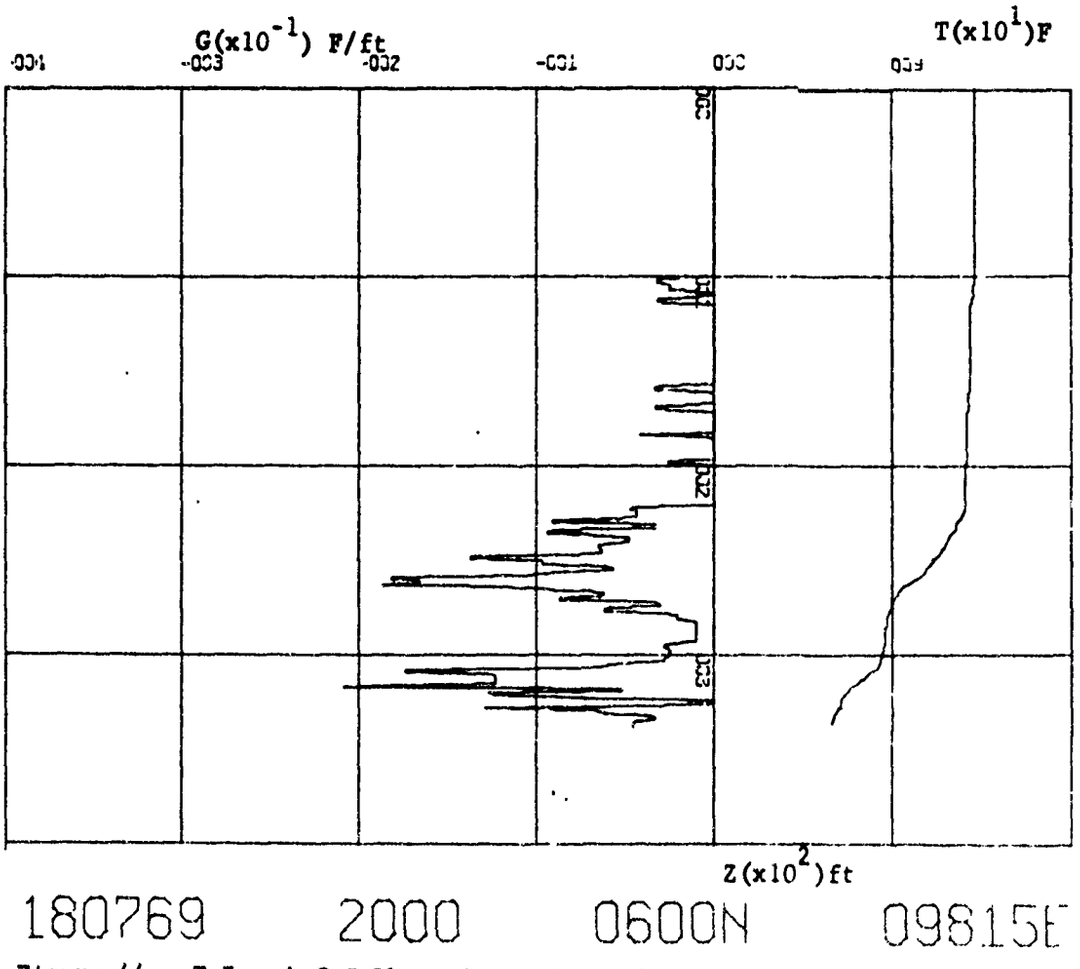

Figure 44. T-Z and G-Z Plots for Andaman Sea Region for 18 July 1969.

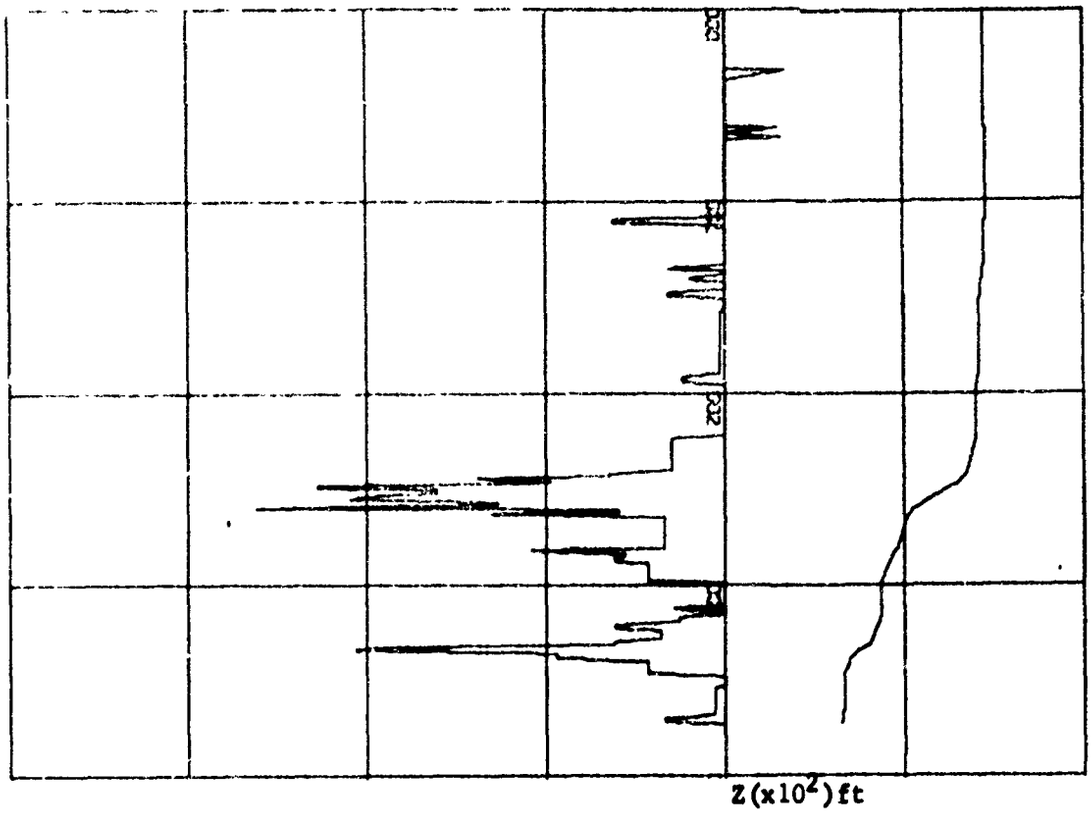

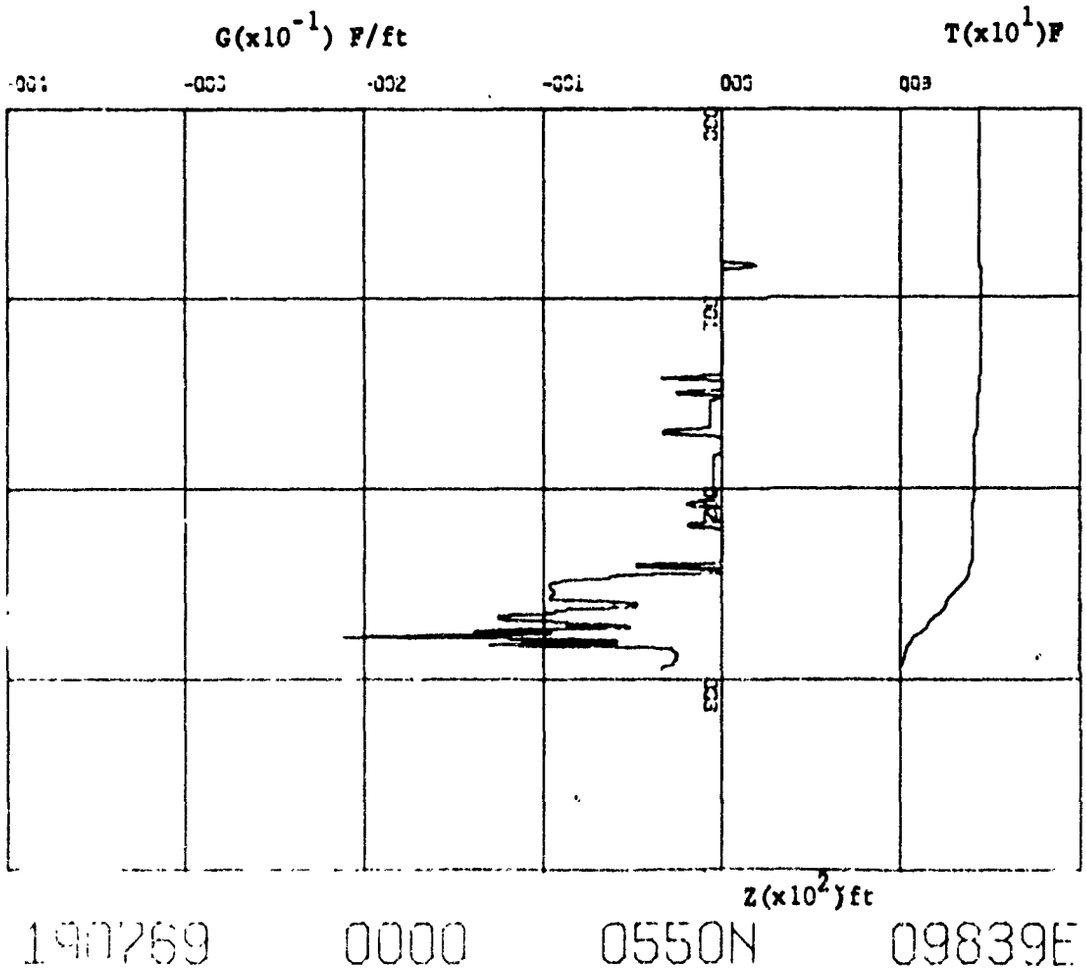

Figure 45. T-Z and G-Z Plots for Andaman Sea Region for 18 and 19 July 1969.

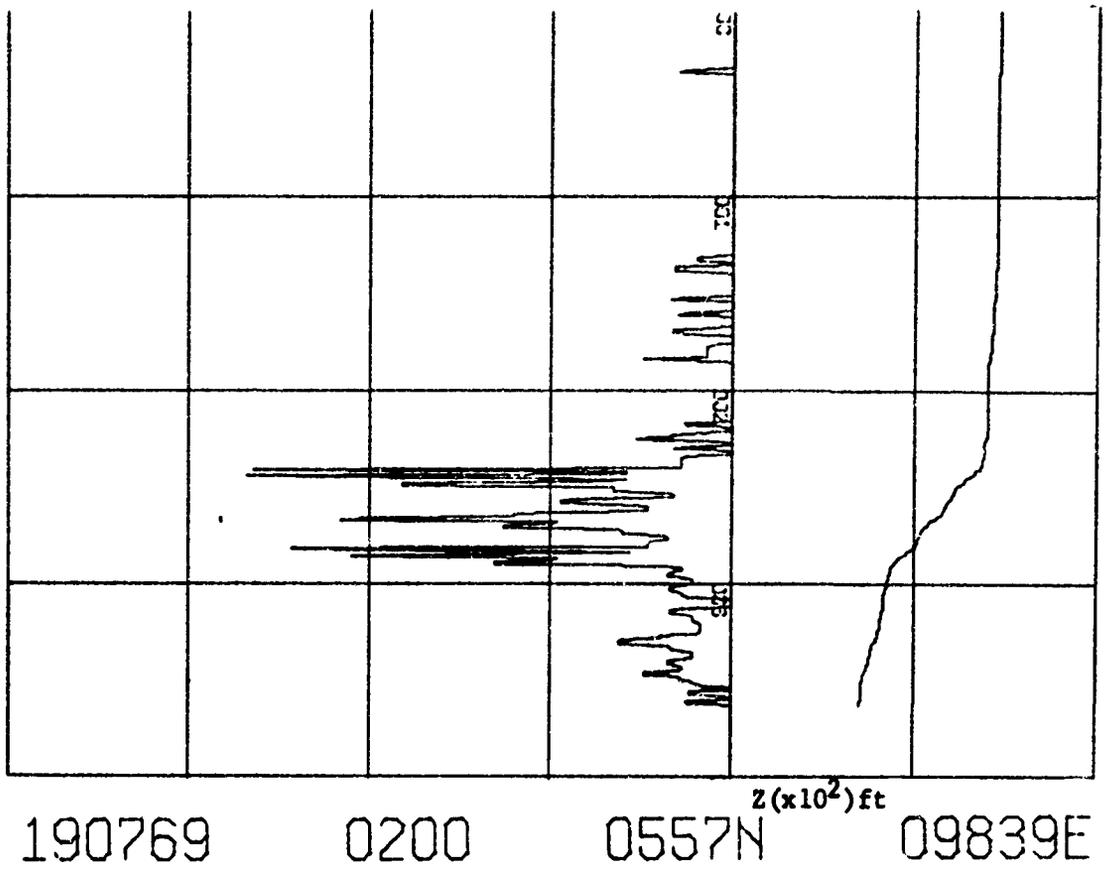

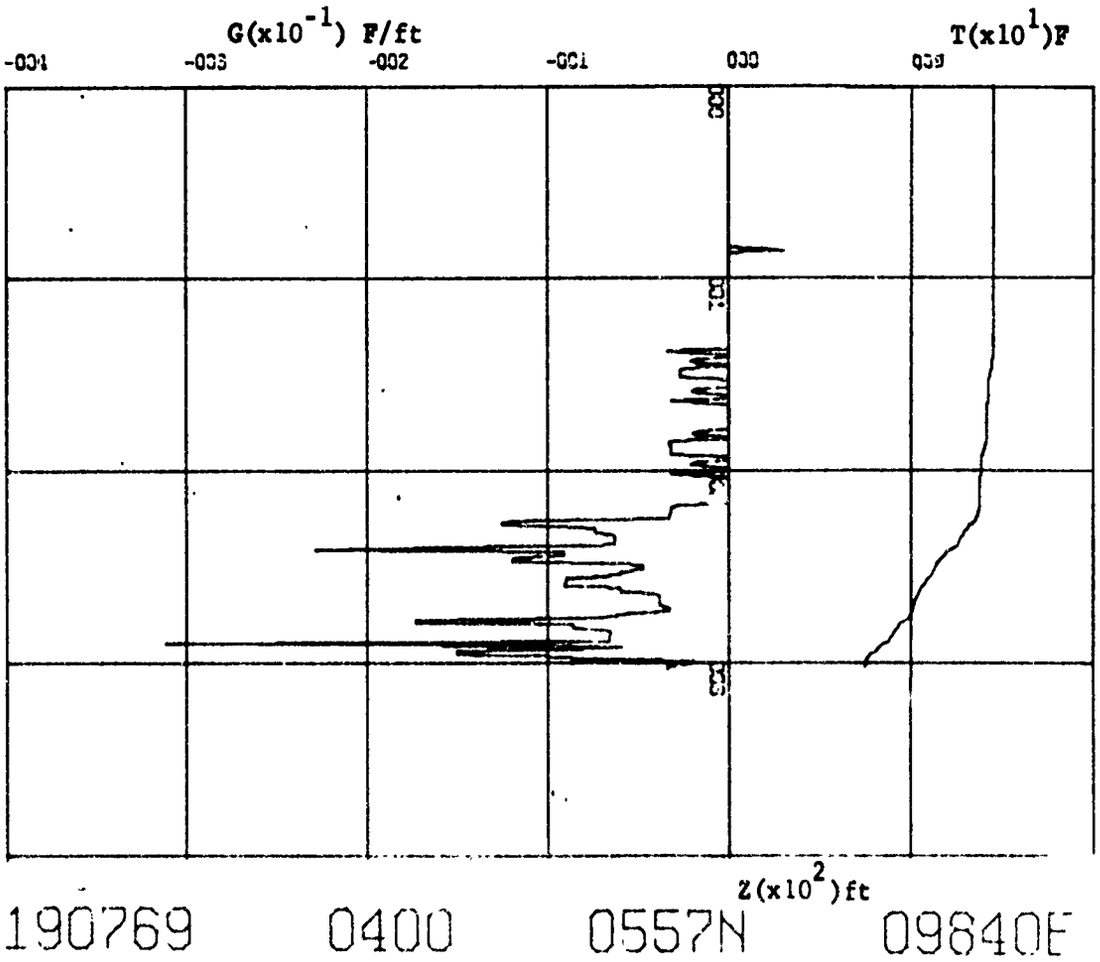

Figure 46. T-Z and G-Z Plots for Andaman Sea Region for 19 July 1969.

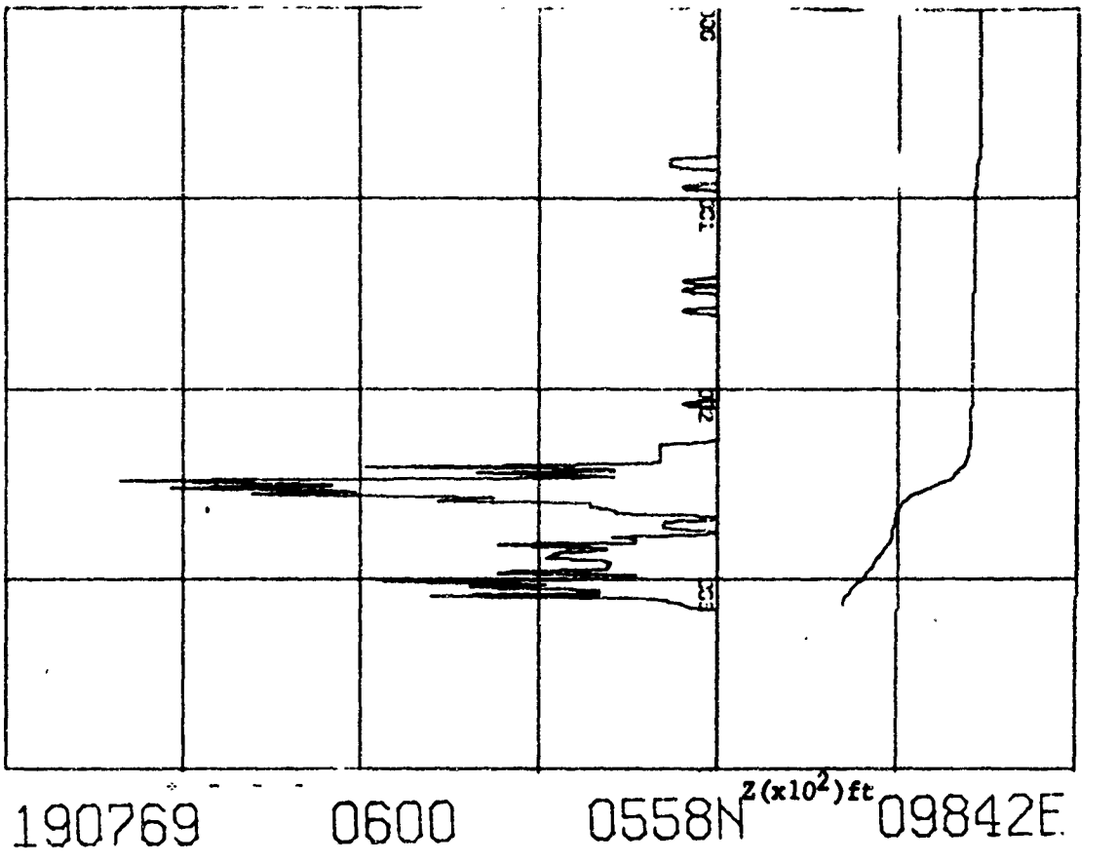

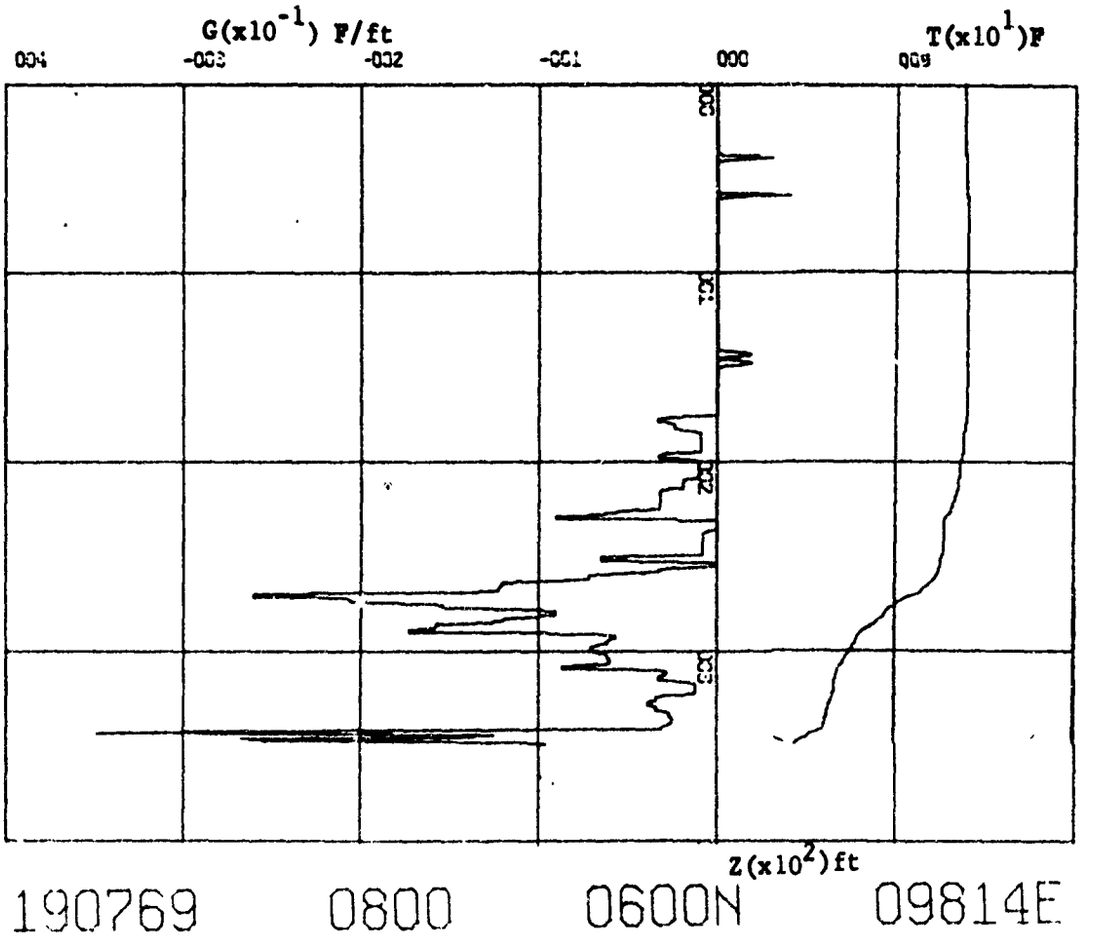

Figure 47. T-Z and G-Z Plots for Andaman Sea Region for 19 July 1969.

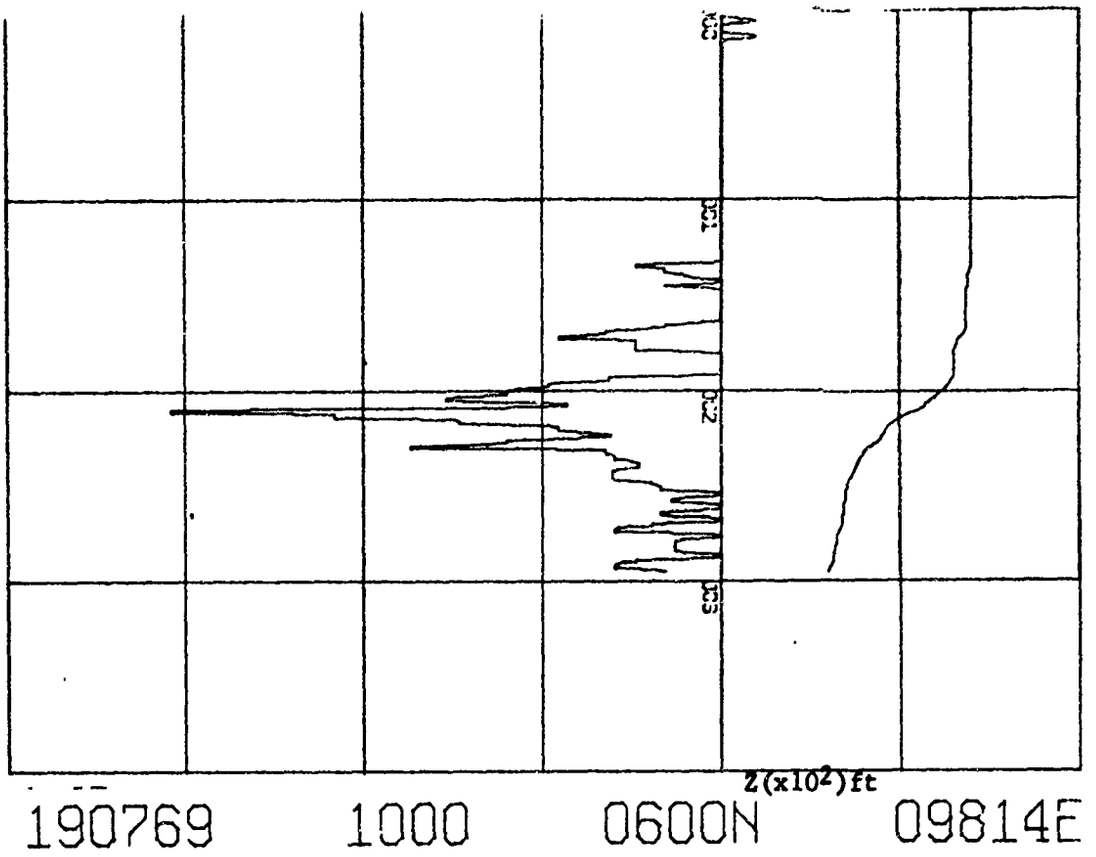

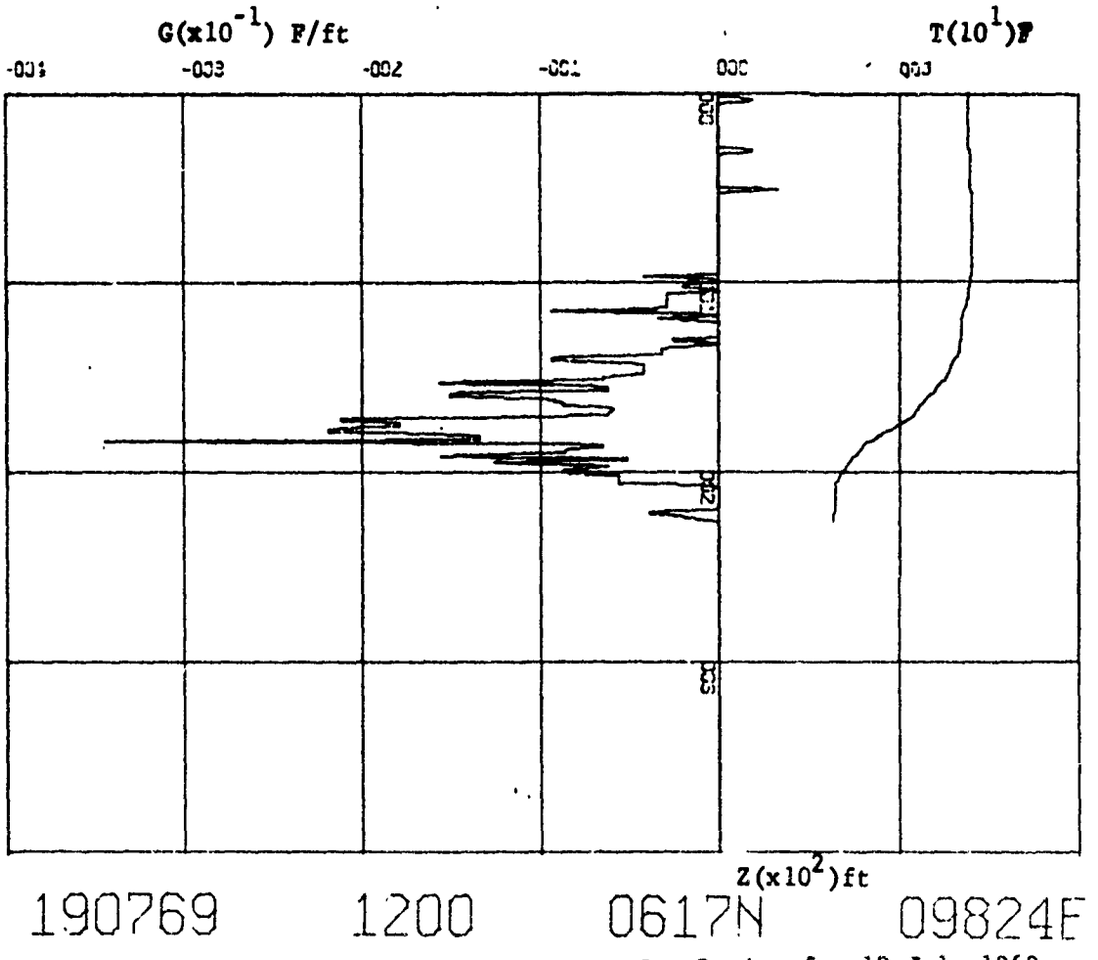

Figure 48. T-Z and G-Z Plots for Andaman Sea Region for 19 July 1969.

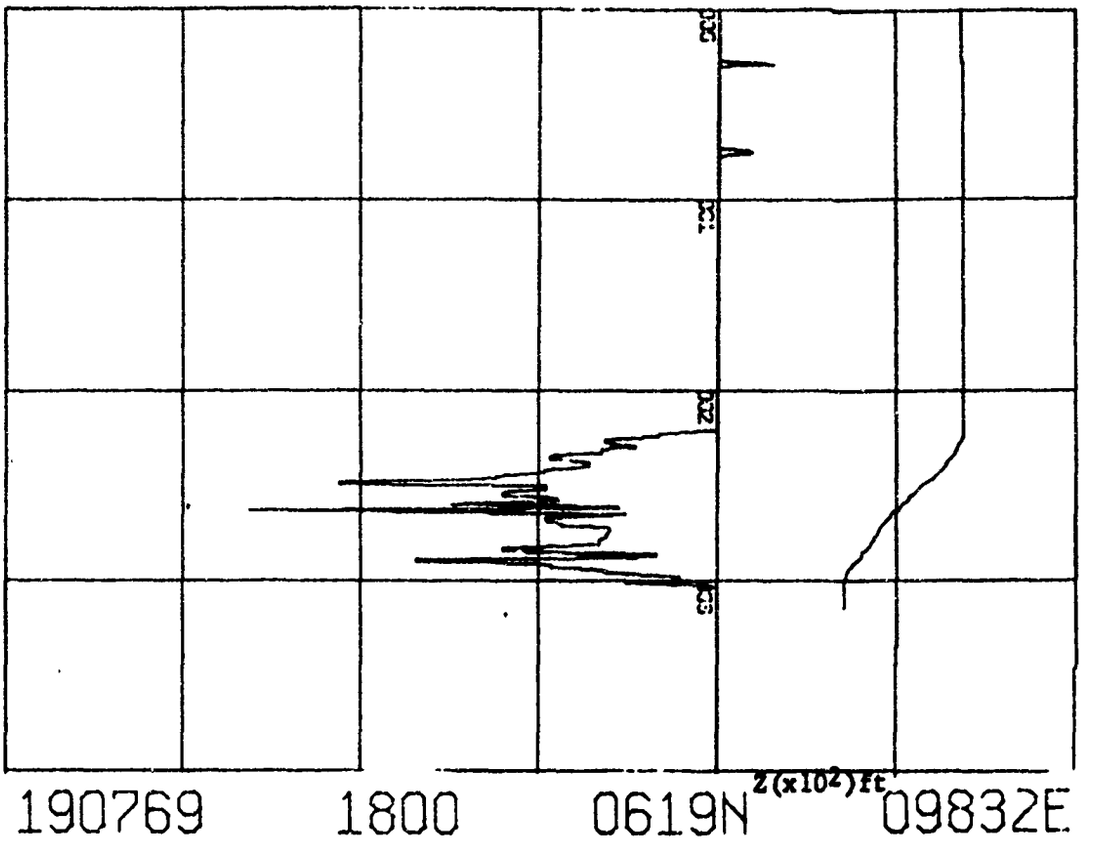

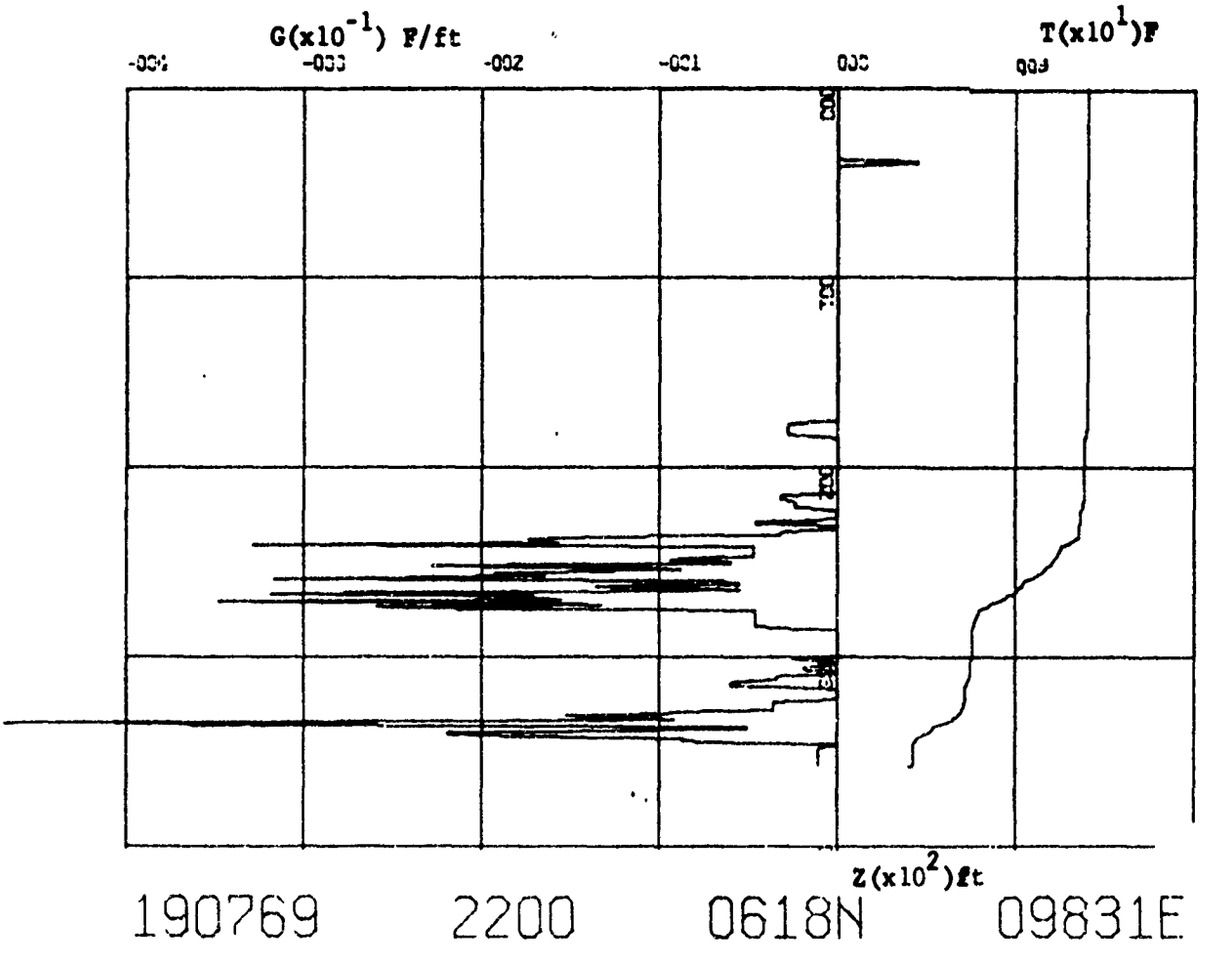

Figure 49. T-A and G-Z Plots for Andaman Sea Region for 19 July 1969.

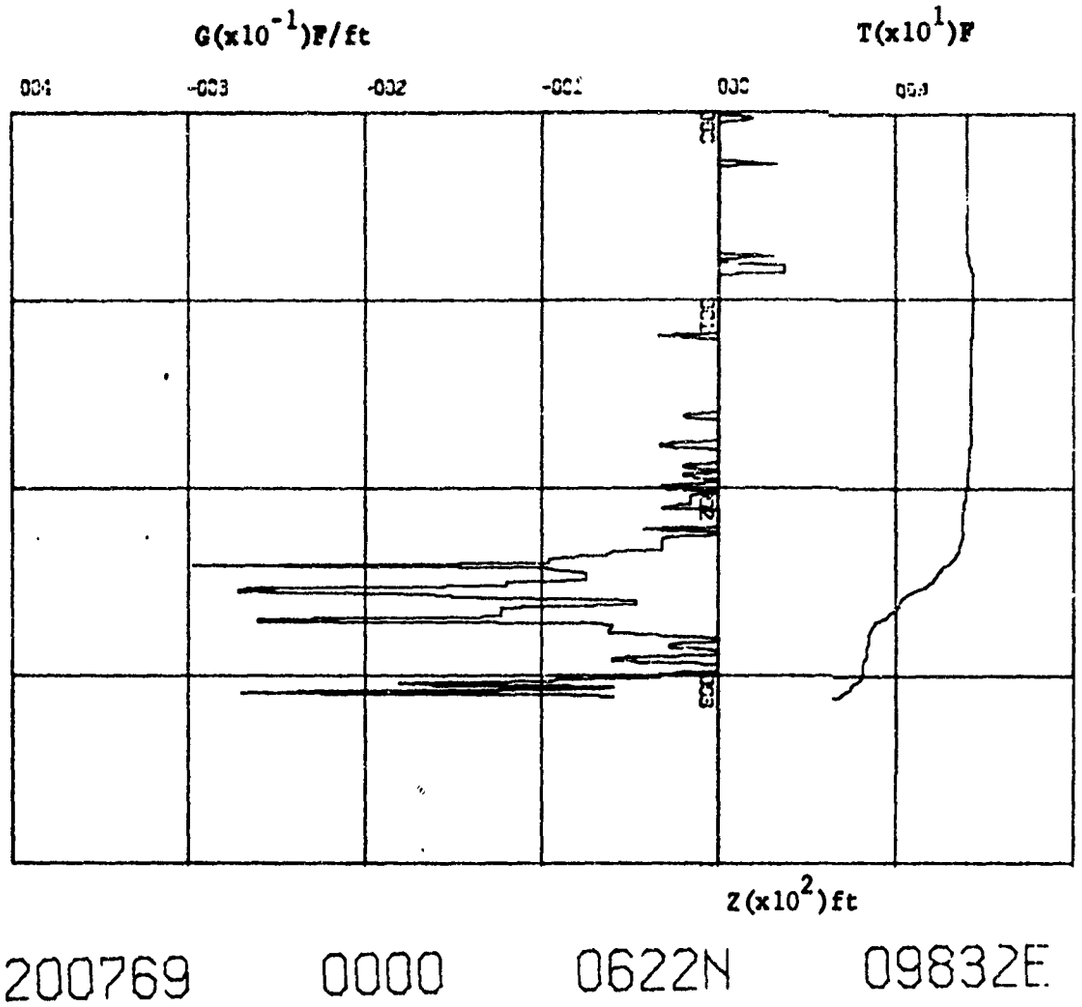

Figure 50. T-Z and G-Z Plots for Andaman Sea Region for 20 July 1969.

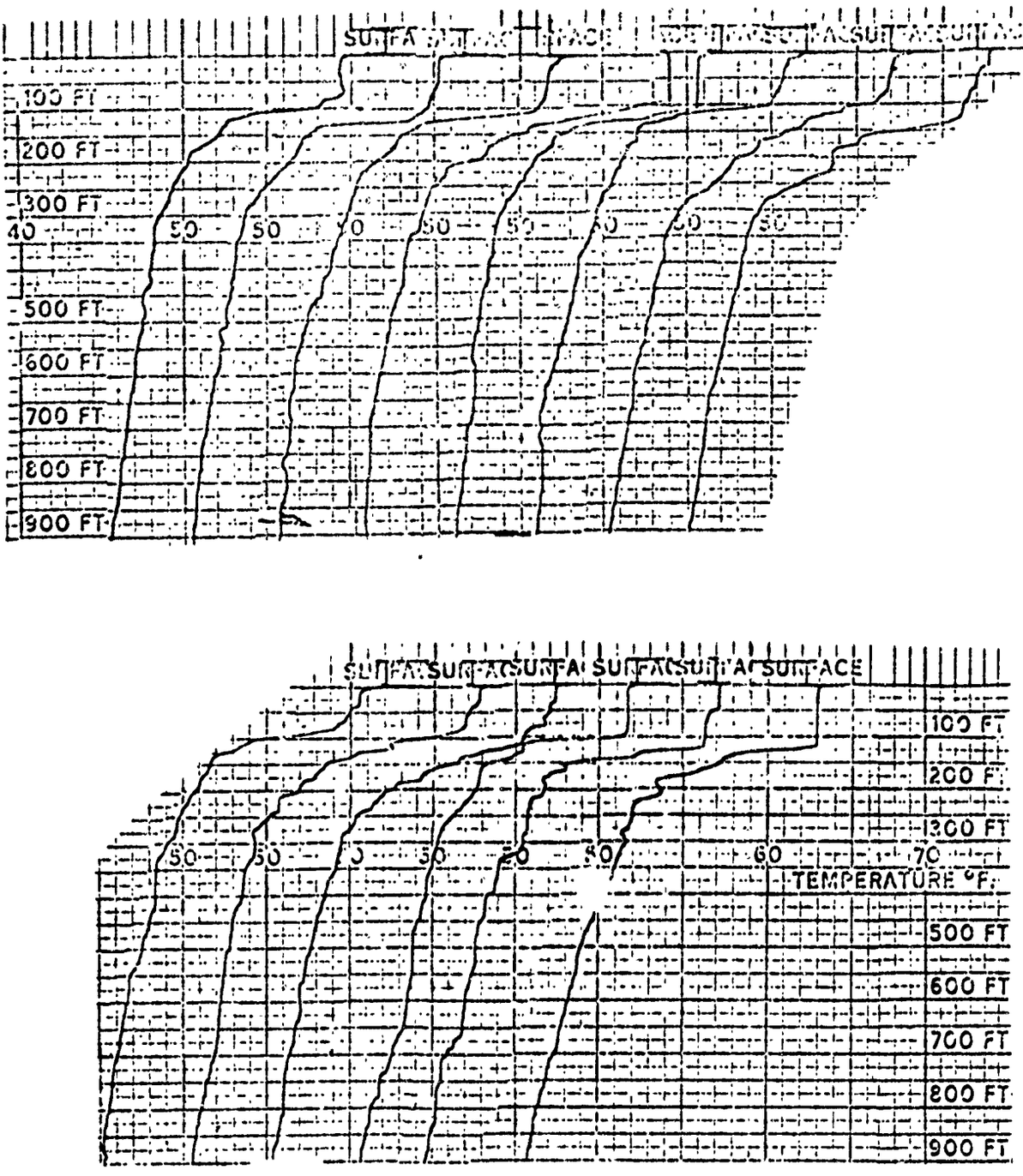

Figure 51. Composite T-Z Plot from Actual XBT Traces Down to 900 feet for Region 100 nm off San Diego. Data are given in time sequence from 10 through 16 October 1968.

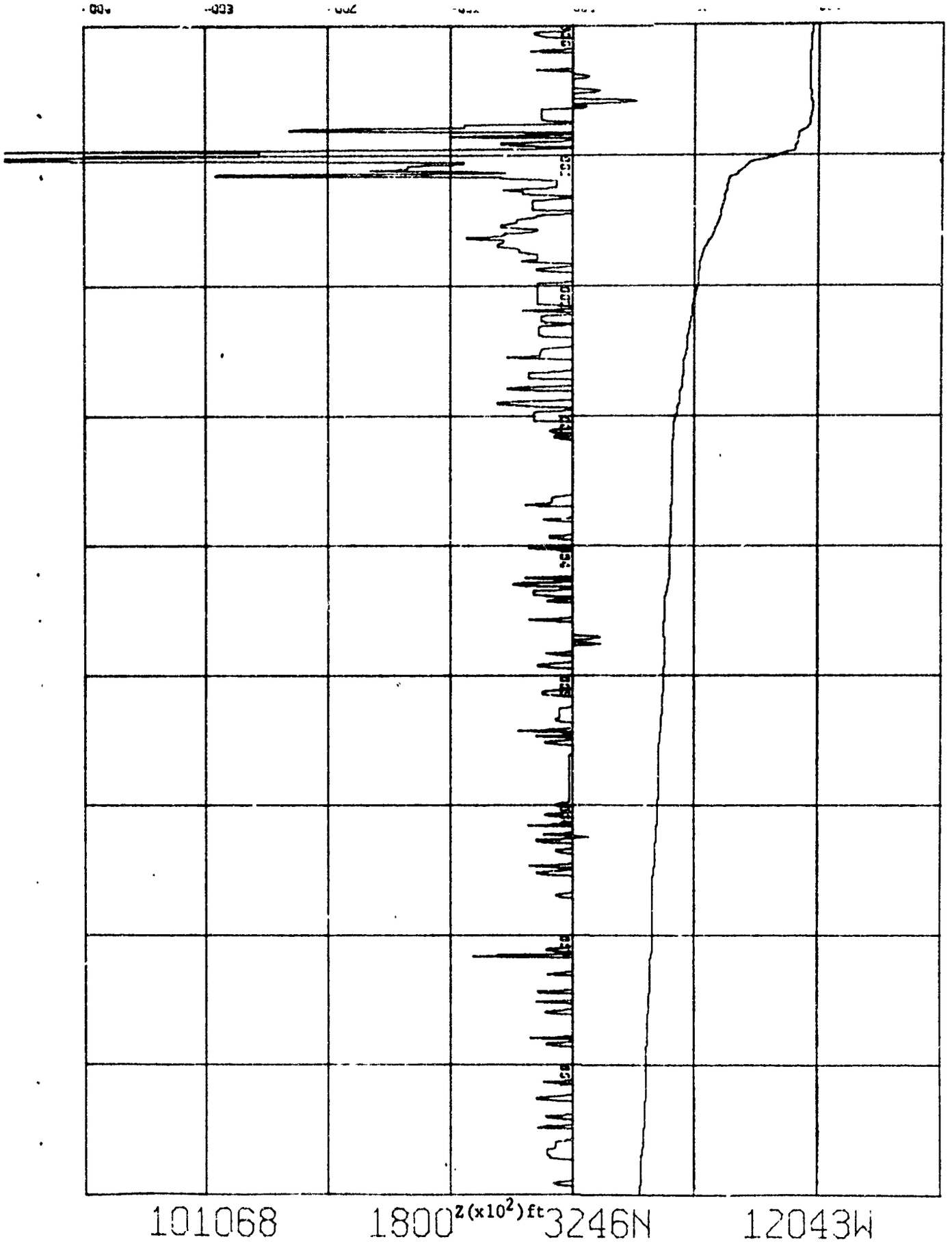

Figure 52. T-Z and G-Z Plots for Eastern North Pacific for 1800Z 10 October 1968.

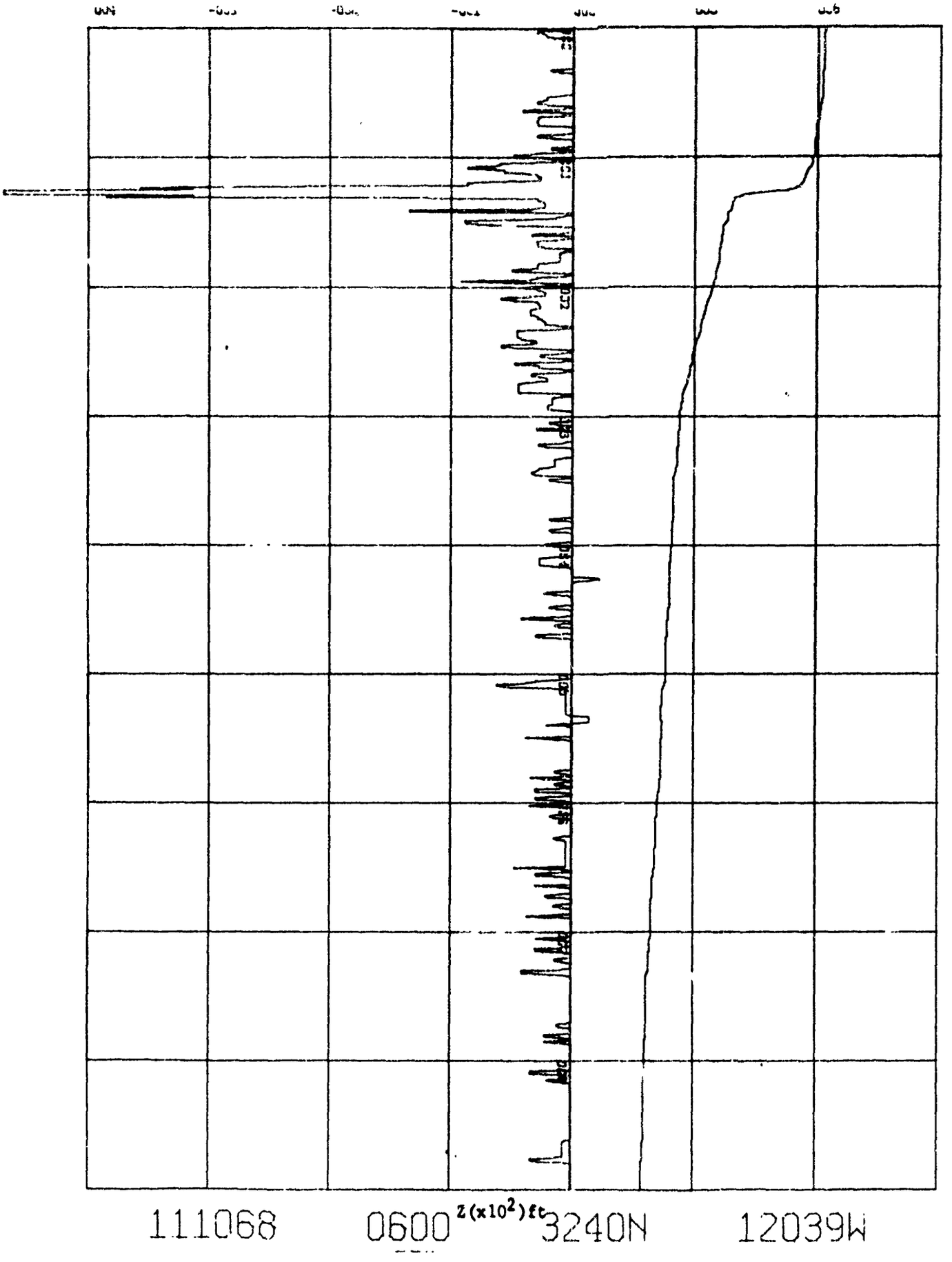

Figure 53. T-Z and G-Z Plots for Eastern North Pacific for 0600Z 11 October 1968.

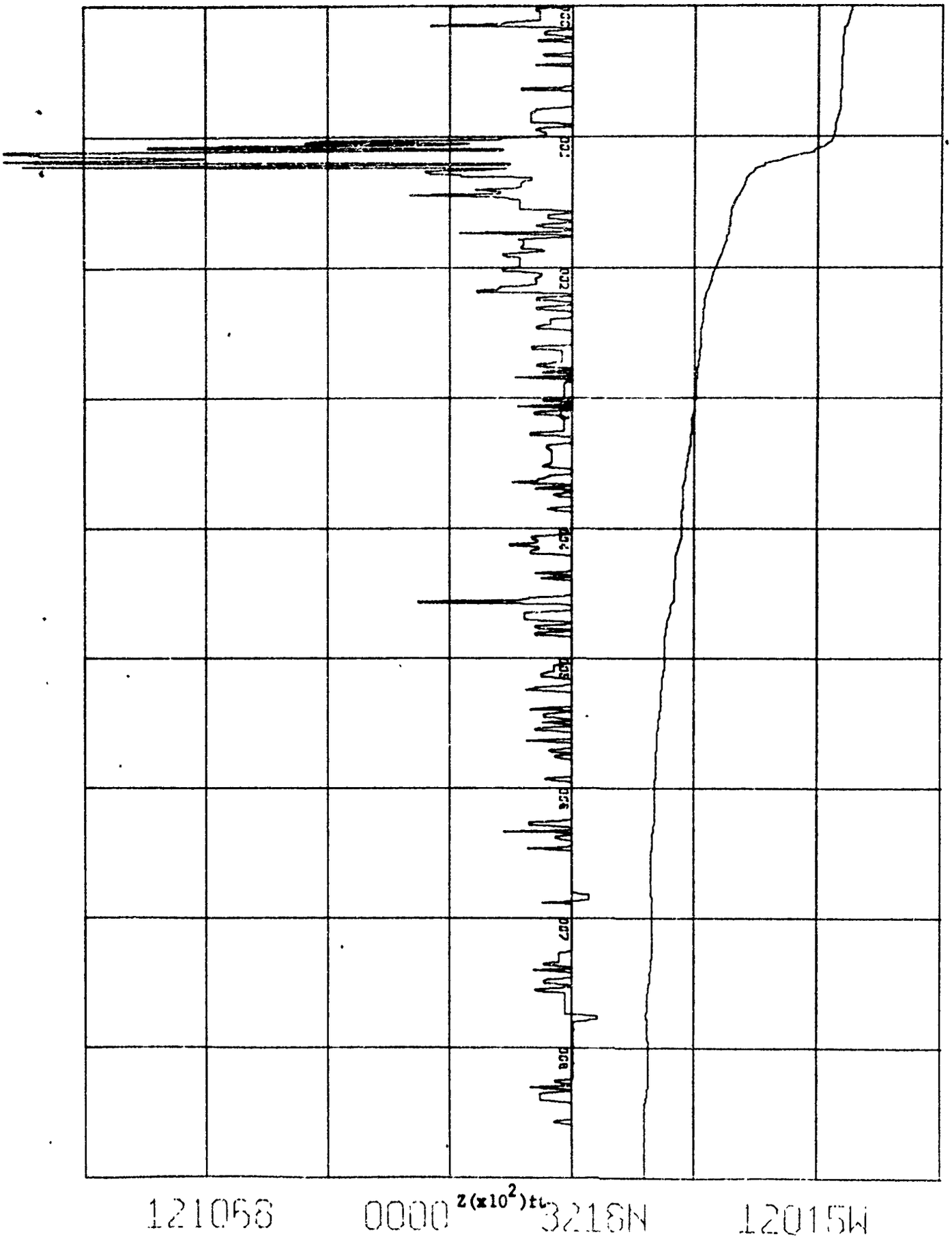

Figure 54. T-Z and G-Z Plots for Eastern North Pacific for 0000Z 12 October 1968.

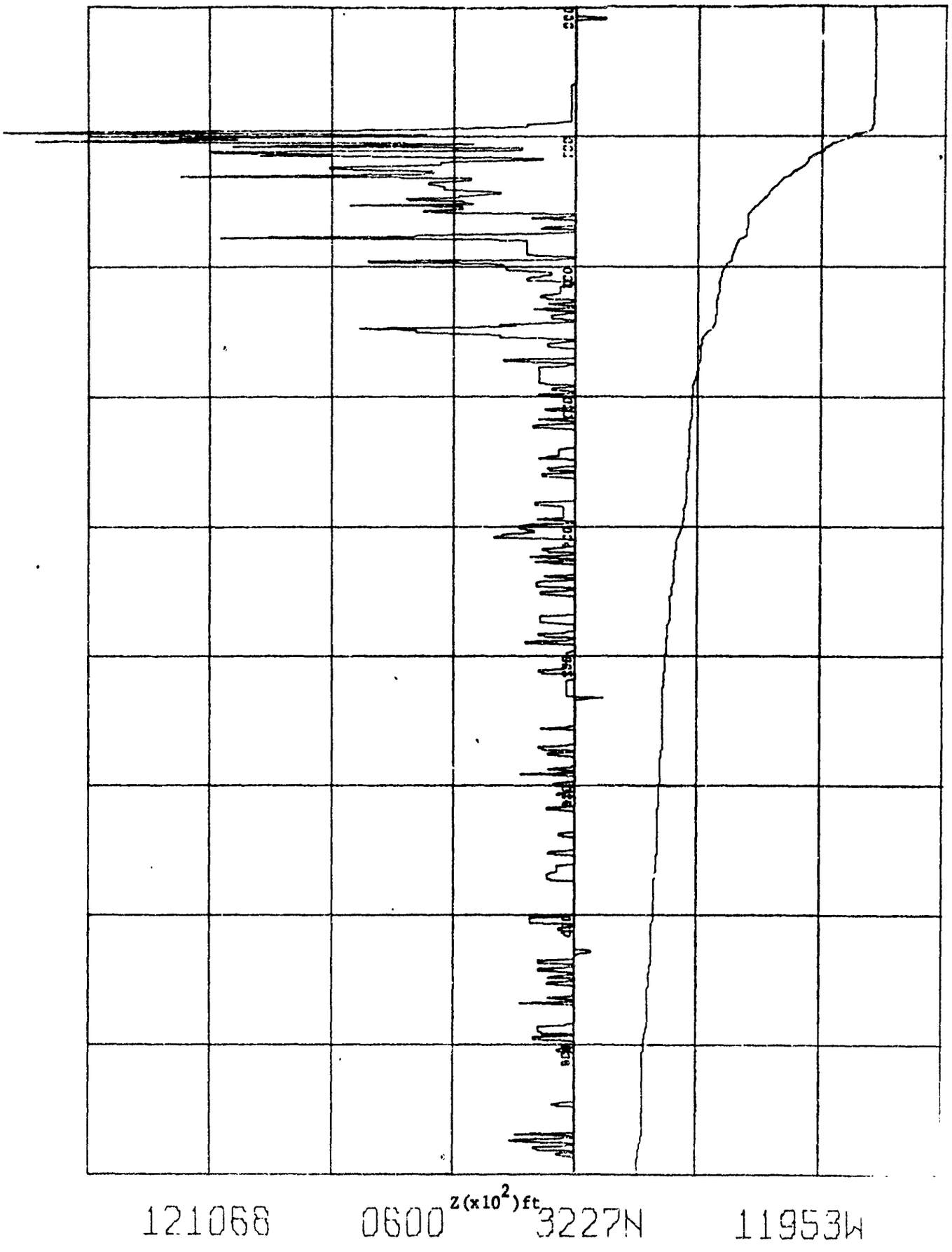

Figure 55. T-Z and G-Z Plots for Eastern North Pacific for 0600Z 12 October 1968.

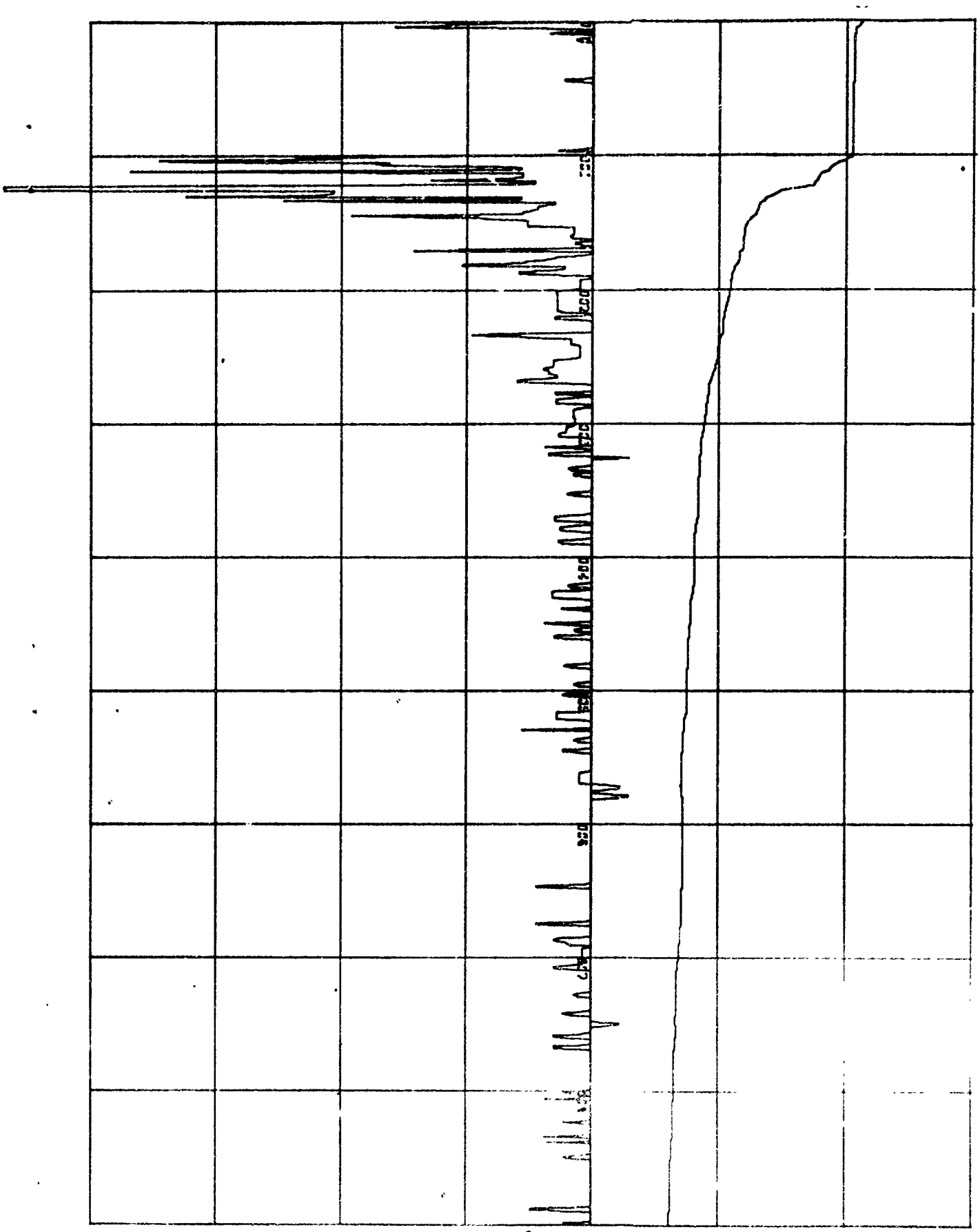

Figure 56. T-Z and G-Z Plots for Eastern North Pacific for 1800Z 12 October 1968.

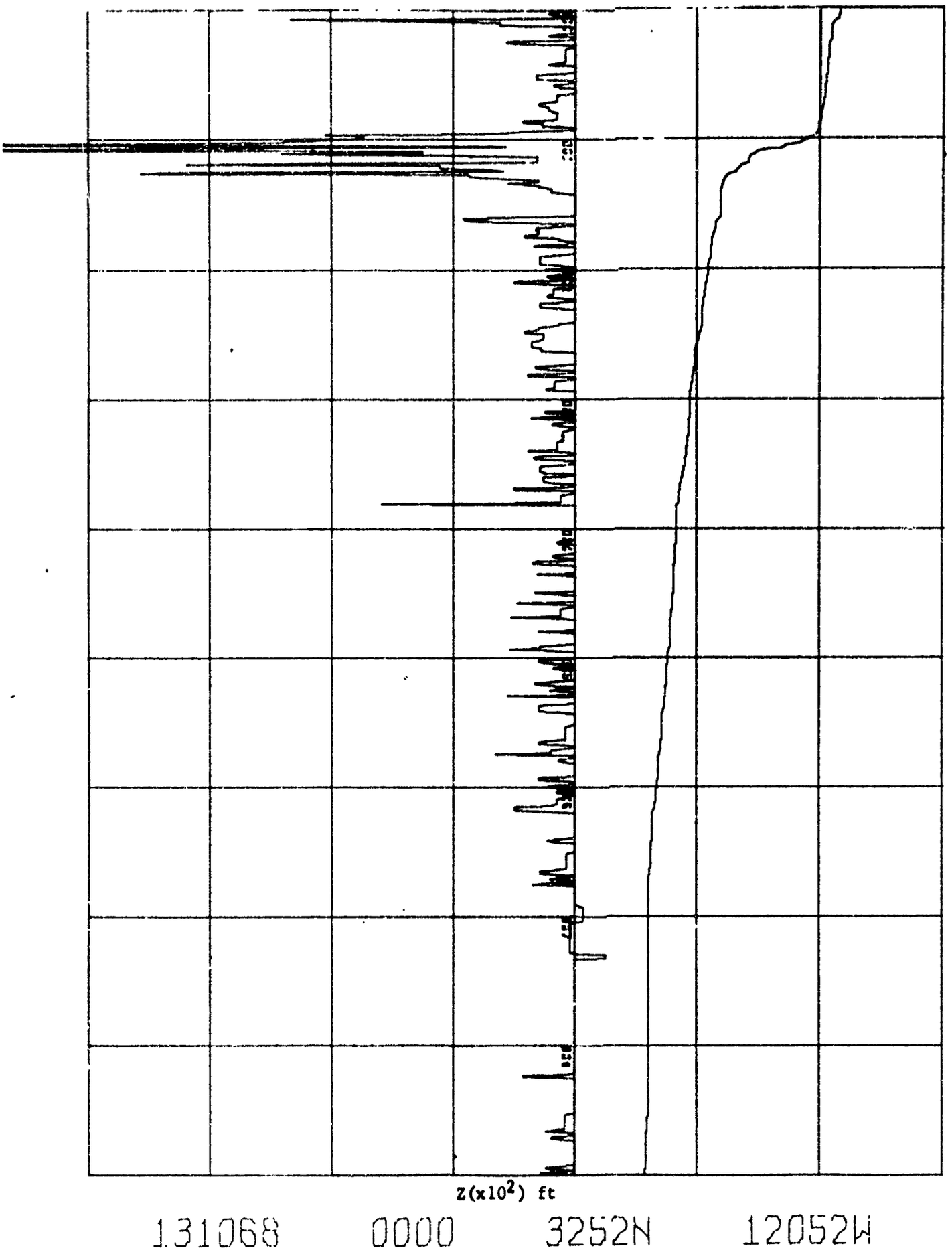

Figure 57. T-Z and G-Z Plots for Eastern North Pacific for 0000Z 13 October 1968.

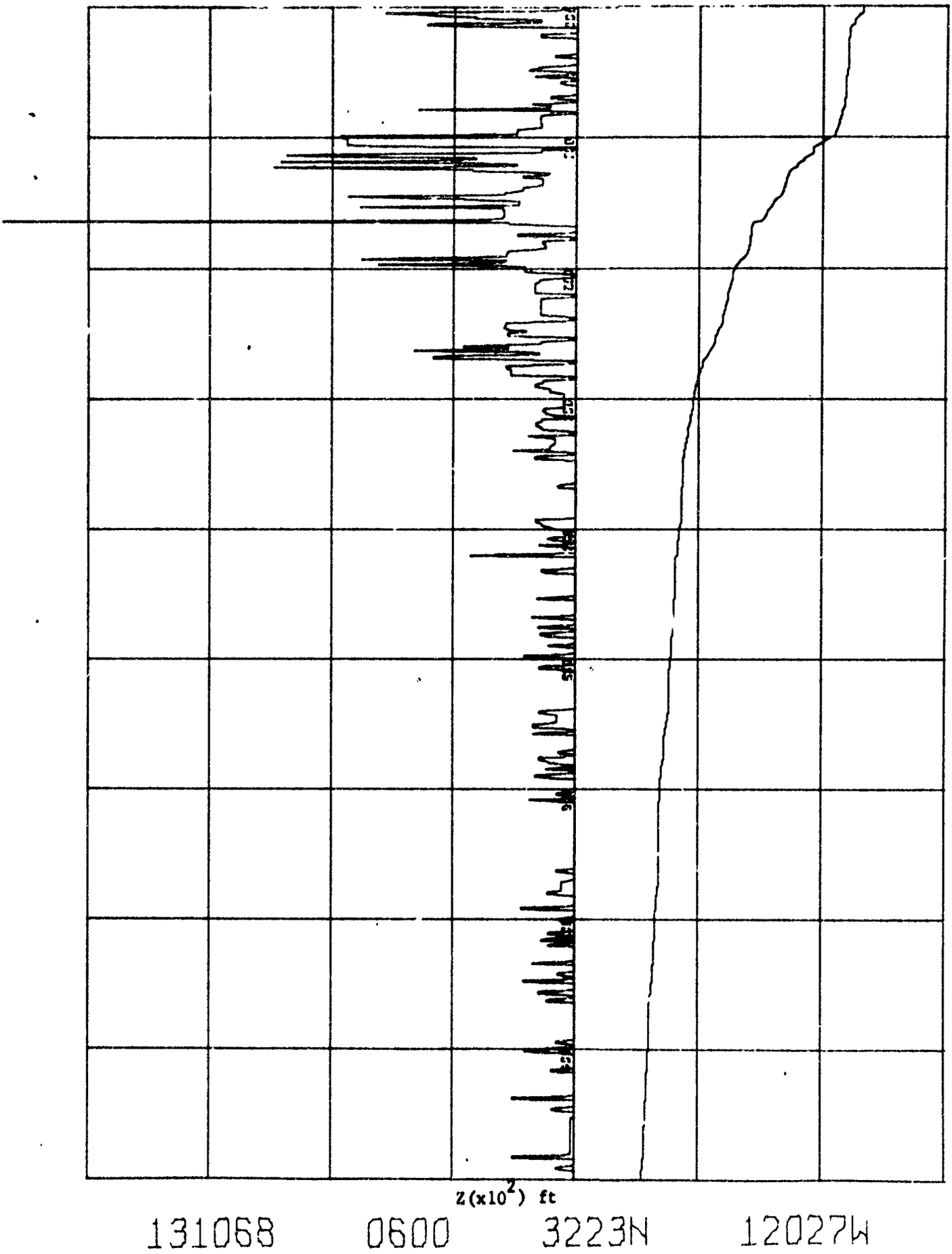

Figure 58. T-Z and G-Z Plots for Eastern North Pacific for 0600Z 13 October 1968.

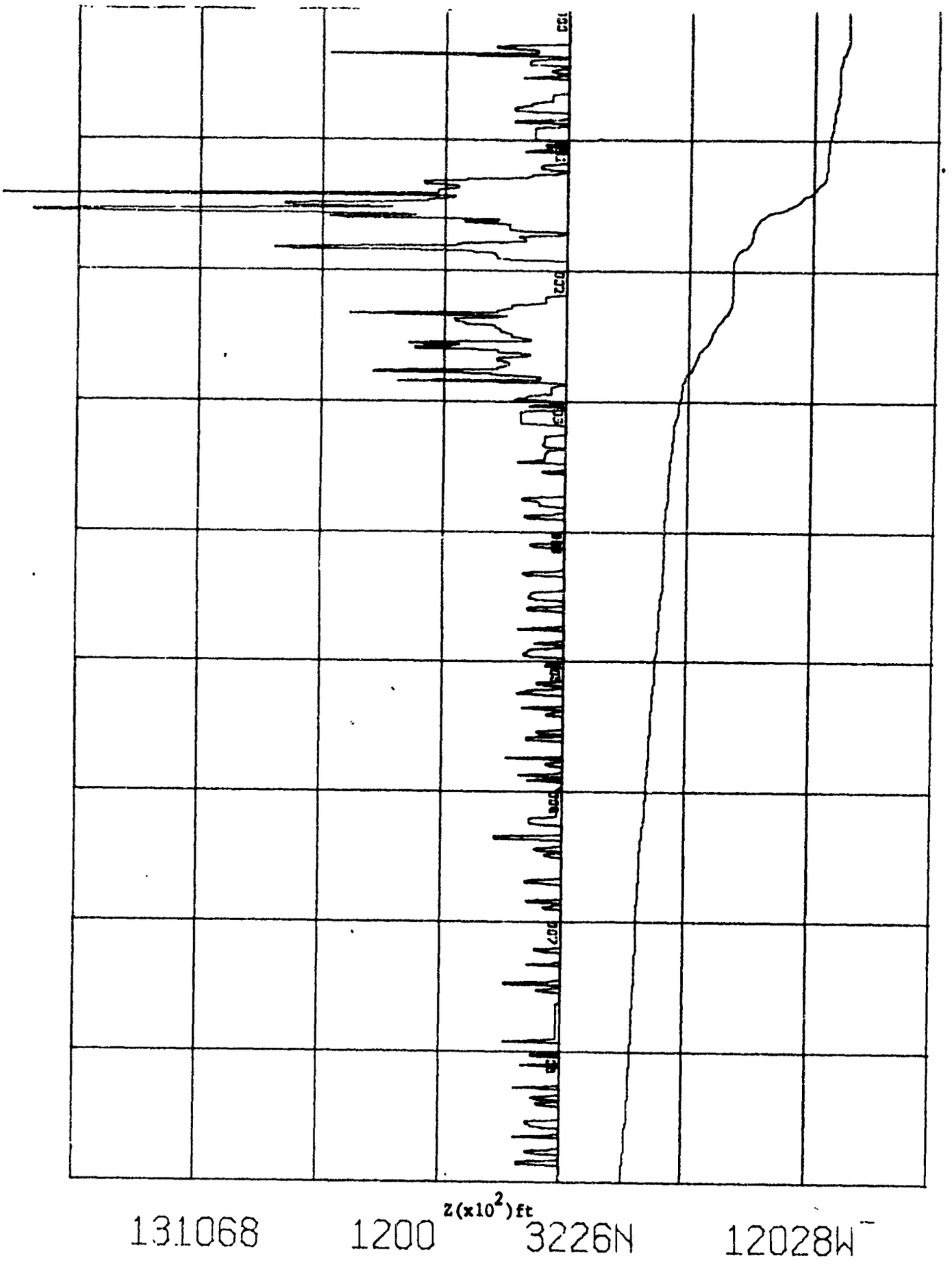

Figure 59. T-Z and G-Z Plots for Eastern North Pacific for 1200Z 13 October 1968.

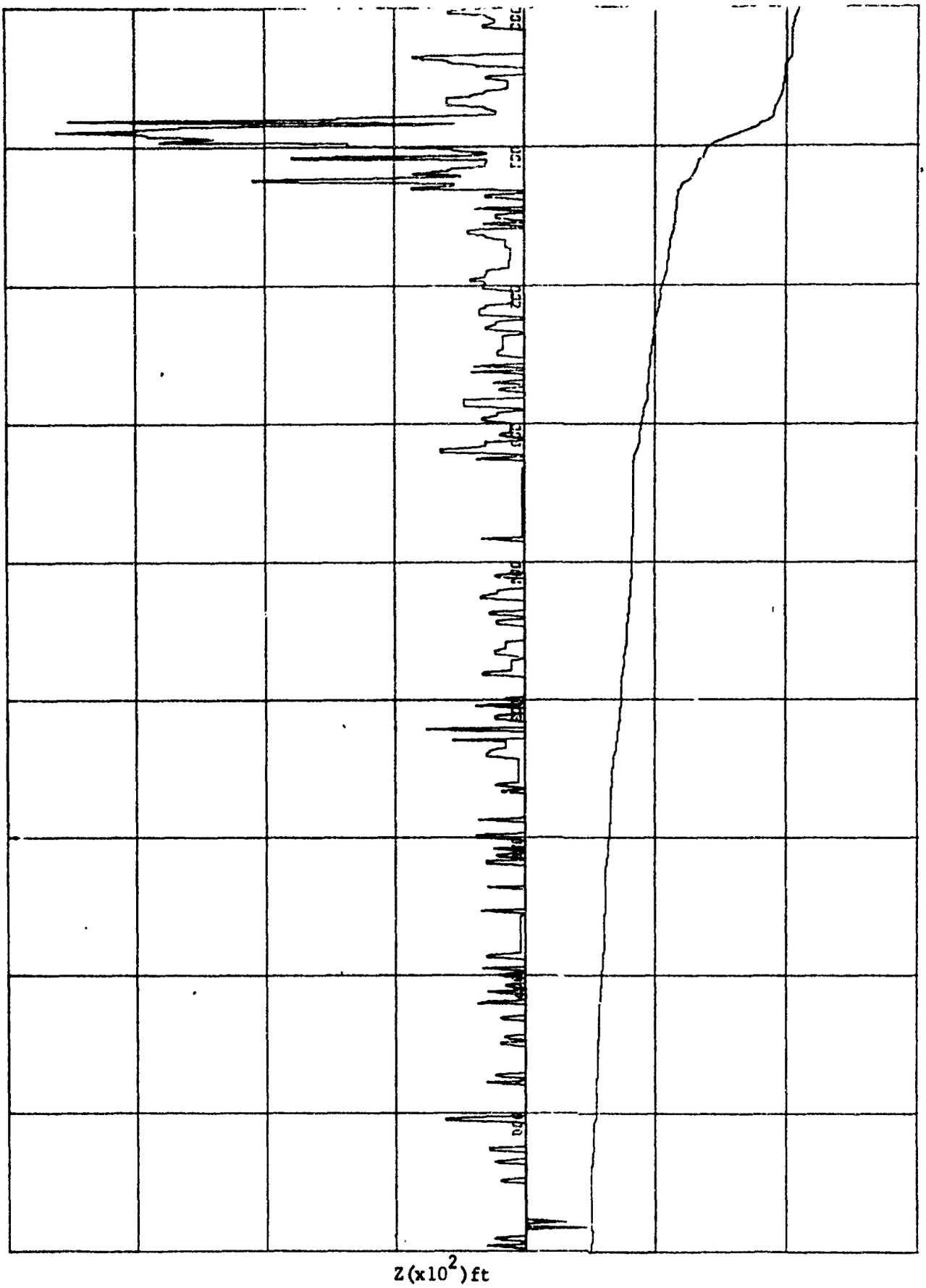

Figure 60. T-Z and G-Z Plots for Eastern North Pacific for 1800Z 13 October 1968.

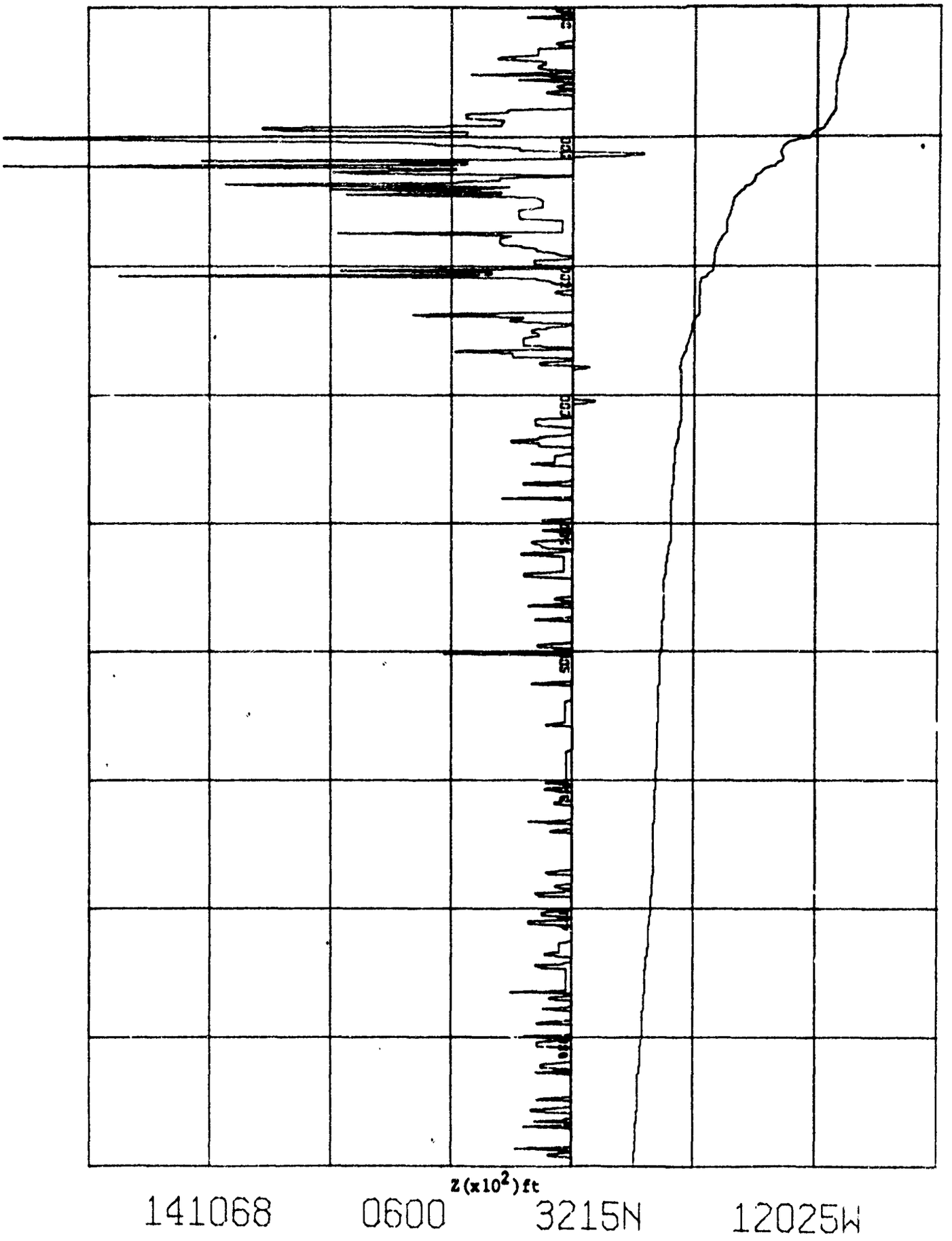

Figure 61. T-Z and G-Z Plots for Eastern North Pacific for 0600Z 14 October 1968.

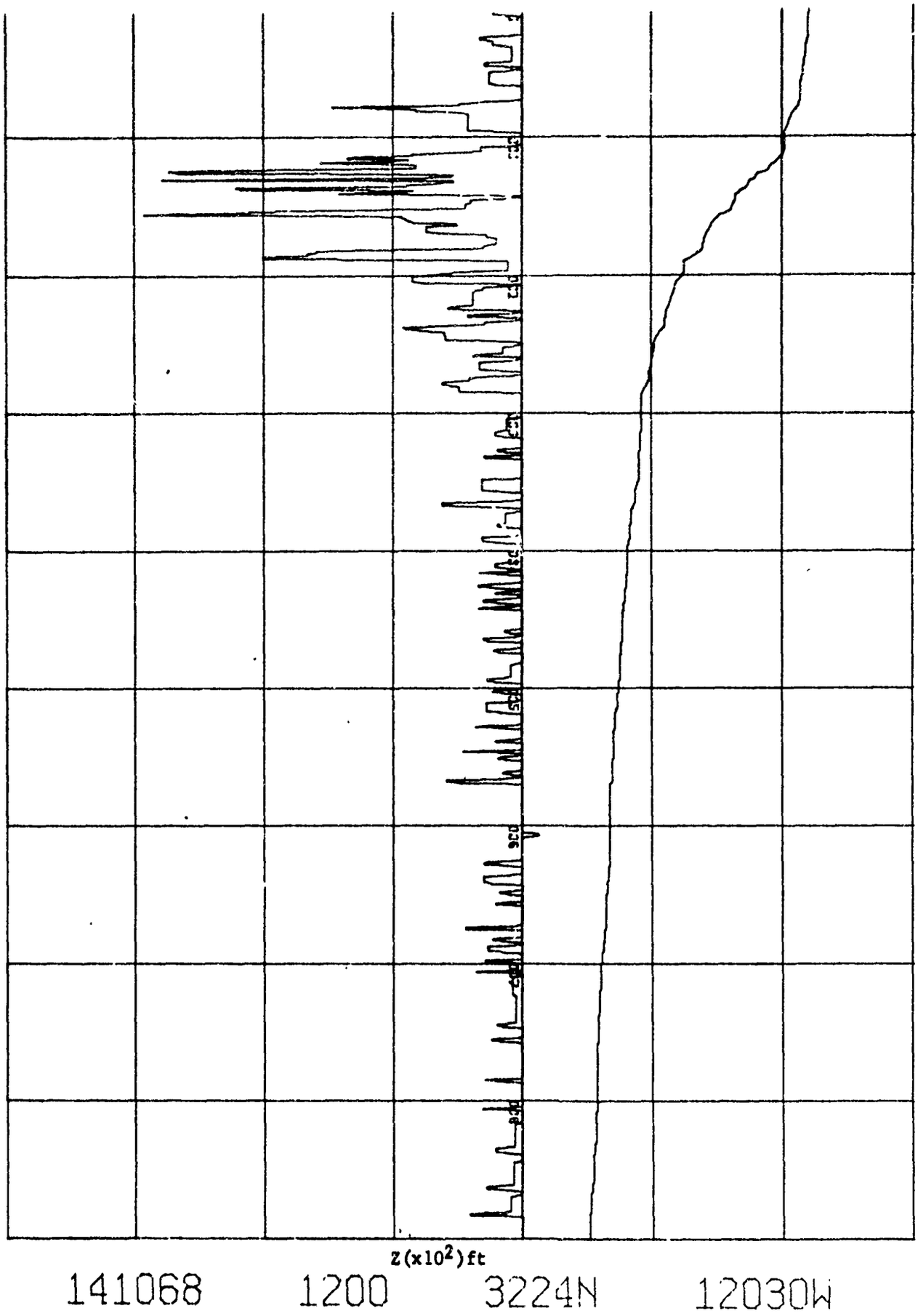

Figure 62. T-Z and G-Z Plots for Eastern North Pacific for 1200Z 14 October 1968.

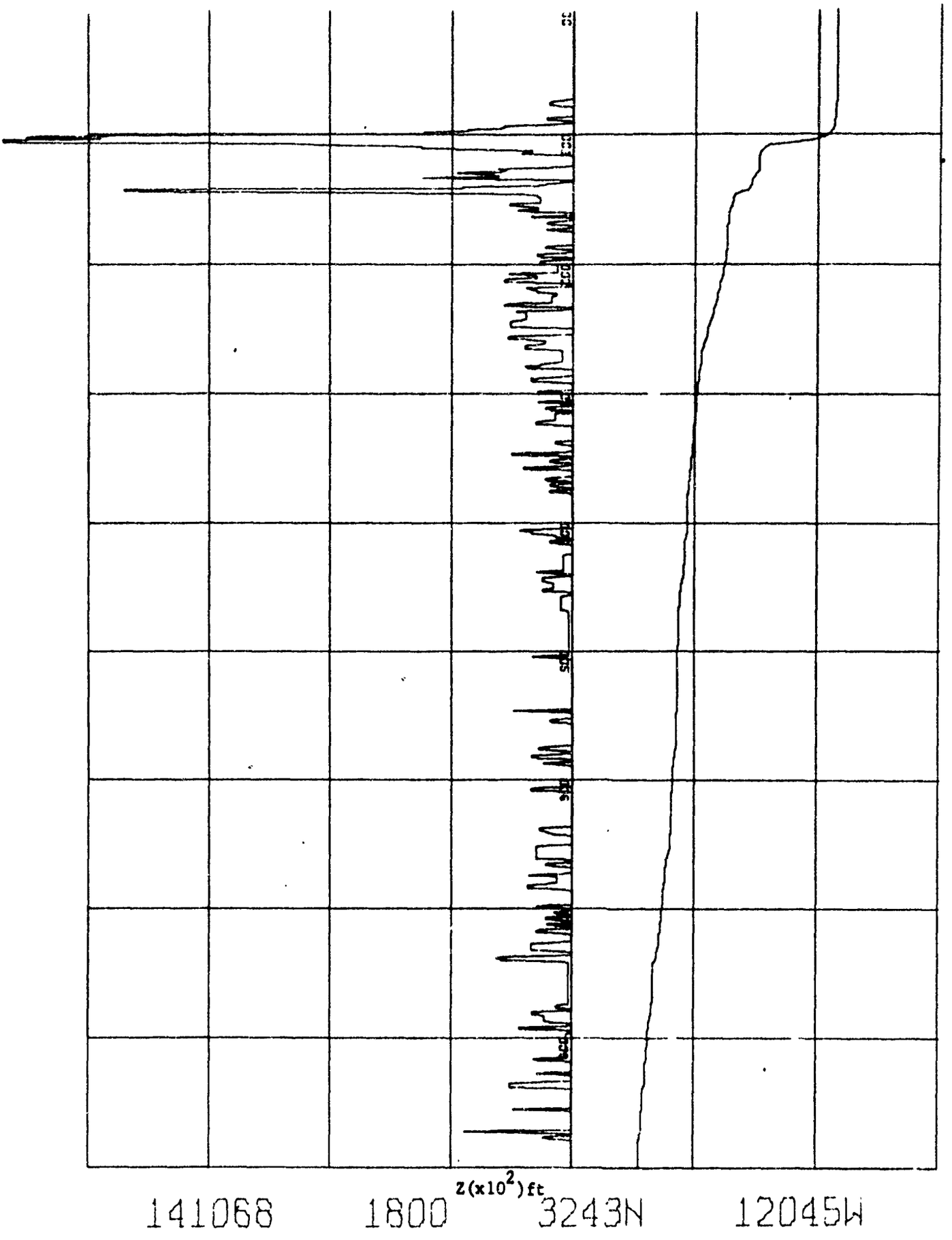

Figure 63. T-Z and G-Z Plots for Eastern North Pacific for 1800Z 14 October 1968.

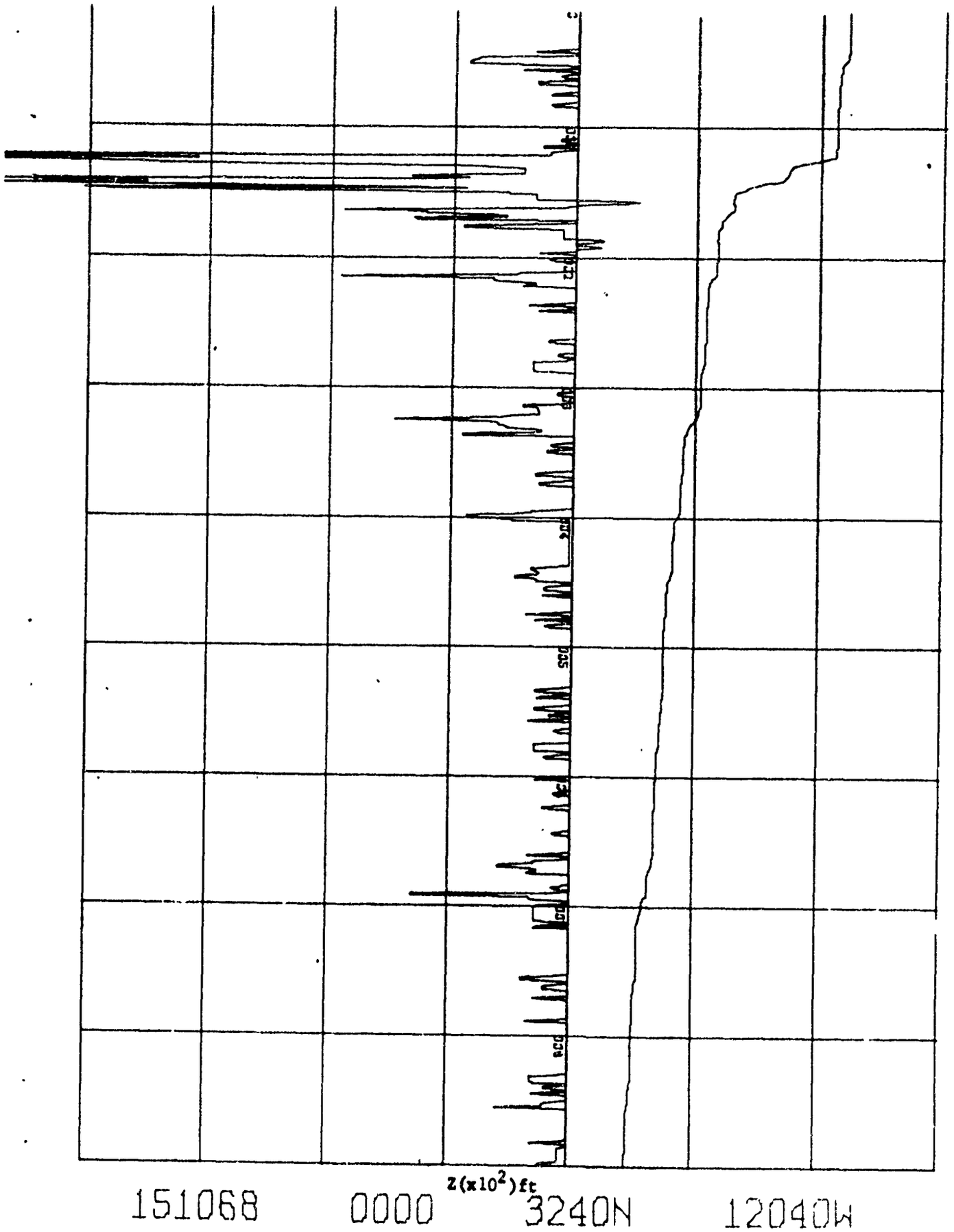

Figure 64. T-Z and G-Z Plots for Eastern North Pacific for 0000Z 15 October 1968.

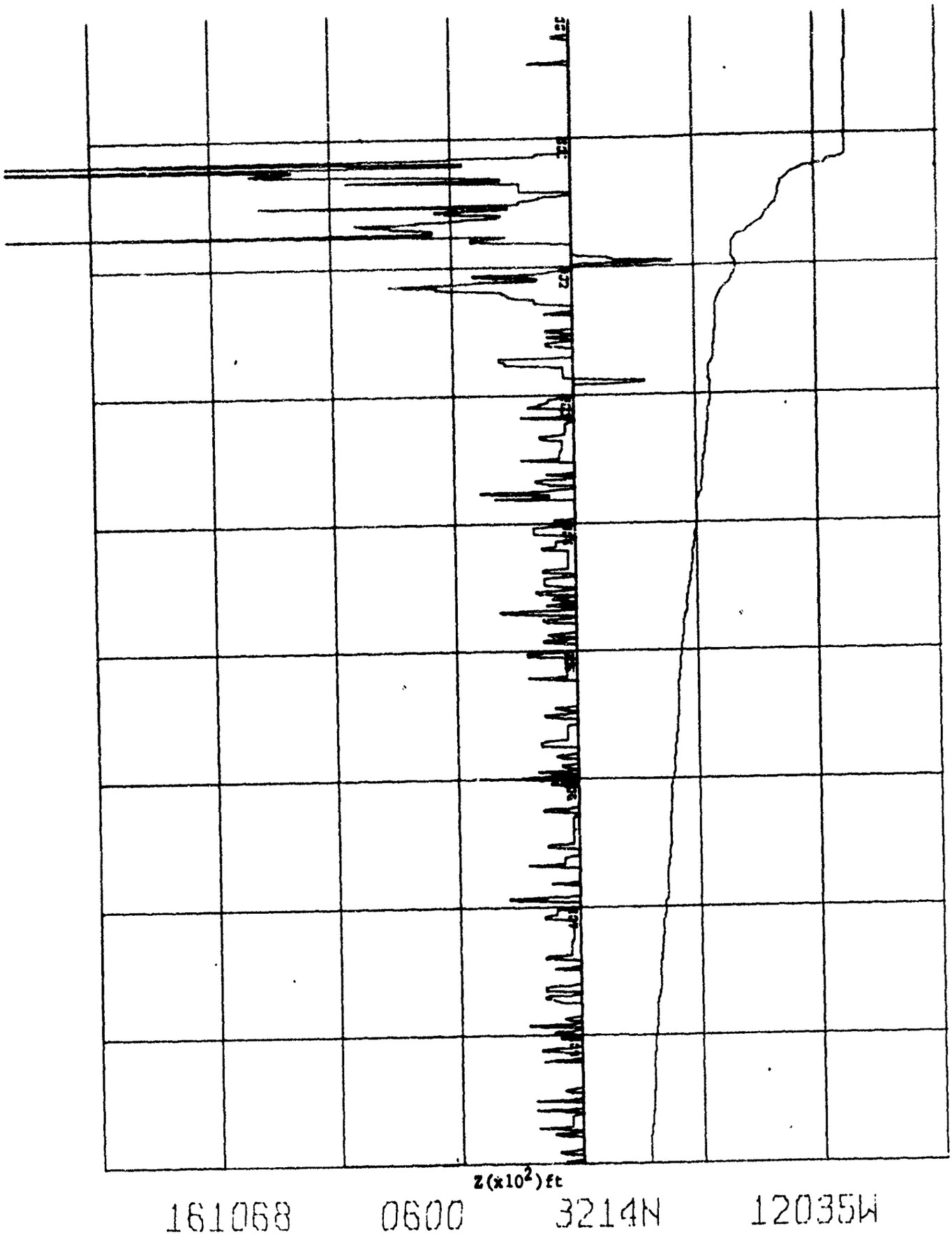

Figure 65. T-Z and G-Z Plots for Eastern North Pacific for 0600Z 16 October 1968.

1968 at 120 feet was clear on both the bathythermogram and the T-Z plot. The steps are quite irregular on the T-Z plot but not as irregular as on the G-Z plot.

4 Gulf Stream Region

Thirteen stations, during the period 11-13 August 1969, were analyzed for the Gulf Stream region (Figures 66 through 80). The ship's track crossed the Gulf Stream boundary several times.

a. Interior of Gulf Stream

For the interior of the Gulf Stream (Figures 70 and 71), the mixed layer is distinct and a typical seasonal and main thermocline are shown. A "boot" in the 100 foot layer is clearly shown by positive gradient values in several of the figures and the actual XBT traces.

b. Frontal Region

Strong gradients are the rule for this region and they are quite distinct in both the T-Z and G-Z plots. The contrast between the frontal and interior regions of the Gulf Stream are quite apparent.

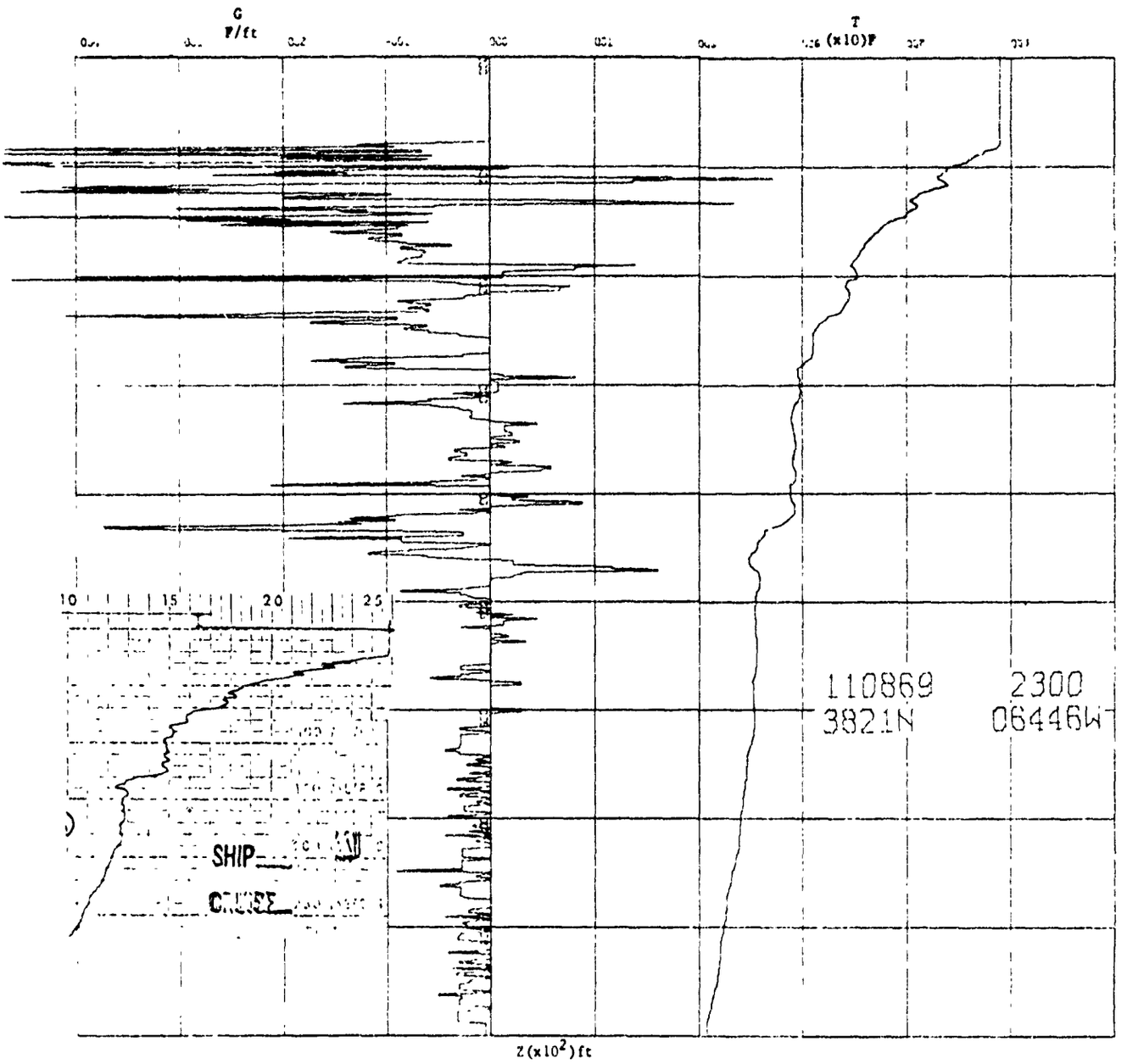

Figure 66 T-Z and G-Z Profile for Transects across Northern Boundary of the Gulf Stream. Actual XBT T-Z Trace Inset.

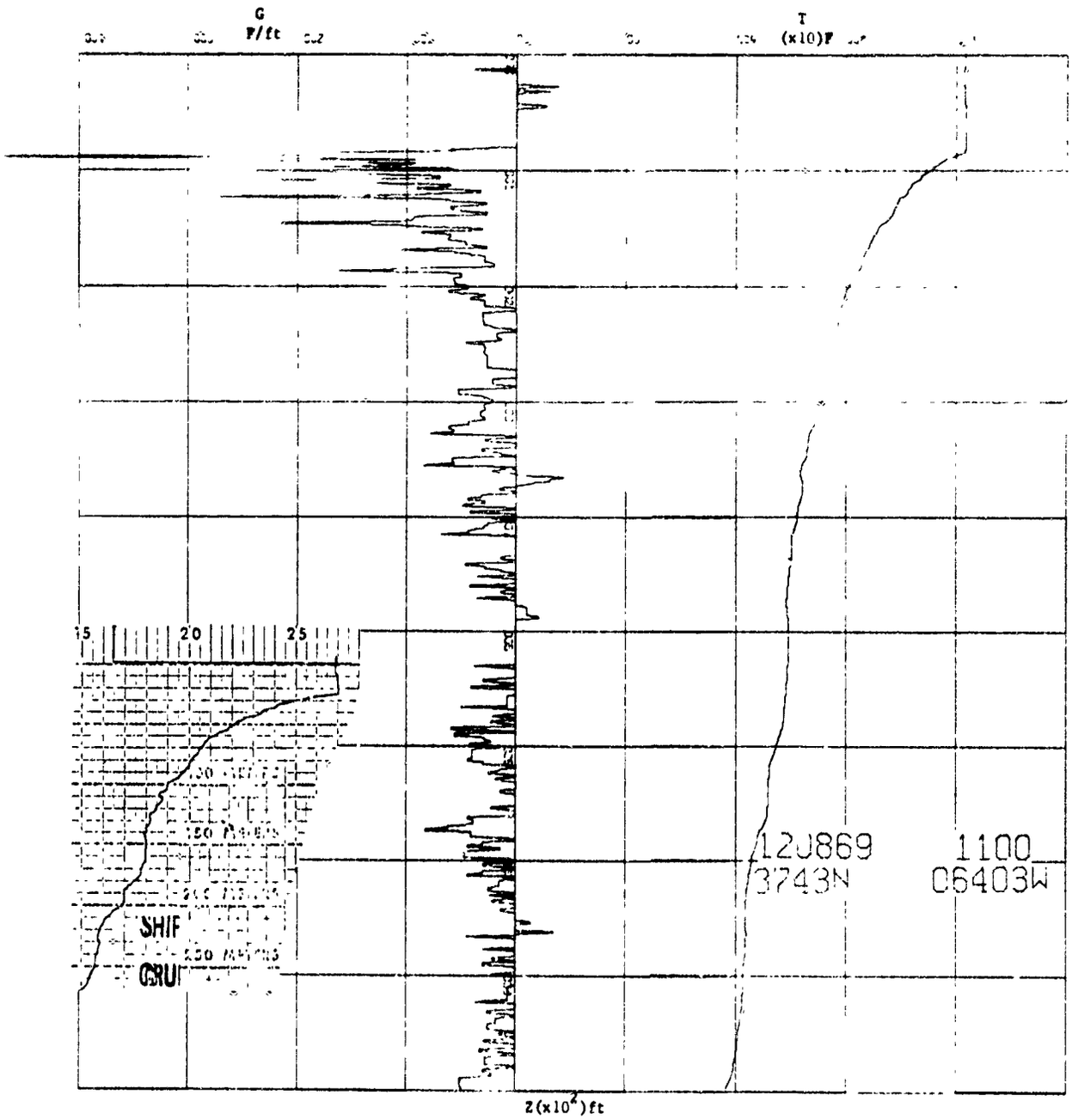

Figure 67. T-Z and G-Z Profile for Transects across Northern Boundary of the Gulf Stream Actual XBT Trace Inset.

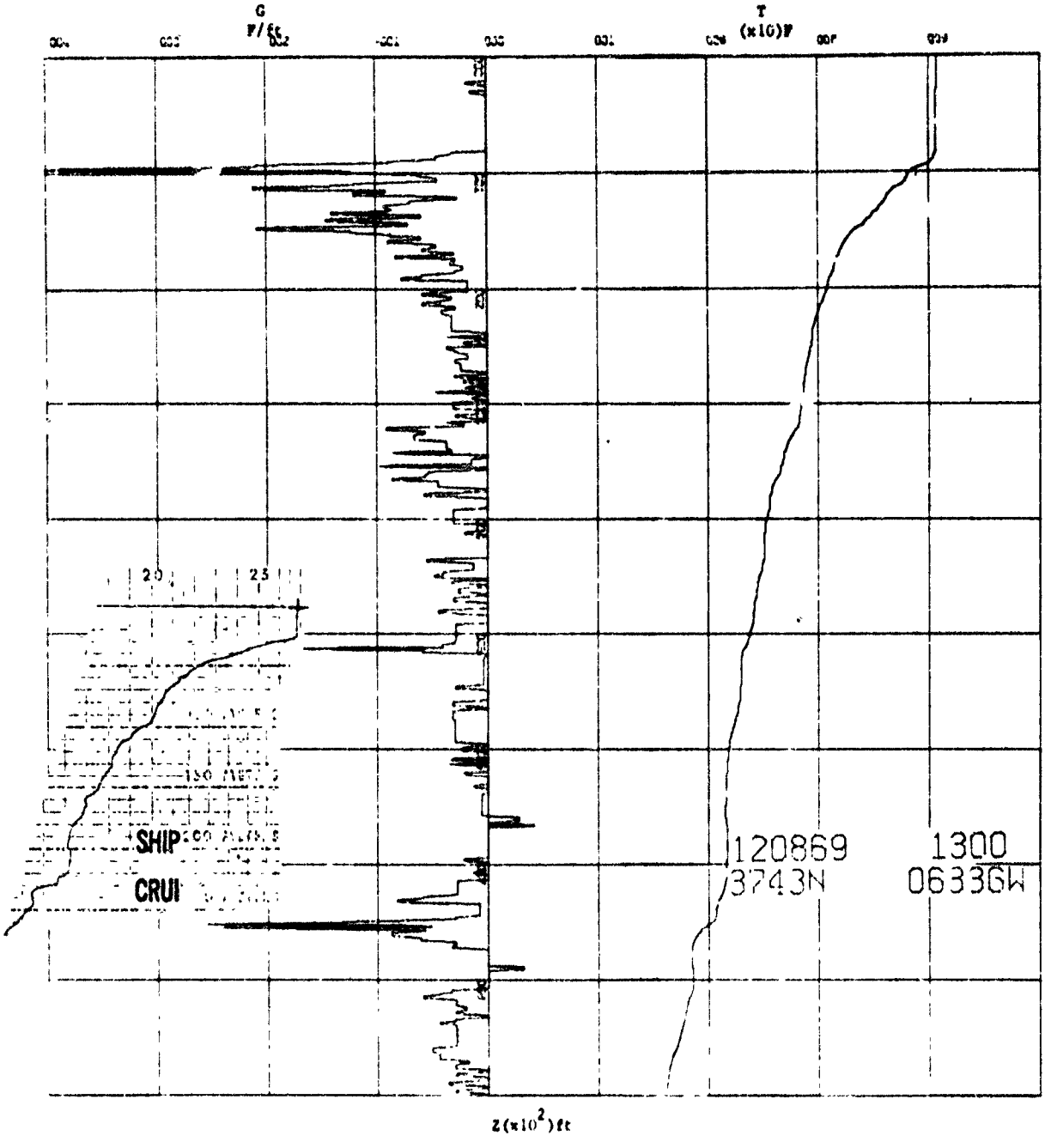

Figure 68. T-Z and G-Z Profile for Transects across Northern Boundary of the Gulf Stream. Actual XBT T-Z Trace Inset.

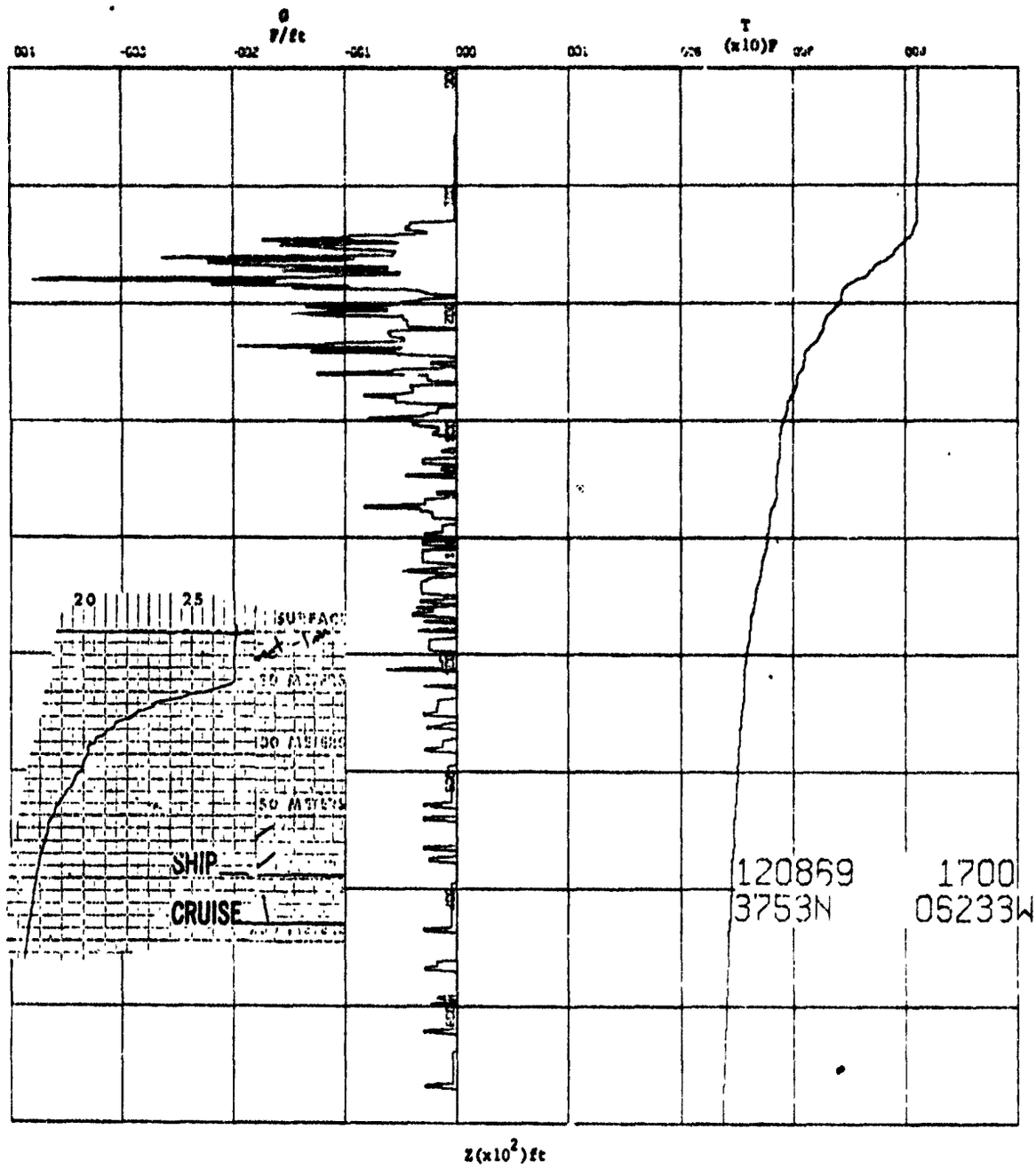

Figure 69. T-Z and G-Z Profile for Transects across Northern Boundary of the Gulf Stream. Actual XBT T-Z Trace Inset.

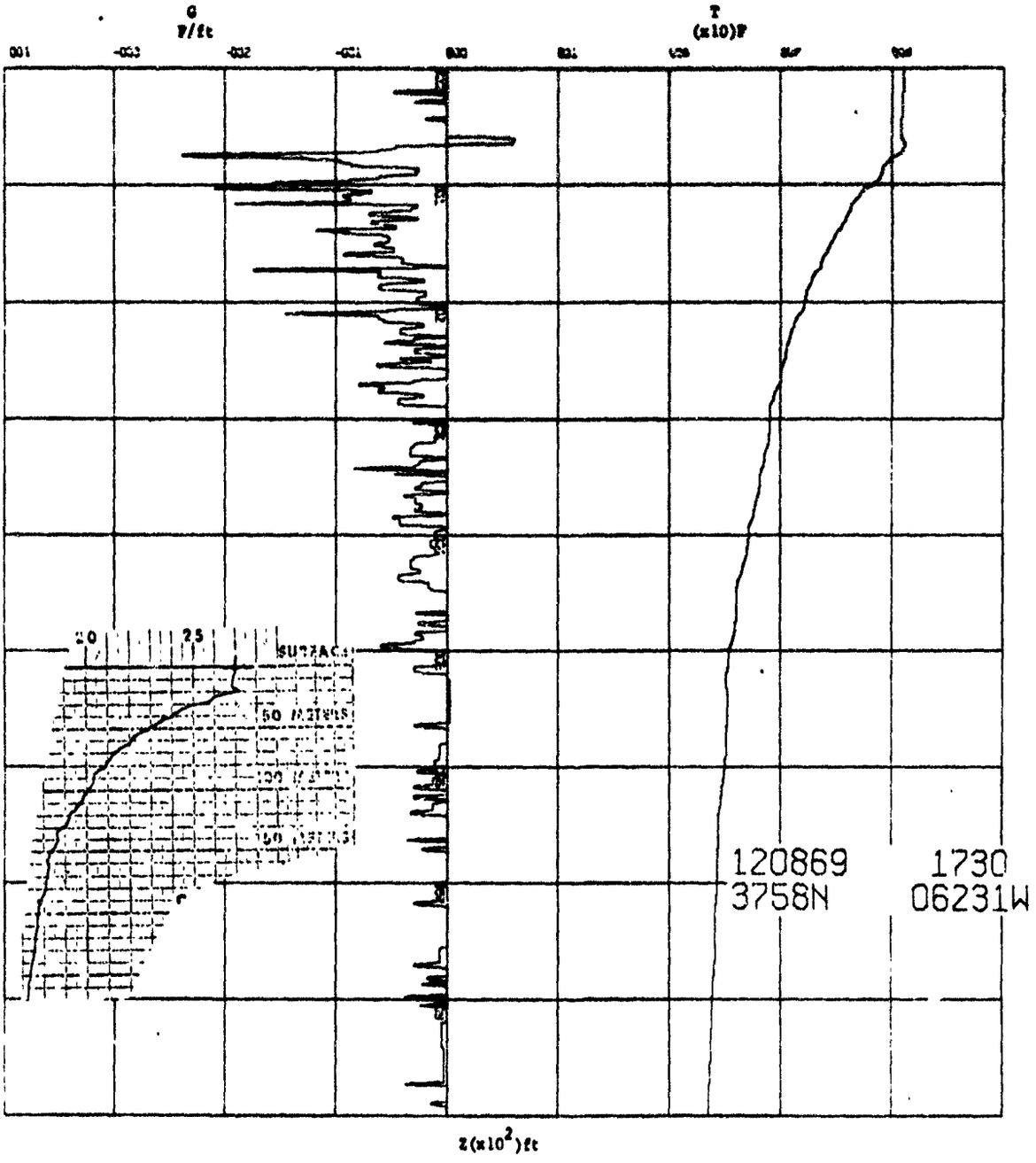

Figure 70. T-Z and G-Z Profile for Transects across Northern Boundary of the Gulf Stream. Actual XBT T-Z Trace Inset.

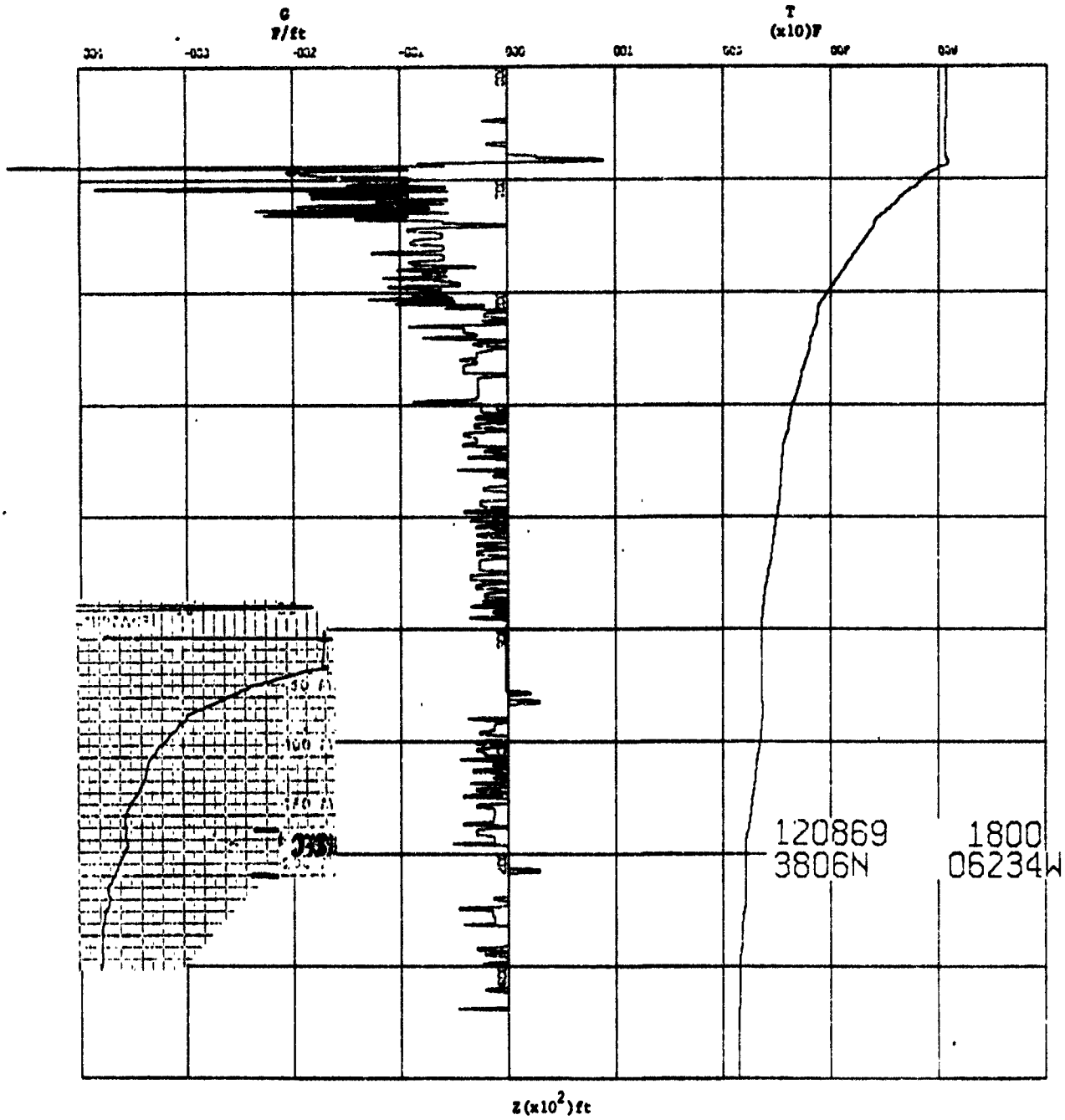

Figure 71. T-Z and G-Z Profile for Transects across Northern Boundary of the Gulf Stream. Actual XBT T-Z Trace Inset.

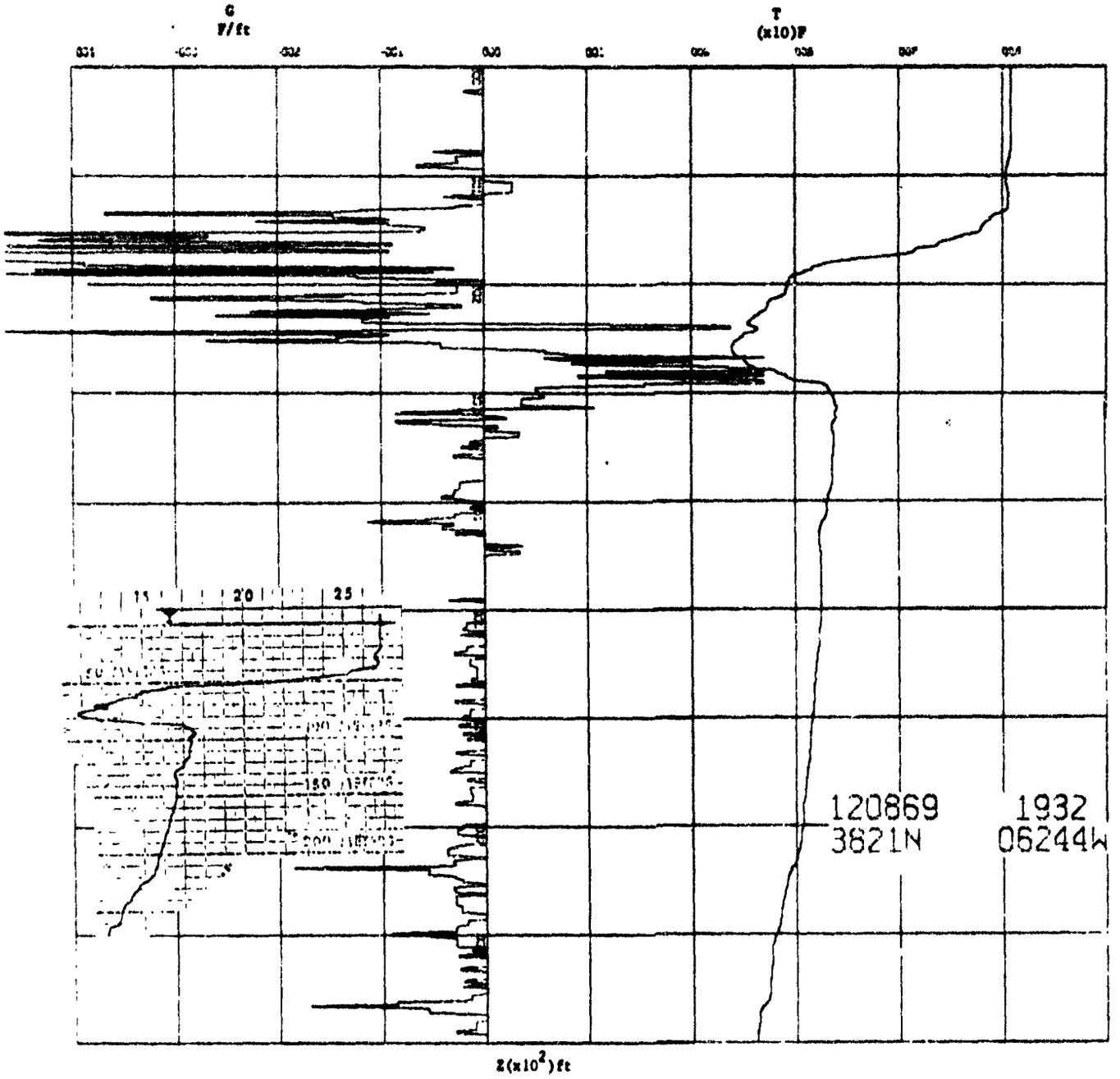

Figure 72. T-Z and G-Z Profile for Transects across Northern Boundary of the Gulf Stream. Actual XBT T-Z Trace Inset.

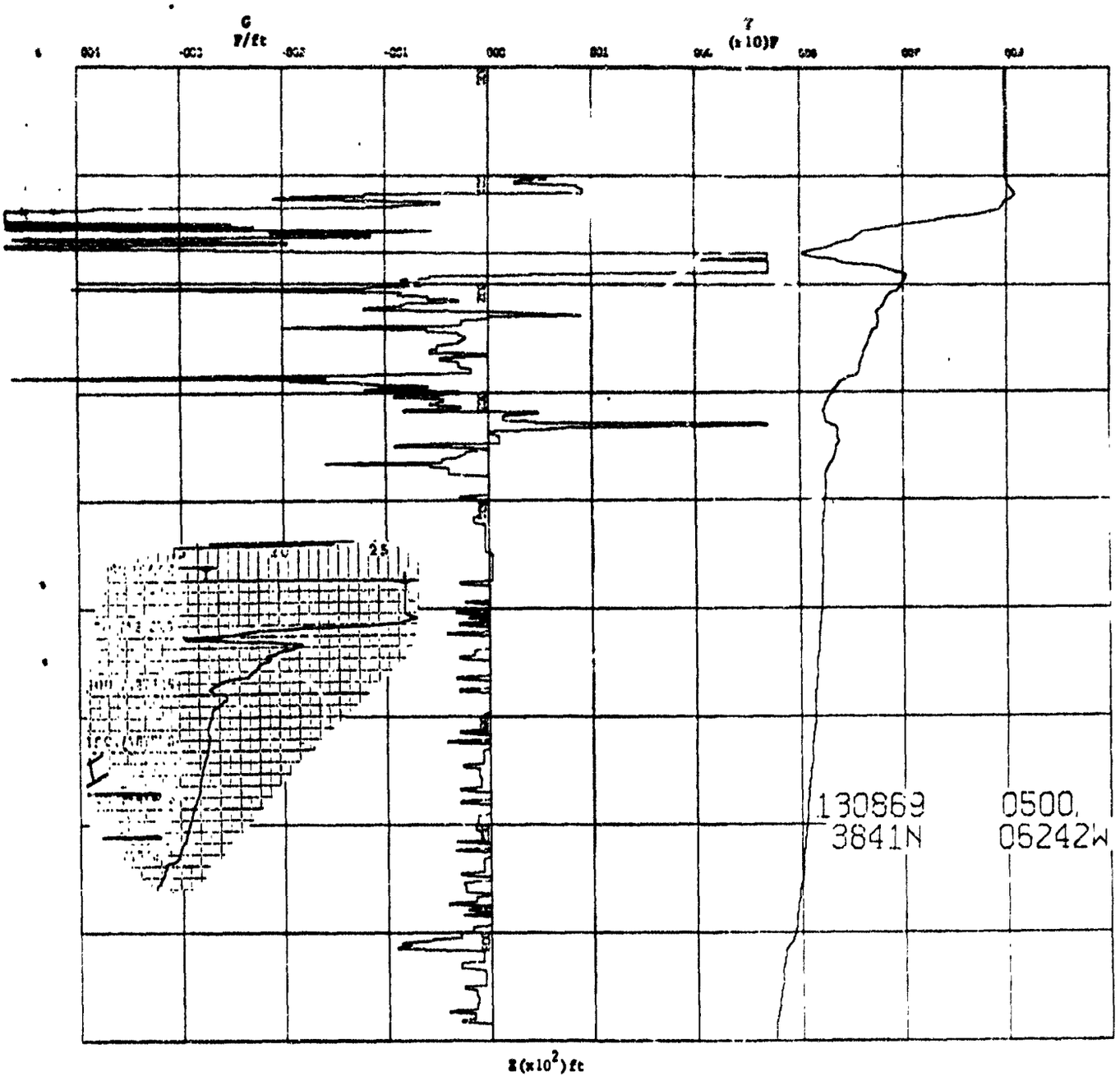

Figure 73. T-Z and G-Z Profile for Transects across Northern Boundary of the Gulf Stream. Actual XBT T-Z Trace Inset.

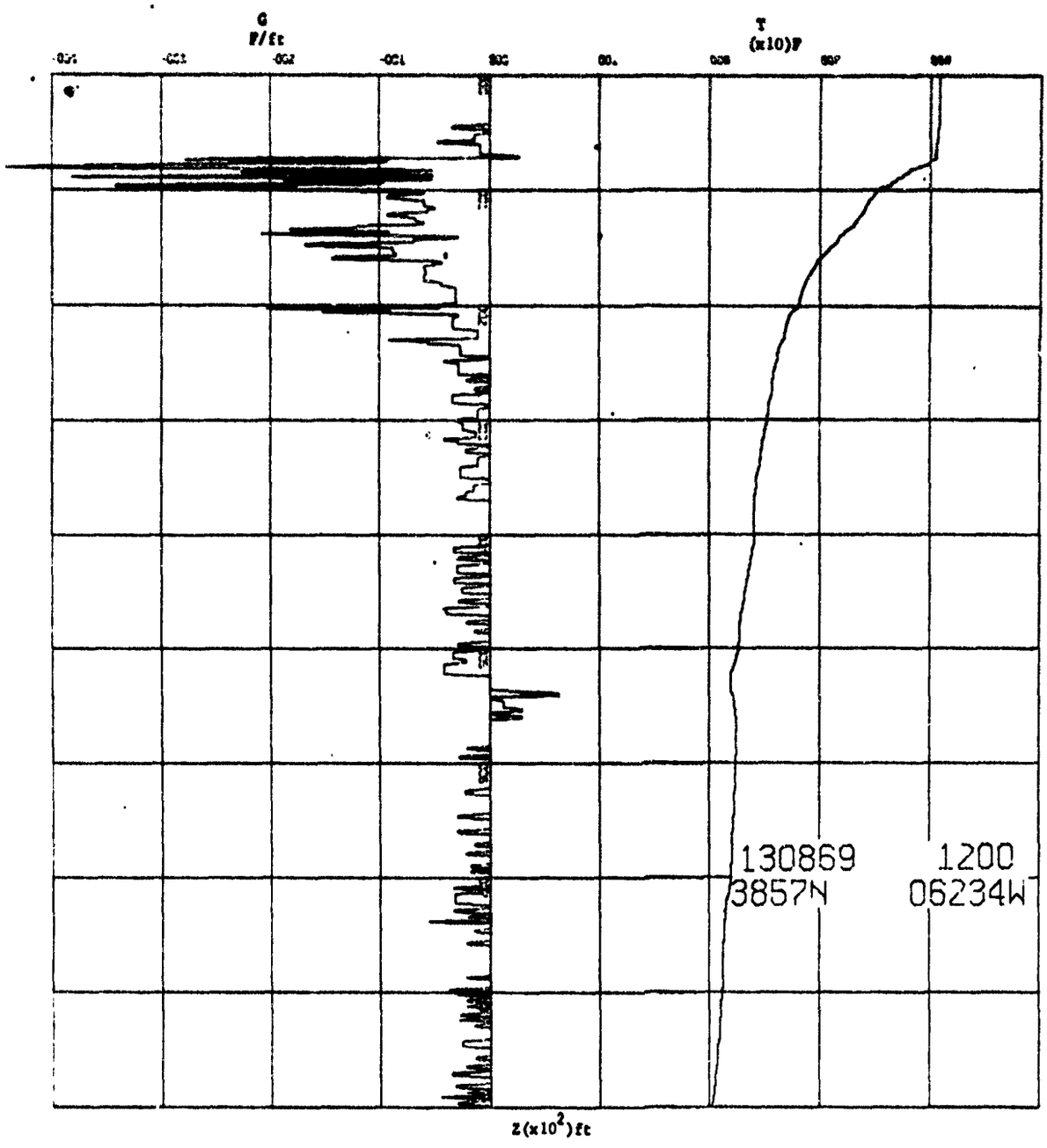

Figure 74. T-Z and G-Z Profile for Transects across Northern Boundary of the Gulf Stream.

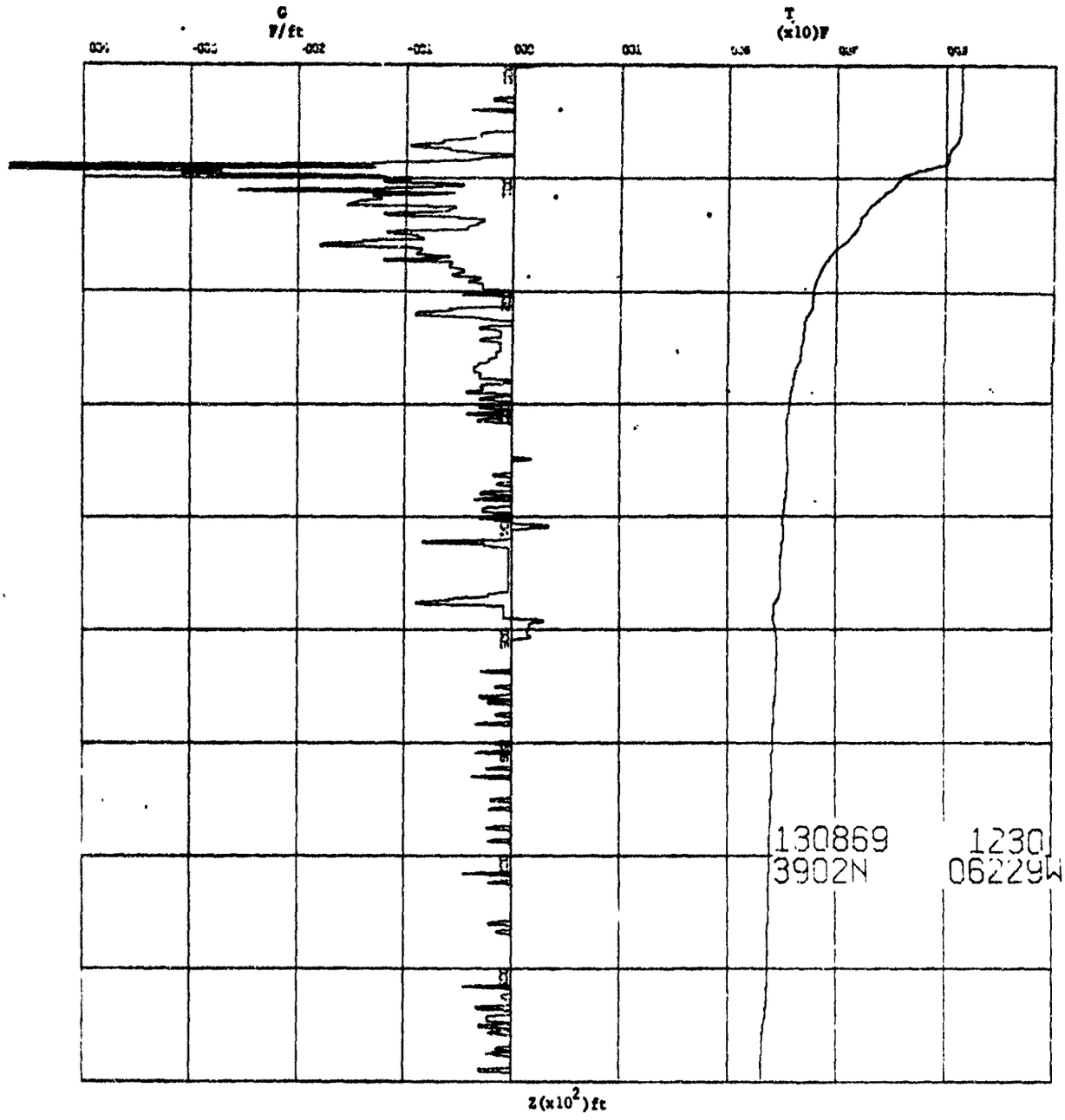

Figure 75. T-Z and G-Z Profile for Transects across Northern Boundary of the Gulf Stream.

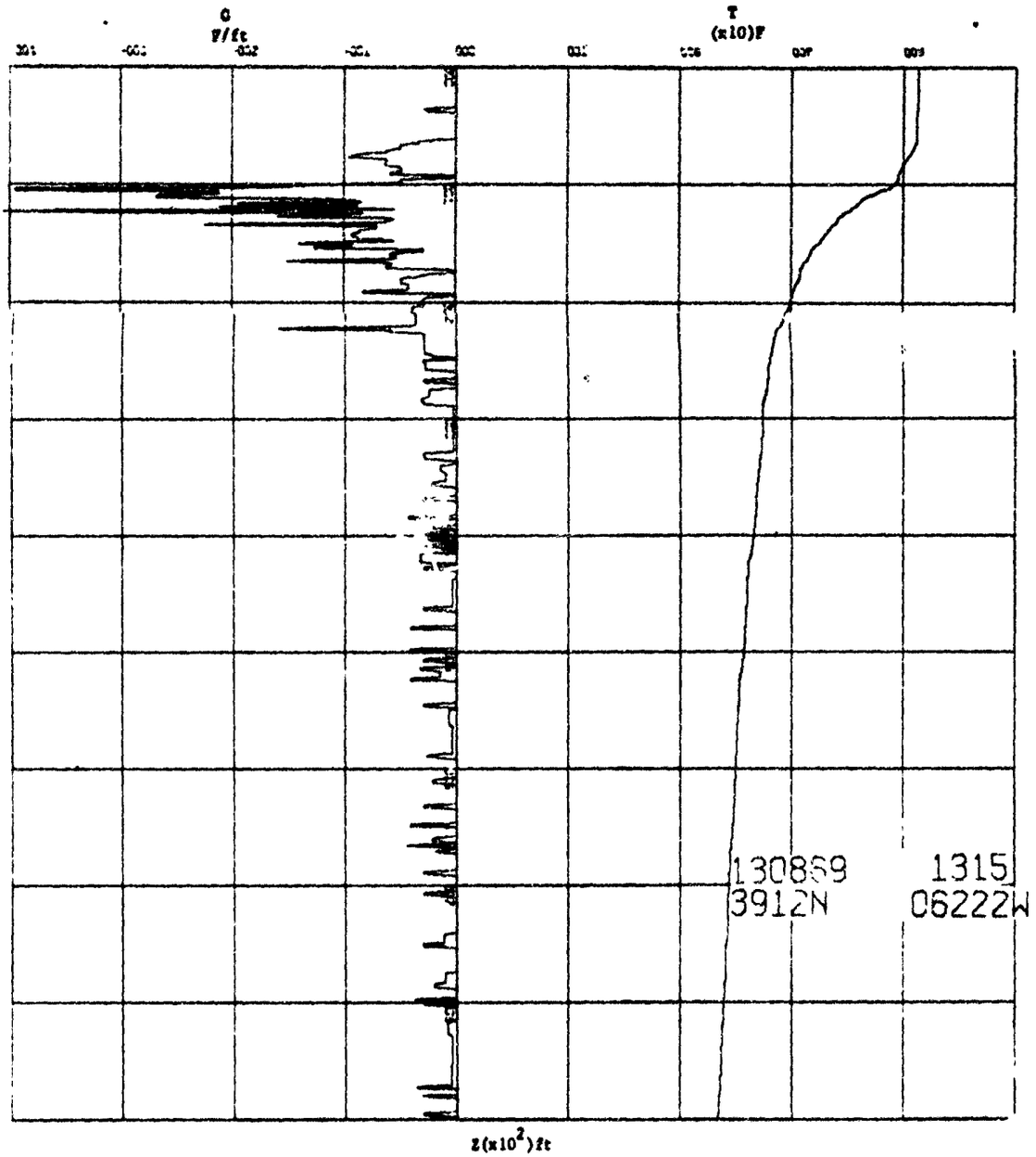

Figure 76. T-Z and G-Z Profile for Transects across Northern Boundary of the Gulf Stream.

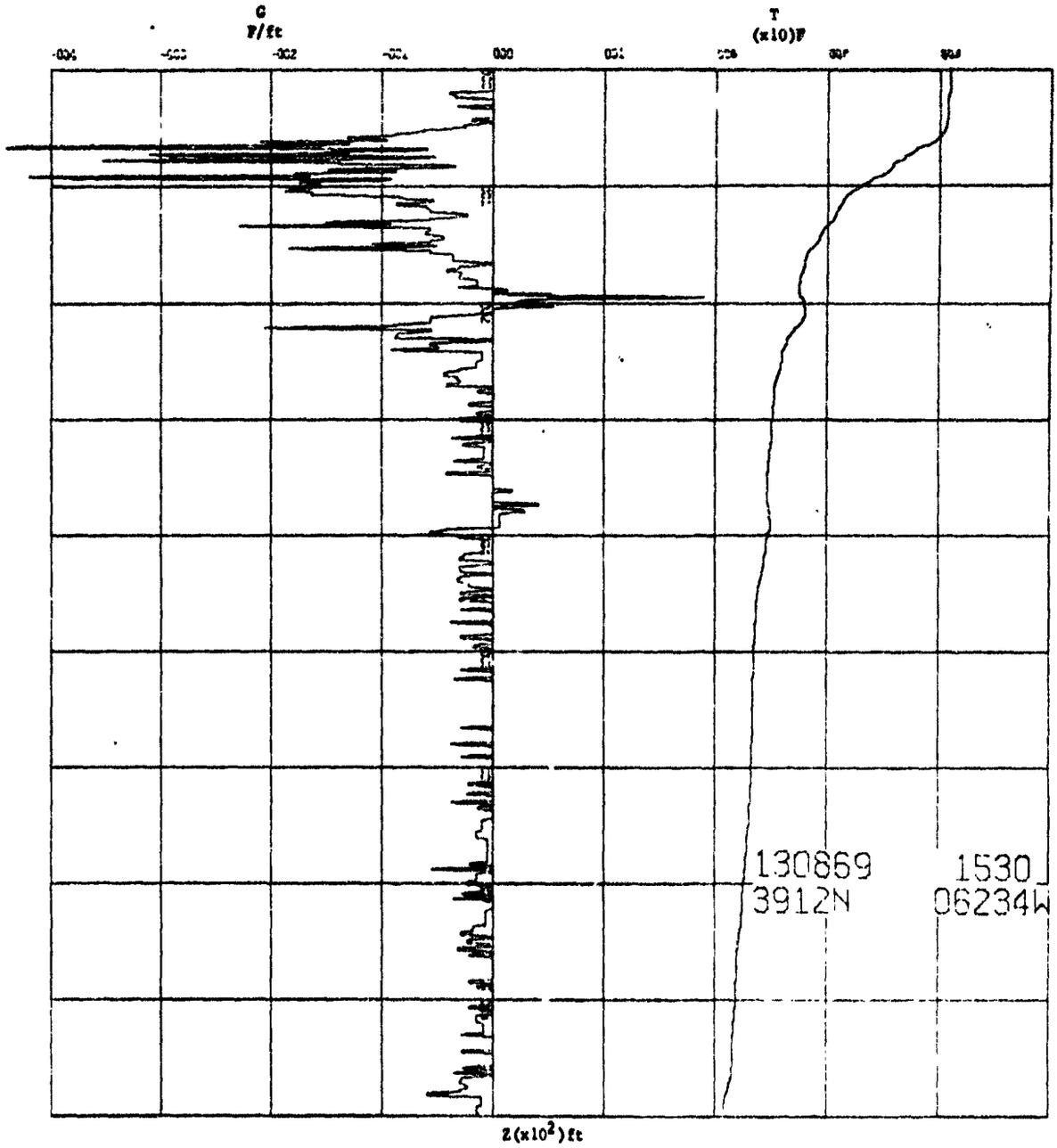

Figure 77. T-Z and G-Z Profile for Transects across Northern Boundary of the Gulf Stream.

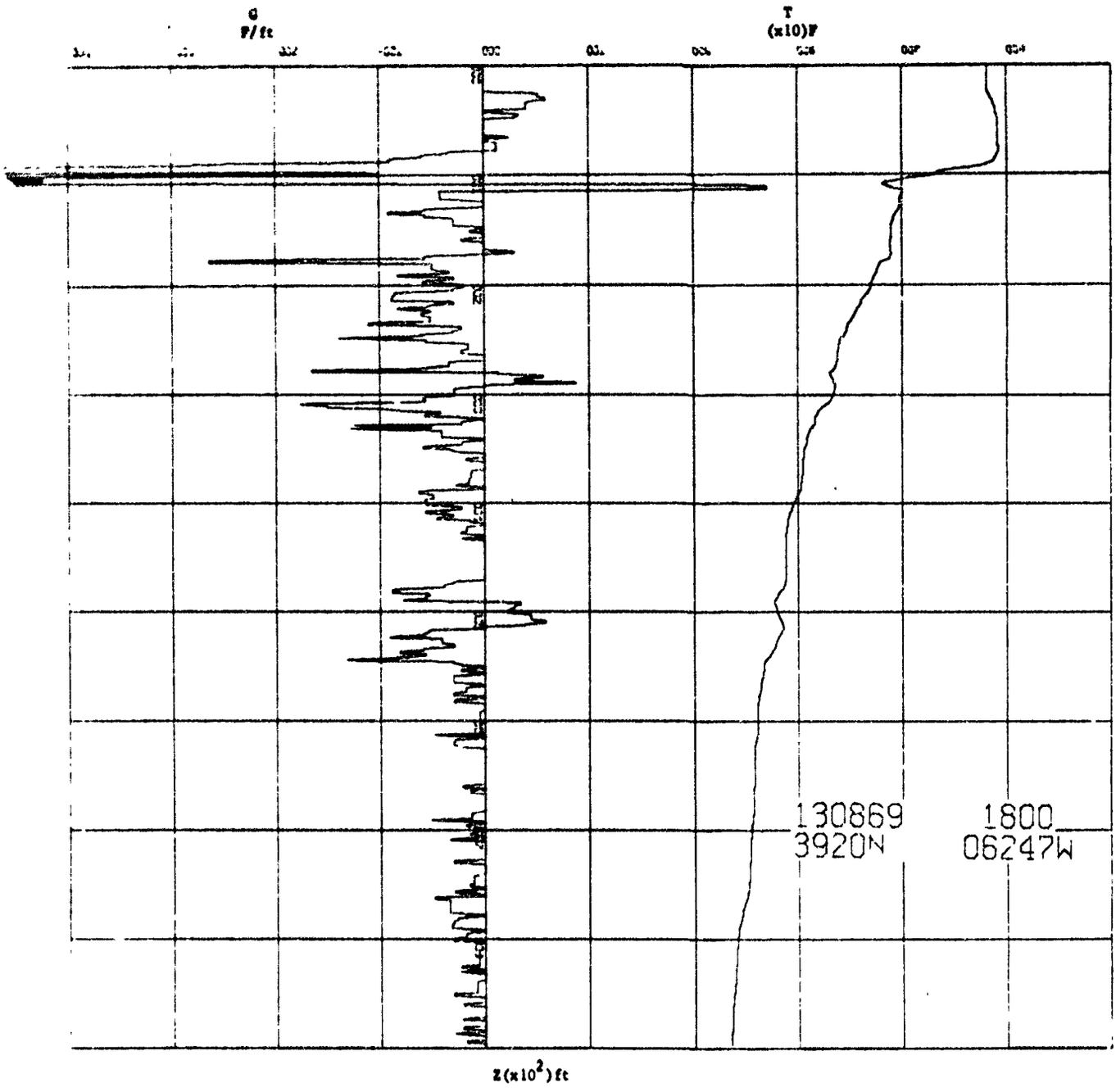

Figure 78- T-Z and G-Z Profile for Transects across Northern Boundary of the Gulf Stream.

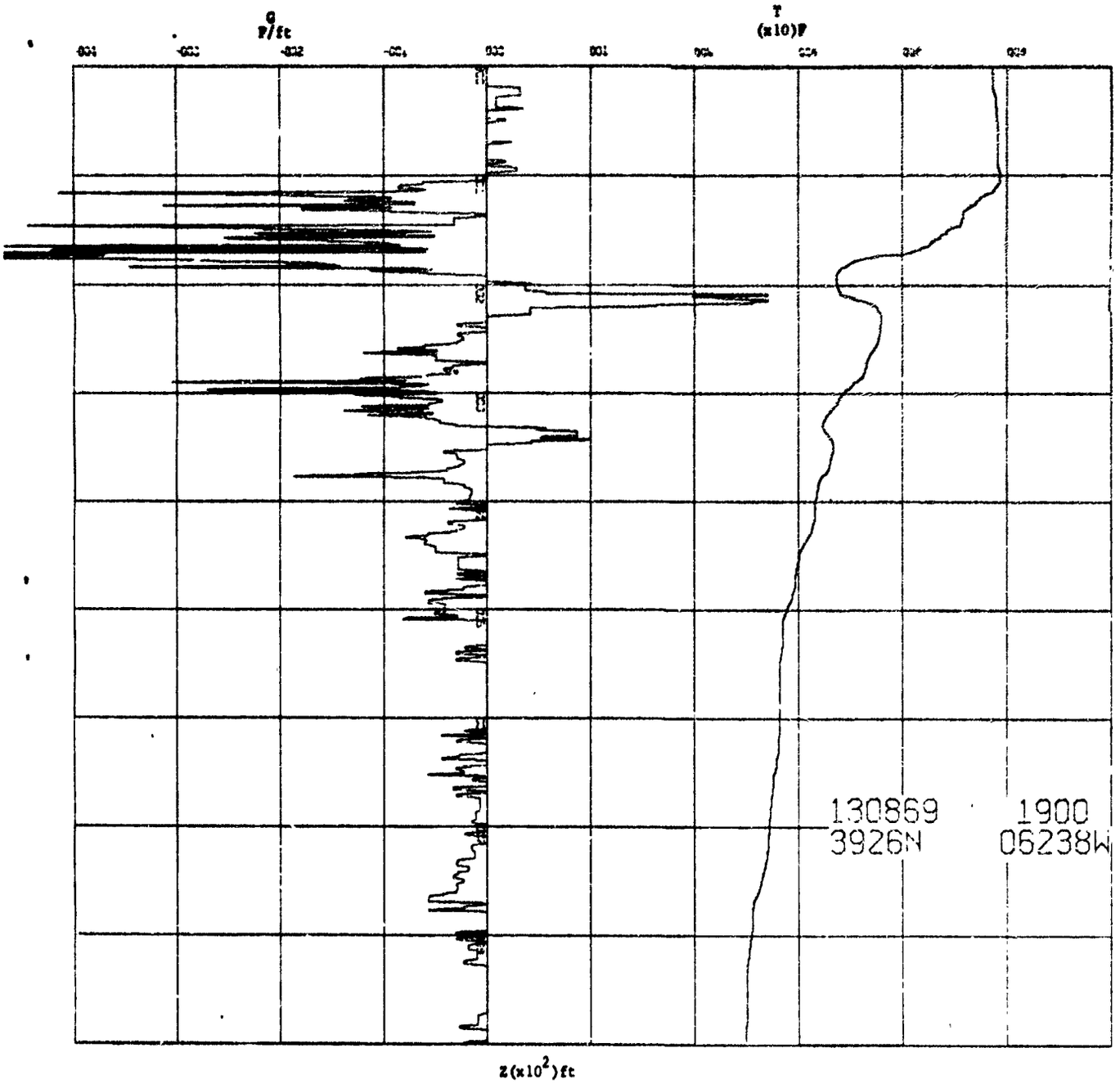

Figure 79. T-Z and G-Z Profile for Transects across Northern Boundary of the Gulf Stream.

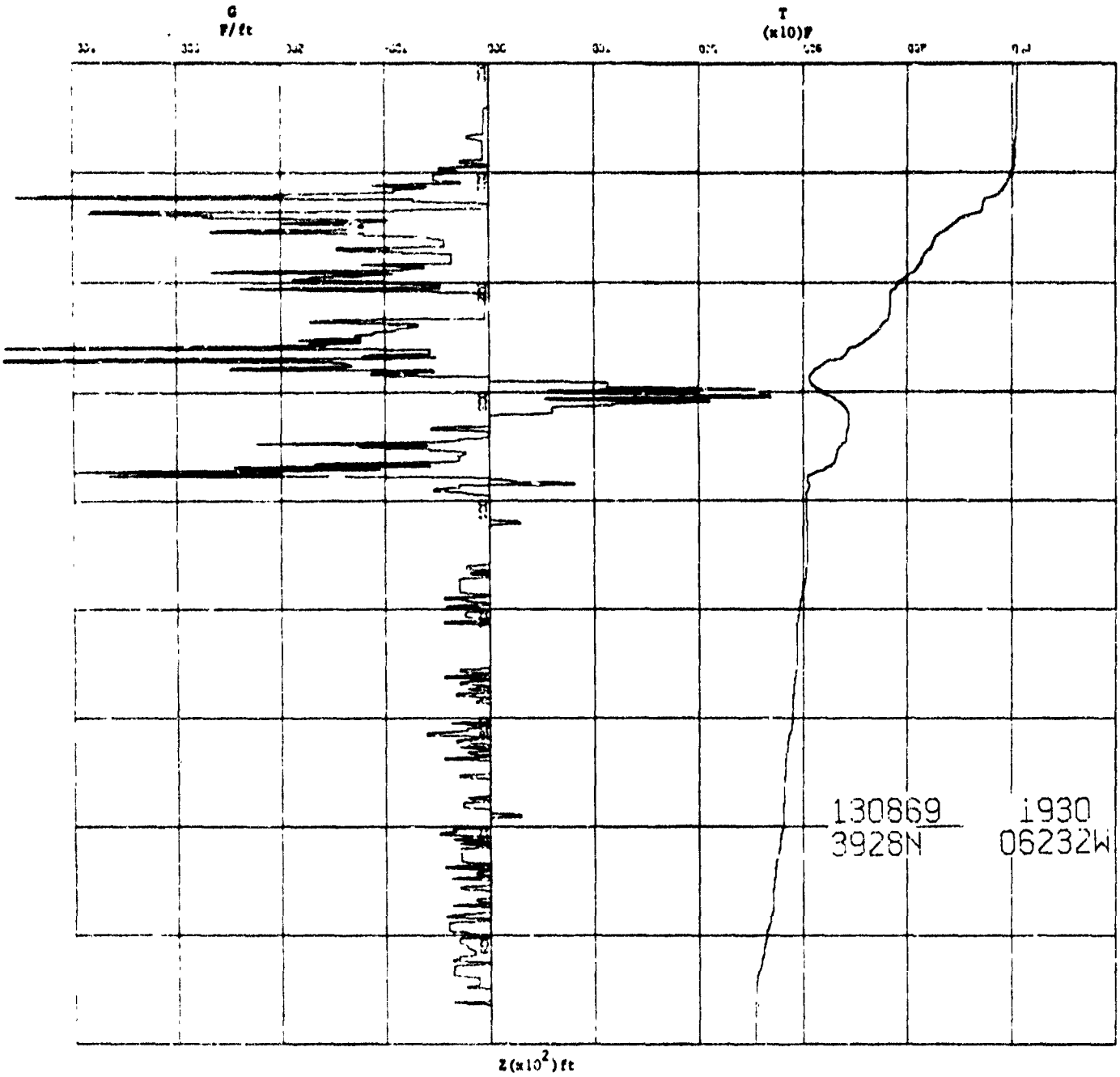

Figure 80. T-Z and G-Z Profile for Transects across Northern Boundary of the Gulf Stream.

VI. CONCLUSIONS

The results give a measure of the microthermal structure obtained with an XBT by the NDM.

A. PHYSICAL SIGNIFICANCE

Microthermal structure statistics have not been adequately explored. This thesis has proposed an easy method to observe the fine-scale thermal structure. Further, this proposed objective analysis scheme does not use the T-Z values but rather the G-Z values. It is the G-Z distribution which is important. The T-Z can always be reconstructed if one additional parameter, the SST, is known.

1. Internal Waves - Väisälä Frequency

The Brunt-Vaisala frequency is the maximum frequency of oscillation of free internal waves. It may be calculated from the density gradient, or from the parameters which define density gradient. In isohaline water, the NDM gives a direct measure of density (or stability). In such waters it could be used to set an upper limit on the maximum frequency of oscillation of internal waves. Further, a time series study would clearly illustrate the amplitudes likely to be encountered since the sheets indicated on the G-Z diagram are readily identified. A correlation study of G-Z, Brunt-Väisälä versus depth diagrams would be useful.

2. Oceanic Fronts

This difficult region to analyze microscopically could possible be better explored by using the NDM for the microthermal processes. The NDM explores the continuously changing conditions in frontal regions.

Frontal regions are usually indicated by extremely complex G-Z plots which illustrate the extreme gradients, both positive and negative, encountered. Based on the admittedly small number of cases examined, there appears to be a tendency of the layers to maintain their characteristics and slide by, over or under each other rather than mix.

3. Sound Propagation

The effect of microthermal structure on sound propagation require better statistical knowledge of the oceans. The NDM gives emphasis to the strongest gradient regions.

The microthermal effects on index or refraction variations (density fluctuations) must be determined. Using the NDM with salinity variations (from an STD cast) and the NDM with sound velocity variations (from an SVTP cast) taken from the two instruments simultaneously, cross-correlation techniques could shed some light on the unresolved micro-processes in the ocean. In particular, what are the exact physical and theoretical correlations among the salinity, temperature, and sound velocity.

B. SUGGESTED STUDIES

Possible studies for the future have suggested themselves while developing this thesis.

1. Mathematical Models

Various mathematical models attempted could be explored further because each method had some merit. Suggested models are limited by their utility.

a. Analysis Methods

The microthermal structure recorded by XBTs can be looked at as a "roughness" factor, the noise level of the water structure. Further

work is required to determine such a factor for practical operational use. This roughness factor should be computed as the XBT trace is being analyzed at FNWC by a program like DIGITBT. This factor could be one number to describe objectively the microthermal structure variations on the G-Z trace.

Variations in the NDM should be used with the variables that have been arbitrarily set. For example, the depth interval of $\Delta T/ft$ at one foot should be varied to find the effects a larger or smaller depth interval would have on the G-Z profiles. As the steps become smaller, the exact derivative is approached. Larger steps should smooth the spikes shown in the G-Z figures. In some cases, this smoothed G-Z profile might be described with curve fitting techniques as suggested by Boston [1966] and Grosfils [1968].

MICROXBT's digitizing interval of 0.01 inches should be changed to 0.005 inches and the program modified to use this interval. This would yield more detailed thermal structure than MICROXBT. Obviously, one cannot make the interval finer than the noise level of the sensor or recording instrument.

b. Physical Processes

The G-Z profiles from the NDM emphasize the changing physical features which are obscure in the T-Z profiles. By using G-Z profiles for parameters other than temperature, clarity in determining distributions of chemical parameters would be similarly emphasized. Limitations in use of the NDM on other chemical properties should be further investigated.

Water mass identification is possible with G-Z profiles. Additional work is required in this area.

2. Experimental Work

A microthermal sheet probe could be designed for investigating the chemical and physical processes inside the sheet and inside the layers. A comparison of actual physical property differences should be made.

A modified expendable temperature gradient (XTG) meter could be designed using two thermistors to obtain the temperature differences in the probe. The standard XBT system equipment already installed could be changed to give analog G-Z profiles to the operational user without any delay.

a. Time Series

The XTG meter could be used to construct G-Z variability at one location by conducting a time series analysis. This needs to be done in order to obtain a roughness factor, an objective microstructure measuring parameter.

b. Transect

An XTG meter could be used in transects across various water masses to obtain the iefinite characteristics for the water masses. The XTG could be used to follow interesting features on the G-Z plots. More important, however, is that the spacial characteristics of microthermal structure could easily be determined.

3. Handling of Data

When the microthermal structure roughness factor is determined, this factor should be made an integral part of the records for that XBT trace. This information should be included as part of the ID data.

Aboard Navy ships the AN/UNQ-7 tape recorder could be used to obtain magnetic tape records of the analog XBT or XTG signals. These tapes could be submitted with the traces to FNOC or NPS for further anal-

4. Naval Applications

Results from microthermal studies show that high frequency sonar performance as influenced by the microstructure receive the greatest microstructure effects. More knowledge of the microstructure is needed before the torpedo and mine-hunting sonar performance could be improved. With a measure of the microstructure, the performance of a sonar system could be predetermined.

Tens of thousands of XBT traces are on file at FNWC. New data are arriving daily. This thesis is an attempt to show how this data can be used both operationally and scientifically. Obviously it represents only a beginning in the way of microstructure analysis and operational utilization.

APPENDIX A

MICROXBT FORTRAN IV PROGRAM FOR CDC 6500

```
      PROGRAM MICROXBT (INPUT,OUTPUT,TAPE2)
*  *  *  *  *  *  *  *  *  *  *  *  *  *  *  *  *  *  *  *  *  *  *  *     A002
*     PROGRAMMER LCDR P. M. MAGRUDER,USN                                  *
*     COMPILED   JANUARY 1970                                             *
*                                                                         *     A005
*     MICROXBT IS A SPECIAL PURPOSE PROGRAM DESIGNED TO                   *
*     INTERPRET THE OUTPUT OF A CALMA COMPANY 303 OR 480 FLATBED          *     A007
*     DIGITIZER USED TO TRACE EXPENDABLE BATHYTHERMOGRAPH ANALOG          *     A008
*     RECORDS ACCORDING TO A SPECIFIC TECHNIQUE.                          *     A009
*                                                                         *
*     THE OUTPUT FROM THIS PROGRAM WILL BE USED IN ANOTHER                *
*     PROGRAM WRITTEN FOR THE IBM/360 AT NPS FOR MICROTHERMAL             *
*     ANALYSIS.   EXTENSIVE USAGE OF THE FNMC PROGRAM DIGITBT             *
*     WRITTEN BY LT N.L.PERKINS, USN, 15 JANUARY 1969, HAS MADE           *
*     THIS MICROTHERMAL ANALYSIS POSSIBLE.                                *
*                                                                         *     A013
*     INPUT TO THE PROGRAM IS BY HOLLERITH CARDS CONTAINING DEPTH         *     A011
*     AND TEMPERATURE CONSTANTS AND BY MAGNETIC TAPE WRITTEN IN           *     A012
*     EXTERNAL BCD CHARACTERS AT 556 BPI, EVEN PARITY, IN VARIABLE        *     A013
*     LENGTH RECORDS.                                                     *     A014
*                                                                         *     A015
*  *  *  *  *  *  *  *  *  *  *  *  *  *  *  *  *  *  *  *  *  *  *  *     A019
      DIMENSION IC(1650),IM(5000),IN(5000),ID(37),IF(40),IG(40),II(10)         A020
      DIMENSION IIS(4500),I1(9),I2(9),I3(9),AO(6000)
      EQUIVALENCE(AO,IP)
      COMMON JD,IT(10),IH(40), IP(6000),ITAPE1(9),IK(37)
      II(1)=1R1  $ II(2)=1R2  $ II(3)=1R3  $ II(4)=1R4  $ II(5)=1R5            A024
      II(6)=1R6  $ II(7)=1R7  $ II(8)=1R8  $ II(9)=1R9  $ II(10)=1R0           A025
      IK(1)=55B  $ IK(2)=50B  $ IK(3)=23B  $ IK(4)=24B  $ IK(5)=25B           A026
      IK(6)=26B  $ IK(7)=27B  $ IK(8)=30B  $ IK(9)=31B  $ IK(10)=32B          A027
      IK(11)=62B $ IK(12)=56B $ IK(13)=51B $ IK(14)=65B $ IK(15)=60B          A028
      IK(16)=67B $ IK(17)=73B $ MASK=2R02 $ IS=1                              A029
      ITAPE1(2)=5LTAPE1.OR.1
      ICA=ICB=ICD=ICF=ICG=ICP=ICR=ICS=ICT=0                                   A031
 1016 FORMAT(R2,R1,X,R3,R1,X,R2,R4,4X,4R4,20X,R4,9X,R4,4R2)                   A049
 1022 FORMAT(X,R4,X,6R1,X,4R1,X,5R1,X,6R1)                                    A056
```

```
 1034 FORMAT(10(X,I8))
 1036 FORMAT(10(X,I7))                                                  A070
*****PAGE EJECT PRINTER.                                                A071
      PRINT 1000                                                        A032
 1000 FORMAT(1H1)                                                       A073
*****REWIND OUTPUT TAPE TO LOAD POINT.                                  A076
*****READ CONSTANTS.  READS PUNCHED CARDS CONTAINING DEPTH AND          A077
*****TEMPERATURE CONSTANTS.  A MAXIMUM OF 25 SETS OF CONSTANTS          A078
*****(75 CARDS) CAN BE READ.                                            A079
      M=0                                                               A080
    1 READ 1001, (IC(J+M),J=1,22)                                       A033
 1001 FORMAT(R1,I2,I1,19I4)                                             A081
      IF(IC(M+1).NE.1) GO TO 2                                          A082
      READ 1002, (IC(J+M),J=23,44)                                      A034
 1002 FORMAT(R1,I2,19I4,R1)                                             A083
      IF(IC(M+23).NE.2) GO TO 2                                         A084
      READ 1003, (IC(J+M),J=45,66)                                      A035
 1003 FORMAT(R1,2I2,18I4,R3)                                            A085
      IF(IC(M+2).NE.IC(M+24).OR.IC(M+24).NE.IC(M+46)) GO TO 2           A086
      IF(IC(M+45).EQ.5) GO TO 51                                        A087
      IF(IC(M+45).NE.3) GO TO 2                                         A088
      IF(M.GE.1584) GO TO 2                                             A089
      M=M+66                                                            A090
      GO TO 1                                                           A091
    2 STOP 1                                                            A092
*****READ IDENTIFICATION RECORD.  A MESSAGE TO THE PRINTER IS           A093
*****TRANSMITTED UPON THE DETECTION OF A FORMAT ERROR NOT SIGNIFIED      A094
*****BY A DELETE RECORD CODE.
   51 GO TO 52                                                          A096
   52 DO 53 J=1,37                                                      A097
   53 ID(J)=0                                                           A098
   54 DO 55 J=1,5                                                       A099
   55 IM(J)=0                                                           A100
      CALL FLIO(4LRBCD,ITAPE1,IM,5)                                     A101
      GO TO (52,57,501,56,501,52)ITAPE1                                 A102
   56 PRINT 1004
```

```
1004 FORMAT(/,25H PARITY IN READING IDENT.)                              A036
     ICP=ICP+1                                                          A103
     GO TO 54                                                           A104
  57 IT(1)=LBYT(55,6,IM(1))                                             A105
     IF(IT(1).NE.73B) GO TO 54                                          A106
     DO 58 J=1,5                                                        A107
     DECODE(10,1005,IM(J)) (IT(K),K=1,10)                               A108
1005 FORMAT(10R1)                                                       A037
     DO 58 K=1,10                                                       A109
     IF(IT(K).EQ.38) GO TO 54                                           A110
  58 CONTINUE                                                           A111
     DECODE(41,1006,IM(1)) (IP(J),J=1,27)                               A112
1006 FORMAT(6X,6R1,2(X,4R1),2X,5R1,2X,2(3R1,X),2R1)                     A038
     DO 60 J=1,27                                                       A113
     DO 59 K=1,10                                                       A114
     IF((IP(J).AND..NOT.II(K)).OR.(II(K).AND..NOT.IP(J))) 59,60         A115
  59 CONTINUE                                                           A116
     PRINT 1007                                                         A117
1007 FORMAT(1H0)                                                        A039
     PRINT 1008, (IM(J),J=1,5)                                          A118
1008 FORMAT(X,R9,3R10,L1)                                               A040
     PRINT 1009                                                         A119
1009 FORMAT(/,39H FORMAT ERROR IN IDENTIFICATION RECORD.)               A041
     ICF=ICF+1                                                          A120
     GO TO 54                                                           A121
  60 CONTINUE                                                           A122
     DECODE(41,1010,IM(1)) (ID(J),J=1,15)                               A123
1010 FORMAT(X,R4,X,3I2,2(X,2I2),R1,X,I3,I2,R1,2(X,I3),X,I2)             A042
     DECODE(30,1011,IM(1)) (ID(J),J=16,37)                              A124
     PRINT 1007                                                         A125
     PRINT 1011, ID(1),(IP(J),J=1,14),ID(9),(IP(J),J=15,19),ID(12),     A126
    1(IP(J),J=20,27)                                                    A127
     WRITE(2,1041)
1041 FORMAT(4HID  )
1011 FORMAT(X,R4,X,6R1,X,4R1,X,5R1,X,6R1,X,2(3R1,X),2R1)                A043
     WRITE(2,1150) ID(1),(IP(J),J=1,14),ID(9),(IP(J),J=15,19),ID(12),
```

```
     1(IP(J),J=28,27)
 1150 FORMAT(4X,R4,4X,6R1,4X,4R1,4X,5R1,4X,6R1,4X,2(3R1,X),2X,2R1)
      JD=ID(1)                                                          A128
      CALL DISBCD                                                       A129
***** READ TWO ASSOCIATED TRACE RECORDS.                               A131
      CALL TRACEV(IE,IR,IM,ICA,ICS,ICR)                                 A132
      IF(IR.NE.0) GO TO 52                                              A133
      IF(IE.NE.0) GO TO 501                                             A134
      CALL TRACEV(IE,IR,IM,ICA,ICS,ICR)                                 A135
      IF(IR.NE.0) GO TO 52                                              A136
      IF(IE.NE.0) GO TO 501                                             A137
***** INSURE NEXT RECORD IS IDENTIFICATION DATA.                        A139
  101 CALL FLIO(4LRBCD,ITAPE1,IP,1)                                     A140
      GO TO (101,102,103,101,103,101)ITAPE1                             A141
  102 IT(1)=LBYT(55,6,IP(1))                                            A142
      IF(IT(1).EQ.739) GO TO 103                                        A143
      PRINT 1012                                                        A144
 1012 FORMAT(/,33H IMPROPER ARRANGEMENT OF RECORDS.)                    A044
      ICA=ICA+1                                                         A145
      GO TO 52                                                          A146
  103 CALL FLIO(4LBKSP,ITAPE1)                                          A147
***** SELECT PROPER SET OF DEPTH AND TEMPERATURE CONSTANTS NEEDED TO    A149
***** CONVERT INCREMENTAL VALUES FOR SIGNIFICANT LEVELS.  DEPTH VALUES  A150
***** ARE SCALED TO THE TENTH TIMES TEN.  TEMPERATURE VALUES ARE SCALED A151
***** TO THE THOUSANDTH TIMES ONE THOUSAND.  INCREMENTAL VALUES ARE     A152
***** SCALED TO THE HUNDREDTH TIMES ONE HUNDRED.                        A153
      DO 151 J=1,40                                                     A154
  151 IF(J)=IG(J)=IM(J)=0                                               A155
      DO 152 J=2,1586,66                                                A156
      IF(IC(J).EQ.ID(14)) GO TO 154                                     A157
      IF(IC(J).EQ.0) GO TO 153                                          A158
  152 CONTINUE                                                          A159
  153 PRINT 1013                                                        A160
 1013 FORMAT(/,43H CONSTANTS MISSING OR GRID NUMBER IN ERROR.)          A045
      ICG=ICG+1                                                         A161
      GO TO 52                                                          A162
```

```
  154 M=J+3 $ I=3 $ L=1 $ IF(2)=IC(J+2)                                    A163
      DO 155 K=M,N                                                        A164
      IF(IC(K).EQ.0) GO TO 156                                            A165
      IF(I)=IC(K)*100 $ IF(I+1)=IC(J+2)*10+IC(J+1)*L*1000                 A166
      I=I+2 $ L=L+1                                                       A167
  155 CONTINUE                                                            A168
      IF(40)=IC(K)*100                                                    A169
      GO TO 157                                                           A170
  156 IF(40)=IC(K-1)*100                                                  A171
  157 IG(2)=IF(2) $ L=1 $ I=3 $ M=J+23 $ N=M+16                           A172
      DO 158 K=M,N                                                        A173
      IF(IC(K).EQ.0) GO TO 160                                            A174
      IG(I)=-IC(K)*100 $ IG(I+1)=IC(J+2)*10-IC(J+1)*L*1000                A175
      I=I+2 $ L=L+1                                                       A176
  158 CONTINUE                                                            A177
      IG(40)=-IC(K)*100                                                   A178
      GO TO 161                                                           A179
  160 IG(40)=-IC(K-1)*100                                                 A180
  161 L=1 $ I=3 $ M=J+46 $ N=M+17                                         A181
      DO 162 K=M,N                                                        A182
      IF(IC(K).EQ.0) GO TO 163                                            A183
      IH(I)=IC(K)*100 $ IH(I+1)=IC(J+45)*L*100                            A184
      I=I+2 $ L=L+1                                                       A185
  162 CONTINUE                                                            A186
  163 JJ=ID(15)*10/IC(J+45) $ IH(40)=IC(J+JJ+45)*100                      A187
      IF(SENSE SWITCH 2) 164,165                                          A188
  164 PRINT 1034, (IF(J),J=1,40),(IG(J),J=1,40),(IH(J),J=1,40)            A189
                                                                          A190
***** EXTRACT X AND Y SUMMATIONS FROM TRACE RECORDS.                      A191
  165 CALL TRACEX(IM)                                                     A192
      CALL TRACEX(IN)                                                     A193
***** COMPARE TRACE RECORDS AND MERGE IF COMPATIBLE.  TRACES ARE MERGED   A195
***** IF FOUND TO BE WITHIN THREE INCREMENTS OF EACH OTHER.               A196
  167 DO 201 J=1,5000
  201 IP(J)=0                                                             A198
      JE=KE=0                                                             A199
```

```
      DO 211 J=1,4999,2                                                          A200
      IF(J.EQ.1) GO TO 202                                                       A201
      IF(IM(J).EQ. M(40).OR.IN(J).EQ.IM(40)) GO TO 212                           A202
      IF((IM(J).EQ.0.AND.IM(J+1).EQ.0).OR.(IN(J).EQ.0.AND.IN(J+1).EQ.0))         A203
     1 GO TO 215                                                                 A204
  202 IF(IM(J)-IN(J)) 203,204,205                                                A205
  203 L=-(IM(J)-IN(J))                                                           A206
      GO TO 206                                                                  A207
  204 L=0                                                                        A208
      GO TO 206                                                                  A209
  205 L=IM(J)-IN(J)                                                              A210
  206 IF(IM(J+1)-IN(J+1)) 207,208,209                                            A211
  207 K=-(IM(J+1)-IN(J+1))                                                       A212
      GO TO 210                                                                  A213
  208 K=0                                                                        A214
      GO TO 210                                                                  A215
  209 K=IM(J+1)-IN(J+1)                                                          A216
  210 IP(J)=(IM(J)+IN(J))/2
      IP(J+1)=(IM(J+1)+IN(J+1))/2
      IF(L.GT.JE)JE=L                                                            A218
      IF(K.GT.KE)KE=K                                                            A219
******COMPATABILITY TEST FOR 0.0350 INCH DIFFERENCE BETWEEN TRACES
 2101 IF(L.GT.350.OR.K.GT.350) GO TO 213
  211 CONTINUE                                                                   A221
      GO TO 214                                                                  A222
  212 IP(J)=IH(40) $ IP(J+1)=(IM(J+1)+IN(J+1))/2 $ J=J+2                         A223
      GO TO 215                                                                  A224
  213 JE=JE/100 $ KE=KE/100                                                      A225
      PRINT 1014, JE,KE                                                          A226
 1014 FORMAT(/,28H DEVIATION TEST FAILED AT X=,I8,4H, Y=,I8,23H HUNDREDT
     1HS OF AN INCH.)                                                            A047
      ICD=ICD+1                                                                  A227
      GO TO 52
  214 PRINT 1015                                                                 A229
 1015 FORMAT(/,35H DATA EXCEEDED LENGTH OF INPUT BIN.)                           A048
      ICB=ICB+1                                                                  A230
```

```
      GO TO 52                                                                  A231
  215 JE=JE/100 $ KE=KE/100 $ IP(1)=0                                           A232
      IF(SENSE SWITCH 2) 216,250                                                A233
  216 J=J+1                                                                     A234
      PRINT 1034, (IP(K),K=1,J)                                                 A235
                                                                                A236
***** SELECT SIGNIFICANT LEVELS FOR OUTPUT.  THOSE POINTS THAT DEVIATE         A237
***** FROM A LINE OF LINEARITY BETWEEN ADJACENT LEVELS BY 175                  A238
***** THOUSANDTHS OF AN INCH OR MORE ARE CONSIDERED SIGNIFICANT.               A239
  250 DO 251 J=1,5000                                                           A240
  251 IM(J)=0                                                                   A241
      I=1 $ J=L=3 $ K=5 $ M=0 $ IM(2)=IP(2)                                     A242
  252 IF(IP(K).EQ.0) GO TO 257                                                  A243
      N=JK=J
  256 IM(L)=IP(N) $ IM(L+1)=IP(N+1) $ I=N $ J=I+2 $ K=J+2 $ M=0 $ L=L+2         A260
      GO TO 252                                                                 A261
  257 IF(IP(JK).EQ.IP(K-2).AND.IP(JK+1).EQ.IP(K-1)) GO TO 258                   A262
      IF(IP(JK).EQ.IM(L-2).AND.IP(JK+1).EQ.IM(L-1)) GO TO 258
      IM(L)=IP(JK) $ IM(L+1)=IP(JK+1) $ L=L+2                                   A264
  258 IM(L)=IP(K-2) $ IM(L+1)=IP(K-1)                                           A265
      DO 259 J=1,5000                                                           A266
  259 IP(J)=0                                                                   A267
      IP(2)=IM(2) $ L=3                                                         A268
      DO 261 K=3,4999,2                                                         A269
      IF(IM(K+2).EQ.0.AND.IM(K+3).EQ.0) GO TO 260                               A270
      IF(IM(K)-IM(K-2).EQ.IM(K+2)-IM(K).AND.IM(K+3)-IM(K+1).EQ.IM(K+1)-I        A271
     1M(K-1)) GO TO 261                                                         A272
      IP(L)=IM(K) $ IP(L+1)=IM(K+1) $ L=L+2                                     A273
      GO TO 261                                                                 A274
  260 IP(L)=IM(K) $ IP(L+1)=IM(K+1) $ LL=L+1                                    A275
      GO TO 262                                                                 A276
  261 CONTINUE                                                                  A277
      LL=L+1                                                                    A278
  262 IF(SENSE SWITCH 2) 263,301                                                A279
  263 PRINT 1034, (IP(J),J=1,LL)                                                A280
```

```
***** CONVERT INCREMENTAL VALUES AT SIGNIFICANT LEVELS TO DEPTH AND          A282
***** TEMPERATURE.  TEMPERATURE VALUES ARE SCALED TO HUNDREDTHS TIMES        A283
***** ONE HUNDRED.  DEPTHS ARE SCALED TO THE NEAREST UNIT.                  A284
  301 DO 312 J=2,LL,2                                                       A285
      IF(IP(J).LT.0) GO TO 305                                              A286
      IF(IP(J).GT.IF(40))IP(J)=IF(40)                                       A287
      IF(IP(J).EQ.0) GO TO 303                                              A288
      DO 302 K=3,37,2                                                       A289
      IF(IP(J).LE.IF(K)) GO TO 304                                          A290
  302 CONTINUE                                                              A291
  303 IP(J)=IF(2)                                                           A292
      GO TO 308                                                             A293
  304 IP(J)=(IP(J)*IF(K+1)-IF(K-2)*IF(K+1)-IP(J)*IF(K-1)+IF(K)*IF(K-1))/    A294
     1(IF(K)-IF(K-2))                                                       A295
      IN(J)=IP(J)
      IF(IN(J)-IN(J)/10*10.GE.5)IN(J)=IN(J)+10                              A297
      IF(IP(J)-IP(J)/10*10.GE.5)IP(J)=IP(J)+10                              A299
      GO TO 309                                                             A301
  305 IF(IP(J).LT.IG(40))IP(J)=IG(40)                                       A302
      DO 306 K=3,39,2                                                       A303
      IF(IP(J).GE.IG(K)) GO TO 307                                          A304
  306 CONTINUE                                                              A305
  307 IP(J)=(IP(J)*IG(K+1)+IG(K)*IG(K-1)-IP(J)*IG(K-1)-IG(K-2)*IG(K+1))/    A306
     1(IG(K)-IG(K-2))                                                       A307
  308 IN(J)=IP(J)
      IF(IN(J)-IN(J)/10*10.GE.5)IN(J)=IN(J)+10                              A309
      IF(IP(J)-IP(J)/10*10.GE.5)IP(J)=IP(J)+10                              A311
  309 IF(IP(J-1).LT.0)IP(J-1)=0                                             A313
      IF(IP(J-1).EQ.0) GO TO 311                                            A314
      IF(IP(J-1).GT.IH(40))IP(J-1)=IH(40)                                   A315
      DO 310 K=3,37,2                                                       A316
      IF(IP(J-1).LE.IH(K)) GO TO 311                                        A317
  310 CONTINUE                                                              A318
  311 IP(J-1)=(IP(J-1)*IH(K+1)-IH(K-2)*IH(K+1)-IP(J-1)*IH(K-1)+IH(K)*       A319
     1IH(K-1))/(IH(K)-IH(K-2))                                              A320
      IN(J-1)=IP(J-1)
```

```
      IF(IN(J-1)-IN(J-1)/10*10.GE.5)IN(J-1)=IN(J-1)+10                    A322
      IF(IP(J-1)-IP(J-1)/10*10.GE.5)IP(J-1)=IP(J-1)+10                    A324
      IF(IP(1).NE.0)IP(1)=0                                               A326
  312 CONTINUE                                                            A327
      K=LL-1 $ L=3 $ IN(1)=0                                              A328
      DO 313 J=3,K,2                                                      A329
      IF(IN(J).EQ.IN(L-2)  GO TO 313                                      A330
      IN(L)=IN(J) $ IN(L+1)=IN(J+1) $ IP(L)=IP(J) $ IP(L+1)=IP(J+1)       A331
      L=L+2                                                               A332
  313 CONTINUE                                                            A333
      LL=L-1                                                              A334
***** PRINT DEPTHS AND TEMPERATURE DATA AND MAXIMUM DEVIATION.           A506
  401 IF(ID(13).LE.180) GO TO 452                                         A508
      DO 451 J=1,LL
  451 AO(J)=FLOAT(IP(J))/10.0                                             A510
      GO TO 454                                                           A511
  452 DO 453 J=1,LL
  453 AO(J)=FLOAT(IN(J))/10.0
  454 DO 455 J=2,LL,2                                                     A513
  455 AO(J)=AO(J)/100.0
      PRINT 1018                                                          A515
 1018 FORMAT(/,2X,7(X,5HDEPTH,2X,5HTEMP ,2X),/)
      WRITE(2,1040) LL
 1040 FORMAT(4HL IS,I4)
      PRINT 1019,(AO(J),J=1,LL)
      WRITE(2,1019)(AO(J),J=1,LL)
 1019 FORMAT(4X,7(F6.1,X,F6.3,2X))
      PRINT 1020, JE,KE                                                   A517
 1020 FORMAT(/,21H MAXIMUM DEVIATION X=,I2,4H, Y=,I2,23H HUNDREDTHS OF A  A053
     1N INCH.,/)                                                          A054
  510 ENCODE(30,1021,IT(1)) (ID(K),K=16,37)
 1021 FORMAT(X,R4,X,6R1,X,4R1,X,5R1,X,6R1)                               A055
      IIS(IS)=IT(1) $ IIS(IS+1)=IT(2) $ IIS(IS+2)=IT(3)                   A519
      IS=IS+3 $ ICT=ICT+1                                                 A520
      GO TO 52                                                            A521
  501 CALL FLIO(4LUNLD,ITAPE1)                                            A524
```

```
      PAUSE 1                                                          A525
      IF (SENSE SWITCH 1) 51,505
  505 END FILE 2
  506 REWIND 2
      PRINT 1000                                                       A543
      IS=IS-1                                                          A544
      PRINT 1023, (IIS(J),J=1,IS)                                      A545
 1023 FORMAT(3X10)                                                     A057
      PRINT 1025, ICD                                                  A546
 1025 FORMAT(/,/,23H FAILED DEVIATION TEST ,I4)                        A059
      PRINT 1026, ICF                                                  A547
 1026 FORMAT 23H FORMAT ERRORS          ,I4)                          A060
      PRINT 1027, ICA                                                  A548
 1027 FORMAT(23H ARRANGEMENT ERRORS     ,I4)                          A061
      PRINT 1032, ICP                                                  A549
 1032 FORMAT(23H PARITY IN ID RECORD    ,I4)                          A066
      PRINT 1033, ICR                                                  A550
 1033 FORMAT(23H PARITY IN TRACE RECORD,I4)                            A067
      PRINT 1028, ICS                                                  A551
 1028 FORMAT(23H SURFACE FLAGS MISSING ,I4)                            A062
      PRINT 1029, ICG                                                  A552
 1029 FORMAT(23H GRID TABLES MISSING    ,I4)                          A063
      PRINT 1030, ICB                                                  A553
 1030 FORMAT(23H DATA EXCEEDED STORAGE ,I4)                            A064
      PRINT 1031, ICT                                                  A554
 1031 FORMAT(23H SATISFACTORY TRACES    ,I4)                          A065
      STOP                                                             A555
      END                                                              A556
```

```
      SUBROUTINE TRACEX(IB)                                                  A599
*  *  *  *  *  *  *  *  *  *  *  *  *  *  *  *  *  *  *  *  *  *  *  *  *   A600
*     TRACEX - SETS UP AND STORES AN ARRAY OF X AND Y SUMMATIONS     *       A601
*     FROM TRACE RECORD CALLED FOR.  X AND Y SUMMATIONS ARE SCALED     *
*     TO THE HUNDREDTH TIMES ONE HUNDRED.                              *
*  *  *  *  *  *  *  *  *  *  *  *  *  *  *  *  *  *  *  *  *  *  *  *   A605
      COMMON JD,IT(10),IH(40), IP(6000),ITAPE1(9),IK(37)
      DIMENSION IB(5000)                                                   A607
      DO 1 J=1,6000
    1 IP(J)=0                                                              A611
      IY=IX=N=0 $ I=1 $ M=3                                                A612
    2 IF(IB(I).EQ.0) GO TO 6                                               A613
      DECODE(10,100,IB(I)) (IT(K),K=1,10)                                  A614
  100 FORMAT(10R1)                                                         A608
      DO 5 J=1,9,2                                                         A615
      IF(N.NE.0) GO TO 4                                                   A616
      IF(IT(J).EQ.39) GO TO 19                                             A617
      CALL COMP(J)                                                         A618
      IY=IY+IT(J)                                                          A619
   19 IF(IT(J+1).EQ.37) GO TO 3                                            A620
      GO TO 5                                                              A621
    3 N=1 $ IP(2)=IY*100                                                   A622
      GO TO 5                                                              A623
    4 CALL COMP(J)                                                         A624
      IX=IX+IT(J) $ J=J+1                                                  A625
      CALL COMP(J)                                                         A626
      IY=IY+IT(J) $ J=J-1 $ K1=IX-IP(M-2)/100 $ L1=IY-IP(M-1)/100          A627
      K=K1                                                                 A628
      IF(K1.LT.0)K=-K1                                                     A629
      L=L1                                                                 A630
      IF(L1.LT.0)L=-L1                                                     A631
      IF(K.GT.5.OR.L.GT.5) GO TO 15
   13 IP(M)=IX*100 $ IP(M+1)=IY*100                                        A633
   14 IF(IP(M).EQ.IP(M-2).AND.IP(M+1).EQ.IP(M-1)) GO TO 6                  A634
      IF(IP(M).GE.IH(40)) GO TO 7                                          A635
      M=M+2                                                                A636
      GO TO 5                                                              A637
```

```
 15 IF(K.EQ.0) GO TO 17                                                    A638
    DO 16 KL=1,K                                                           A639
    IP(M)=IP(M-2)+K1/K*100 $ IP(M+1)=IP(M-1) $ M=M+2                       A640
 16 CONTINUE                                                               A641
 17 IF(L.EQ.0) GO TO 14                                                    A642
    LK=L-1                                                                 A643
    DO 18 KL=1,LK                                                          A644
    IP(M)=IP(M-2) $ IP(M+1)=IP(M-1)+L1/L*100 $ M=M+2                       A645
 18 CONTINUE                                                               A646
    GO TO 13                                                               A647
  5 CONTINUE                                                               A648
    I=I+1                                                                  A649
    GO TO 2                                                                A650
  6 IP(M)=IP(M+1)=0 $ M=M-2                                                A651
  7 DO 8 J=1,5000                                                          A652
  8 IB(J)=0                                                                A653
    I=N=3 $ IB(2)=IP(2)                                                    A654
    DO 11 J=I,M,2                                                          A655
    IF(J.LE.3) GO TO 10                                                    A656
    IF(IP(J).EQ.IP(J-4-K).AND.IP(J+1).EQ.IP(J-3-K)) GO TO 9                A657
    GO TO 10                                                               A658
  9 IP(J-1)=IP(J-2)=IP(J-3-K)=IP(J-4-K)=0                                  A659
    K=K+4                                                                  A660
    GO TO 11                                                               A661
 10 K=0                                                                    A662
 11 CONTINUE                                                               A663
    DO 12 J=3,M,2                                                          A664
    IF(IP(J).EQ.0.AND.IP(J+1).EQ.0) GO TO 12                               A665
    IB(N)=IP(J) $ IB(N+1)=IP(J+1) $ N=N+2                                  A666
 12 CONTINUE                                                               A667
    IF(SENSE SWITCH 2) 20,21                                               A668
 20 M=M+1                                                                  A669
    PRINT 101, (IB(J),J=1,M)                                               A670
101 FORMAT(16(X,I10))                                                      A609
 21 RETURN                                                                 A671
    END                                                                    A672
```

```
      SUBROUTINE TRACEY(IE,IR,IB,ICA,ICS,ICR)                          A557
*  *  *  *  *  *  *  *  *  *  *  *  *  *  *  *  *  *  *  *  *  *  *  *  A558
*     TRACEY READS INTO MEMORY AN ERROR FREE TRACE RECORD.  THE      *  A559
*     TERM ERROR FREE MEANS CORRECT FORMAT.  NO SCALING OF DATA IS   *  A560
*     PERFORMED IN THIS ROUTINE.                                     *  A561
*  *  *  *  *  *  *  *  *  *  *  *  *  *  *  *  *  *  *  *  *  *  *  *  A562
      COMMON JD,IT(10),IH(40), IP(6000),ITAPE1(9),IK(37)
      DIMENSION IB(5000)                                               A564
    1 I=IE=IR=0                                                        A569
      DO 2 J=1,5000                                                    A570
    2 IB(J)=0                                                          A571
      CALL FLIO(4LRBCD,ITAPE1,IB,5000)                                 A572
      GO TO (7,4,9,7,9,7)ITAPE1                                        A573
    4 DO 5 J=1,5000                                                    A574
      IF(IB(J).EQ.0) GO TO 6                                           A575
      DECODE(10,100,IB(J)) (IT(K), K=1,10)                             A576
  100 FORMAT(10R1)                                                     A565
      DO 5 L=1,10                                                      A577
      IF(IT(L).EQ.38) GO TO 1                                          A578
      IF(IT(L).NE.37) GO TO 5                                          A579
      I=1                                                              A580
    5 CONTINUE                                                         A581
    6 IT(1)=LBYT(55,6,IB(1))                                           A582
      IF(IT(1).EQ.39) GO TO 8                                          A583
      CALL FLIO(4LBKSP,ITAPE1)                                         A584
      PRINT 102                                                        A585
  102 FORMAT(/,33H IMPROPER ARRANGEMENT OF RECORDS.)                   A567
      ICA=ICA+1                                                        A586
    7 IR=1                                                             A587
      PRINT 103                                                        A588
  103 FORMAT(/,25H PARITY IN READING TRACE.)                           A568
      ICR=ICR+1                                                        A589
      GO TO 10                                                         A590
    8 IF(I.EQ.1) GO TO 10                                              A591
      PRINT 101                                                        A592
  101 FORMAT(/,22H SURFACE FLAG MISSING.)                              A566
```

```
      ICS=ICS+1                                                          A593
      IR=1                                                               A594
      GO TO 10                                                           A595
    9 IE=1                                                               A596
   10 RETURN                                                             A597
      END                                                                A598
```



```
      SUBROUTINE COMP(J)                                                 A673
*  *  *  *  *  *  *  *  *  *  *  *  *  *  *  *  *  *  *  *  *  *  *  *  A674
*     COMP - CONVERTS CODED INTEGERS OF DIGITIZER OUTPUT TO ABSOLUTE     A675
*                                                                        A676
*     INTEGERS FOR SUMMING.                                              A677
*  *  *  *  *  *  *  *  *  *  *  *  *  *  *  *  *  *  *  *  *  *  *  *  A678
      COMMON JD,IT(10),IH(40), IP(6000),ITAPE1(9),IK(37)
      DO 1 K=1,16                                                        A680
      IF(IT(J).EQ.0) GO TO 3                                             A681
      IF(IT(J).EQ.IK(K))IA=K-1                                           A682
      IF(IT(J).EQ.IK(K)) GO TO 2                                         A683
    1 CONTINUE                                                           A684
      IT(J)=IT(J)-27                                                     A685
      GO TO 3                                                            A686
    2 IT(J)=0                                                            A687
      IF(IA.NE.0)IT(J)=-IA                                               A688
    3 RETURN                                                             A689
      END
```

```
          IDENT  DISBCD                                                    A690
          ENTRY  DISBCD                                                    A691
*  *  *  *  *  *  *  *  *  *  *  *  *  *  *  *  *  *  *  *  *  *  *  *     A692
*         DISBCD - CONVERTS INTERNATIONAL SHIPS CALL OR                  *  A693
*         IDENTIFICATION LABEL OF REPORTING UNIT FROM CONSOLE            *  A694
*         DISPLAY CODE TO EXTERNAL BCD CHARACTERS.  NO SCALING OF        *  A695
*         DATA IS PERFORMED IN THIS ROUTINE.                             *  A696
*  *  *  *  *  *  *  *  *  *  *  *  *  *  *  *  *  *  *  *  *  *  *  *     A697
          VFD    36/0HDISBCD,24/0                                          A698
DISBCD    BSSZ   1                                                         A699
          SA1    JD                                                        A700
          SB1    10B                                                       A701
          RJ     =XCHARCVT                                                 A702
          MX0    36                                                        A703
          BX6    -X0*X6                                                    A704
          SA6    JD                                                        A705
          JP     DISBCD                                                    A706
          BSS    0                                                         A707
          USE    //                                                        A708
JD        BSS    1                                                         A709
          USE    *                                                         A710
          END                                                              A711
```

Input Data Cards

```
A012620000220044006600880110013101520173019402150235025502750294031303320350000
B010022004400660088011001310152017301940215023502550275029403130332035000000000
C015001580318048206490816000000000000000000000000000000000000000000000000000000
A022620000220044006600870109013101520174019502160237025702770296031503330351000
B020022004400660087010901310152017401950216023702570277029603150333035100000000
C025001590320046506530821000000000000000000000000000000000000000000000000000000
A035600000140028004300580073008901050122000000000000000000000000000000000000000
B030014002900440059007500910105000000000000000000000000000000000000000000000000
E035005001000150025000000000000000000000000000000000000000000000000000000000000
```

APPENDIX B

MICROTHERMAL STRUCTURE ANALYSIS FORTRAN SOURCE PROGRAM

FOR IBM 360/67

```
      DIMENSION DATA(34),T(902),TEMP(902),Z(902),D(902),A(902),AMON(12)
      DIMENSION ITI(4)
      INTEGER TIME,DAY,YR,BL,DI,DATA,SHP
      REAL*4 LAT,LONG
      REAL*4 L1/4H    /
      REAL*8 ADATA(12)
C
      DATA IN,IS,IE,IW/'N   ','S   ','E   ','W   '/
      DATA BL/'L IS'/
      DATA DI/'ID  '/
      DATA AMON/'JAN ','FEB ','MAR ','APR ','MAY ','JUNE','JULY',
     *'AUG ','SEPT','OCT ','NOV ','DEC '/
      DATA IT/'N001'/
      DATA ITI/'N002','N003','N004'/
      DATA ADATA(12)/' BOX   M'/
C
      KKK=0
      II=0
      III=1
C
    5 READ(4,40,END=20,ERR=38)DATA
   40 FORMAT(34A4)
C     WRITE(6,41)(DATA(I),I=1,25)
   41 FORMAT(1X,25A4)
   38 IF(DATA(1).EQ.DI)GOTO 500
      GO TO 5
C
  500 READ(4,1205,END=34,ERR=5) ID,SHP,DAY,MON,YR,TIME,LAT1,LAT2,INS,
     *LONG1,LONG2,IEW,IREFT,IGRID,IDXBT
 1205 FORMAT(A4,A4,4X,3I2,4X,I4,4X,2I2,A4,1X,I3,I2,A4,2(1X,I3),3X,I2,31X
     *)
      BACKSPACE 4
      READ(4,501)(ADATA(I),I=1,11)
  501 FORMAT(4X,11A8)
      WRITE(6,35)SHP,IT
      IF(SHP.NE.IT)GO TO 5
      READ(4,40)DATA
      KKK=KKK+1
      REFT=FLOAT(IREFT)/10.0
      LAT=FLOAT(LAT1)+FLOAT(LAT2)/60.0
      IF(INS.EQ.IS) LAT=-LAT
      LONG=FLOAT(LONG1)+FLOAT(LONG2)/60.0
      IF(IEW.EQ.IW) LONG=-LONG
C
      IF(DATA(1).EQ.BL)GOTO 42
      BACKSPACE 4
      GO TO 5
C
```

```
   42 DO 1 J=1,902
      Z(J)=0.0
      TEMP(J)=0.0
      D(J)=0.0
      T(J)=0.0
    1 CONTINUE
C
      WRITE(6,9999)KKK
 9999 FORMAT(1X,'XBT NUMBER IS ',I5,2X)
      WRITE(6,107) SHP,DAY,AMON(MON),YR,TIME,LAT,INS,LONG,IEW,REFT
  107 FORMAT(1HO,1X,'SHIP CODE',T25,A4/' DATE OF XBT DROP',T25,I2,2X,A4,
     *2X,I5/' TIME OF XBT DROP(GCT)',T25,I4,' Z',/' LATITUDE',T25,F9.2,
     *A4,/' LONGITUDE',T25,F9.2,A4/' REFERENCE TEMPERATURE',T25,F5.2///)
      WRITE(6,1015)
 1015 FORMAT(1HO,'Z(J) AND TEMP(J) ARRAYS',///)
C
      DO 2 J=1,900,7
      JJ=J+6
      READ(4,1019,END=3,ERR=4)(DATA(I),(Z(I),TEMP(I),I=J,JJ))
      WRITE(6,1019)(DATA(I),(Z(I),TEMP(I),I=J,JJ))
 1019 FORMAT(A4,7(F6.1,1X,F6.3,2X))
      IF(Z(JJ).LT.1.0)GOTO 3
      IF(Z(JJ).LT.Z(J))GOTO 3
      IF(DATA(1).EQ.DI) GO TO 4
      IF(TEMP(J).LT.1.0)GOTO 4
    2 CONTINUE
      GO TO 3
C
    4 K=0
      BACKSPACE 4
      K=J
      GOTO 7
    3 K=JJ
      IF(K.GT.902)K=902
    7 SST=TEMP(1)
      ZMAX=Z(JJ)
C
      DO 51 I=1,10
      IF(Z(J+I-2).GT.ZMAX)ZMAX=Z(J+I-2)
      IF((J+I-2).GE.JJ)GOTO 49
   51 CONTINUE
C
      BACKSPACE 4
   49 NT=J-3+I
C
C     COMPUTING VALUES FOR EACH FOOT IN DEPTH FROM THE FINEST DIGITIZED
C     INPUT XBT TRACE FROM FNWC
C
```

```
      D(1)=0.0
      T(1)=SST
      K=IFIX(ZMAX+0.5)
C
      I=1
      DO 8 J=2,K
      D(J) = FLOAT(J-1)
      IF((D(J)+D(J+1)).LT.0.4) GO TO 9
      IF(Z(I+1).GE.D(J)) GO TO 50
      I=I+1
   50 T(J)=TEMP(I)+(TEMP(I+1)-TEMP(I))/(Z(I+1)-Z(I))*(D(J)-Z(I))
      A(J-1)=T(J)-T(J-1)
      IF(J.GE.901)GOTO 9
      IF((Z(I+1)-Z(I)).LT.0.05) GO TO 9
    8 CONTINUE
C
    9 N=J-1
      KK=900
      CALL DRAW(N,D,A,0.0,0,L1,ADATA,100.0,0.1,4,0,2,0,9,6,1,L)
      CALL DRAW(KK,D,T,0,0,L1,ADATA,100.0,10.0,0,0,2,0,9,9,1,L)
      WRITE(6,510)(J,A(J),J=1,N)
  510 FORMAT(8(I5,1X,F8.5,2X))
   18 II=II+1
      IF(II.EQ.15)GO TO 20
C
C      CHECKING LATITUDE
      ALTMX=70.0
      ALTMN=10.0
      IF(LAT.LT.ALTMN.OR.LAT.GT.ALTMX) GO TO 5
      YMAX=15.0
      ALGMN=120.0
      ALGMX=180.0
C     CHECKING TO SEE IF EAST LONGITUDE
      IF(LONG.LT.ALGMN.OR.LONG.GT.ALGMX) GO TO 5
      ALGMN=-180.0
      ALGMX=-110.0
C     CHECKING TO SEE IF WEST LONGITUDE
      IF(LONG.LT.ALGMN.OR.LONG.GT.ALGMX) GO TO 5
   19 GO TO 5
C
   20 REWIND 4
      III=III+1
      IF(III.GT.4)GO TO 21
      IT=ITI(III)
      II=0
      GO TO 5
   21 STOP
      END
```

APPENDIX C

JOB CONTROL LANGUAGE (JCL) FOR READING FNWC TAPES

```
//(Job name)   JØB (Acct. no., Job no., Section), '(Your name)'  Note 1
//      EXEC   FØRTCLGP,REGION=100K,TIME.GØ=2                    Note 2
//FØRT.SYSIN   DD *

               FØRTRAN Source Deck

/*                                                              Note 3
//GØ.FT06F001  DD  SYSØUT=A,SPACE(CYL,6)                        Note 4
//GØ.FT04F001  DD  UNIT=2400-1,VØL=SER=NPSXXX,LABEL=(,NL),      Note 5
//               DCB=(DEN=1,RECFM=F,LRECL=136,BLKSIZE=136,TRTCH=ET),  " 5
//               DISP=(ØLD,KEEP)                                Note 5
//GØ.FT04F002  DD AFT=FT04F001,VØL=SER=NPSXXX,LABEL(2,NL),      Note 6
//               DCB=(DEN=1,RECFM=F,LRECL=136,BLKSIZE=136,TRTCH=ET),  " 6
//               DISP=(ØLD,KEEP)                                Note 6
//GØ.SYSIN     DD *                                            Note 7

               DATA Cards, if any

/* (Orange Card)
```

Notes

1. Standard JØB, green card, for program submission.

2. If not plotting or card punching, the FØRTCLGP can be changed to FØRTCLG.

3. Must be a white card.

4. Optional card for additional storage for output.

5. The XXX following NPS is the NPS tape number. These three cards are for reading the first file on the input tape. These cards assign input unit 4 for the source programs READ statements. Further note that the record length is 136 characters, all of which may be read. This is the standard record length from the CDC 3600.

6. For a third file to be read, these three cards must be repeated with F002 changed to F003 and LABEL(2,NL) changed to LABEL(3,NL) and so forth for additional files. Also the UNIT=2400-1 should be changed to AFT=FT04F001 for all files after the first file. If only one file is to be read, then these three cards are not required.

7. Not required if there are no input data cards.

APPENDIX D

JOB CONTROL LANGUAGE (JCL) FOR DUMPING FNWC TAPE DATA

```
//(Job name)   JØB (Acct. no., Job no., Section), '(Your name)'      Note 1
//DUMPTAPE     EXEC PGM=IEBPTPCH
//SYSPRINT     DD SYSØUT=A
//SYSUT1       DD UNIT=2400-1,DI3B=ØLD,LABEL=(,NL),VØLUME=SER=NPSXX, Note 2
//                DCB=(DEN=1,RECFM=F,LRECL=136,BLKSIZE=136,TRTCH=ET)  Note 2
//SYSUT2       DD SYSØUT=A
//SYSIN        DD *,DCB=BLKSIZE=80
                PRINT MAXFLDS=1,STØPAFT=1000                         Note 3
                RECORD FIELDS=(120)                                  Note 4

/* (Orange Card)
```

Notes

1. Standard JØB, green card, for program submission.

2. If more than one file is on the tape then separate two cards for each file identified by file number by the file number in the LABEL (X,NL) where S is the file number, which is implied 1 when omitted.

3. The STØPAFT limits the number of lines of printed output, in this example 1000 lines is used before printing is terminated.

4. The field is recorded at the maximum amount that this program will dump which is 120 characters. If there are any characters between 120 and 133 in the records then this routine will not dump those characters.

BIBLIOGRAPHY

Arthur D. Little Inc., 1965. Experimental Evaluation of Expendable Bathythermographs, Report 4071165.

Arthur D. Little Inc., 1966. Internal Waves: Their Influence Upon Naval Operations, Report 4090266.

Arthur D. Little Inc., 1966a. Expendable Bathythermograph (XBT) System Evaluation for Tactical Sonar Application, Report 4150866.

Arthur D. Little Inc., 1966b. Acoustic Transmission in an Ocean Surface Duct, Report 4171166.

Arthur D. Little Inc., 1967. Internal Waves in the Ocean, Report 4321267.

Arthur D. Little Inc., 1968. An Assessment of Expendable Bathythermograph (XBT) Data and Recorder Requirements, Report 4250268.

Arthur D. Little Inc., 1968a. Experimental Evaluation of Deep (6000 ft.) Expendable Bathythermographs, Report 4391168.

Ayers, E., Wolff, P. M., Carstensen, L., and Ayers, H. C., 1966. A Ray Tracing Program for a Digital Computer, paper presented at NATO Symposium on the Operational Evaluation of ASW Weapons Systems, Paris, France on 28 June 1966.

Barakos, P. A., 1968. Acoustic Wave Scattering and Refraction by Internal Waves in a Model Tank, U. S. Navy Underwater Sound Laboratory Report 905, Ph.D. Thesis, University of Washington, Seattle.

Bauer, R. A., 1969. Fleet Numerical Weather Central's XBT Digitizing System, Computer Applications Report.

Berkerle, J. C., Reitzell, J. S., Payne, R. E., and Hersey, J. B., 1968. Variations in Sound Between Bermuda and the Antilles, lectures given at AGU meeting on 20 April 1966, Woods Hole Oceanographic Institute Reference 68-19 (Unpublished manuscript).

Bergmann, P. G., 1946. "Propagation of Radiation in a Medium with Random Inhomogeneities," Physical Review, v. 70, p. 486-492.

Boston, N. E. J., 1966. Objective Definition of the Thermocline, Texas A&M Reference 66-19T, Project 286-D.

Choate, T. V., 1970. (Marketing Manager, Sippican Corporation), personal communication.

Cohen, J. S., and Weinberg, H., 1969. CONGRATS Ray Plot Program, USL Technical Memorandum 2070-110-69.

Cook, J. C., and Kenyon, K. E., 1963. "Fast-Response Thermistor Probes for Temperature Microstructure Studies at Sea," Review of Scientific Instruments, v. 34, p. 496-499.

Cooper, J. W., and Stommel, H., 1968. "Regularly Spaced Steps in the Main Thermocline near Bermuda," Journal of Geophysical Research, v. 73, p. 5849-4854.

Cooper, L. H. N., 1967. "Stratification in the Deep Ocean," Sci. Prog. (Oxf.), v. 55, p. 73-90.

Demeo, R. P., 1968. The Validity of Expendable Bathythermograph Measurements, Paper presented at MTS Meeting, 4th, Miami, Florida.

Denner, W. W., 1966. A Comparison of the Sippican and General Motors Expendable Bathythermograph to a Mechanical Bathythermograph, Fleet Numerical Weather Central Technical Note 16.

Denner, W. W., 1968. "Separation of the Residual Instrument Noise from the Significant Variability for Expendable Bathythermographs," Marine Sciences Instrumentation, v. 4, Plenum Press, p. 635-641.

Denner, W. W., 1969. The T-S Gradient Method, a New Method of Computing Geostrophic Currents over Large Ocean Areas, U. S. Naval Postgraduate School Technical Report NPS-58DW9072A.

General Motors Defense Laboratories, 1965. Observations on Expendable Instrumentation.

DiNapoli, F. R., 1969. Acoustic Propagation in a Stratified Medium, USL Report 1046, Ph.D. Thesis, University of Rhode Island.

Einstein, L. T., and Cohen, J. S., 1969. Acoustic Field Modeling with Constant and Continuous Velocity Gradients, USL Technical Memorandum 2070-237-69.

Frankignoul, C., 1969. Note on Internal Waves in a Simple Thermocline Model, Woods Hole Ref. 69-47 (Unpublished manuscript).

Glennon, A. N., 1965. "Practicalities of Sonar Range Prediction," U. S. Naval Institute Proceedings, v. 91, p. 128-132, March 1965.

Gouzie, M. W., Sanders, M. R., and Littlehale, A. D., 1966. Laboratory and Engineering Evaluation of Three Models of Expendable Bathythermography, USL Report 732.

Grant, H. L., Moilliet, A., and Vogel, W. M., 1968. "Some Observations of the Occurrence of Turbulence in and above the Thermocline," Journal of Fluid Mechanics, v. 34, p. 443-448.

Green, E. L., 1967. Diffraction Theory of Lensless Correlation, USL Report 842.

Grosfils, E. F., 1968. Objective Digital Analysis of Bathythermograph Traces, M.S. Thesis, Naval Postgraduate School, Monterey, California.

Haurwitz, B., Stommel, H., and Munk, W. H., 1959. "On the Thermal Unrest in the Ocean," in The Atmosphere and the Sea in Motion, ed. by B. Boiln, Rockefeller Institute Press, N. Y., p. 74-94.

Hazelworth, J. B., 1966. Quantitative Analysis of Some Bathythermograph Errors, U. S. Naval Oceanographic Office TR-180, ASWEPS Report 111.

Hecht, A., and White, R. A., 1968. "Temperature Fluctuations in the Upper Layer of the Ocean," Deep-Sea Research, v. 15, p. 339-353.

Hubert, W. E., and T. Laevastu., 1966. Short-Period Changes and Anomalies of Temperature in the Oceans and Their Effects on Sound Propagation, Fleet Numerical Weather Facility Technical Note 10.

Ingham, M. C., 1968. "The 'Mixed Layer' in the Western Tropical Atlantic Ocean," Bulletin of Marine Science, v. 18, p. 561-571.

James, R. W., 1966. Ocean Thermal Structure Forecasting, NavOceanO, SP-105, ASWEPS Manual v. 5.

James, R. W., 1967. Data Requirements for Synoptic Sea Surface Temperature Analyses, NavOceanO, SP-111.

Knollman, G. C., 1964. "Wave Propagation in a Medium with Random, Spheroidal Inhomogeneities," Journal of the Acoustical Society of America, v. 36, p. 681-688.

Krauss, W., 1966. Internal Tides off Southern California, U. S. Naval Electronics Laboratory Report 1389.

LaFond, E. C., 1959. Slicks and Temperature Structure in the Sea, NEL Report 937.

LaFond, E. C., and Cox, S. S., 1962. "Internal Waves," in The Sea, v. 1, ed. by W. M. Hill, Interscience Publishers, p. 731-763.

LaFond, E. C., and LaFond, K. G., 1966. Vertical and Horizontal Structures in the Sea, NEL Report 1395.

Laevastu, T., 1960. "Factors Affecting the Temperature of the Surface Layer of the Sea," Soc. Scient. Fennica. Comm. Phys-Mathem, v. 25, p. 1-136.

Lee, O. S., 1961. "Effect of an Internal Wave on Sound in the Ocean," Journal of the Acoustical Society of America, v. 33, p. 677-681.

Lee, O. S., 1961a. "Observations on Internal Waves in Shallow Water," Limnology and Oceanography, v. 6, p. 312-321.

Liebermann, L. N., 1951. "The Effect of Temperature Inhomogeneities in the Ocean on the Propagation of Sound," Journal of the Acoustical Society of America, v. 23, p. 563-57-.

Lovett, J. R., 1968. "Vertical Temperature Gradient Variations Related to Current Shear and Turbulence," Limnology and Oceanography, v. 13, p. 127-142.

Meyer, R. F., and Romberg, B. W., 1963. Acoustic Scattering in the Ocean, Arthur D. Little Report 1360863.

Miles, J. W., 1961. "On the Stability of Heterogeneous Shear Flows," Journal of Fluid Mechanics, v. 10, p. 496-501.

Miles, J. W., 1963. "On the Stability of Heterogeneous Shear Flows, Part 2," Journal of Fluid Mechanics, v. 16, p. 209.

Mintzer, D., 1953. "Wave Propagation in a Randomly Inhomogeneous Medium, I," Journal of the Acoustical Society of America, v. 25, p. 922-927.

Mintzer, D., 1953a. "Wave Propagation in a Randomly Inhomogeneous Medium, II," Journal of the Acoustical Society of America, v. 25, p. 1007-1111.

Mintzer, D., 1954. "Wave Propagation in a Randomly Inhomogeneous Medium, III," Journal of the Acoustical Society of America, v. 26, p. 186-190.

Mooers, C. N. K., 1966. A Study of Ocean Variability at a Depth of One Mile, USL Report 693.

National Oceanographic Data Center, 1968. Unclassified letter to all Sippican XBT Users, Subject: Procedures for Disposition of XBT Traces, 21 February 1968.

National Oceanographic Data Center, 1968a. Instructions for Preparing the Bathythermograph Log Sheet, NODC EXP-3167/10-A (Rev. 1-68).

National Defense Research Committee, 1946. The Application of Oceanography to Subsurface Warfare, Summary Technical Report of Division 6, v. 6A.

Naval Weather Service, 1967. U. S. Naval Weather Service Computer Products Manual, Naval Air Systems Command Report NAVAIR 50-1G-522.

Neshyba, S., Neal, V. T., and Denner, W. W., 1969. "The Significance of Temperature Stratification in the Arctic," paper presented at Symposium on Military Oceanography, 6th, Seattle, Washington.

Officer, C. B., 1958. Introduction to the Theory of Sound Transmission with Application to the Ocean, McGraw-Hill.

Osborn, T. R., 1969. Oceanic Fine Structure, Ph.D. Dissertation, University of California at San Diego.

Pao, Y-H., 1969. "Origin and Structure of Turbulence in Stably Stratified Media," Clear Air Turbulence and Its Detection, Plenum Press, p. 73-99.

Pederson, M. A., 1961. "Acoustic Intensity Anomalies Introduced by Constant Velocity Gradients, Journal of the Acoustical Society of America, v. 33, p. 465-474.

Pedersen, J. A., and Gordon, D. F., 1965. "Normal-Mode Theory Applied to Short-Range Propagation in an Underwater Acoustic Surface Duct," Journal of the Acoustical Society of America, v. 37, p. 105-110.

Pipp, A. T., 1964. "Fine Structure and Stability of the Sound Channel in the Ocean," Journal of the Acoustical Society of America, v. 36, p. 1948-1953.

Pingree, R. D., 1969. "Small-Scale Structure of Temperature and Salinity Near Station Cavall," Deep-Sea Research, v. 16, p. 275-295.

Pond, S., 1968. "Microscale Phenomena in the Ocean and the Atmospheric Boundary Layer," Proceedings of Region Six IEEE Conference 1-C-4, p. 1-10.

Potter, D. S., and Murphy, S. R., 1957. "On Wave Propagation in a Random Inhomogeneous Medium," Journal of the Acoustical Society of America, v. 29, p. 197-198.

Rasmussen, R. A., 1962. "Application of Thermistors to Measurements in Moving Fluids," Review of Scientific Instruments, v. 33, p. 38-42.

Rattray, M., 1962. "Interpolation Errors and Oceanographic Sampling," Deep-Sea Research, v. 9, p. 25-37.

Reid, W. L., 1964. Bathythermograph Evaluation, (Unpublished manuscript).

Richardson, W. M., 1958. Measurement of Thermal Microstructure, Woods Hole Ref 58-11 (Unpublished manuscript).

Roden, G. I., 1963. "On Sea Level, Temperature, and Salinity Variations in the Central Tropical Pacific and on Pacific Ocean Islands," Journal of Geophysical Research, v. 68, p. 455-472.

Rossby, C. G., and Montgomery, R. B., 1934. "The Layer of Frictional Influence on Wind and Ocean Currents," Papers in Physical Oceanography and Meteorology, v. 3.

Sagar, F. H., 1960. "Acoustic Intensity Fluctuations and Temperature Microstructure in the Sea," Journal of the Accoustical Society of America, v. 32, p. 112-121.

Schulkin, M., 1969. The Propagation of Sound in Imperfect Ocean Surface Ducts, USL Report 1013.

Sederowitz, W. J., and Favret, A. G., 1969. "Covariance Between Acoustic Signals Traveling Diverging Paths in a Random Medium," Journal of the Acoustical Society of America, v. 45, p. 386-391.

Sheehy, M. J., 1950. "Transmission of 24-Kc Underwater Sound from a Deep Source," Journal of the Acoustical Society of America, v. 22, p. 24-28.

Shonting, D. H., and Kadis, A. L., 1968. The Thermiprobe: A System for Measuring Thermal Microstructure in the Sea, paper presented at National ISA, Marine Sciences Instrumentation Symposium, 4th, Pittsburg, Pennsylvania on 22 January 1968.

Siedler, G., 1969. "On the Fine Structure of Density and Current Distribution and its Short-Time Variations if Different Areas," in Progress in Oceanography, v. 5, ed. by M. Sears, Pergmanon Press, p. 81-94.

Sippican Corporation, 1968. Instructions for Installation, Operation and Maintenance of Sippican Expendable Bathythermograph System, Sippican Report R-467B.

Skudrzyk, E., 1957. "Scattering in an Inhomogeneous Medium," Journal of the Acoustical Society of America, v. 29, p. 50-60.

Smith, E. L., 1967. A Predictive Horizontal-Temperature Gradient Model of the Upper 750 Feet of the Ocean, NEL Report 1445.

Spilhaus, A. F., 1938. "A Bathythermograph," Journal of Geophysical Research, v. 1, p. 95-100.

Stern, M. E., 1968. "T-S Gradiants on the Micro-Scale," Deep-Sea Research, v. 15, p. 245-250.

Stern, M. E., and Turner, J. S., 1969. "Salt Fingers and Convecting Layers," Deep-Sea Research, v. 16, p. 495-511.

Stommel, H., 1966. The Gulf Stream, University of California Press.

Stommel, H., and Federov, K. N., 1967. "Small Scale Structure in Temperature and Salinity Near Timor and Mindanao," Tellus, v. 19, p. 306-325.

Stone, R. G., and Mintzer, D., 1962. "Range Dependence of Acoustic Fluctuations in a Randomly Inhomogeneous Medium," Journal of the Acoustical Society of America, v. 34, p. 647-653.

Sverdrup, H. U., Johnson, M. W., and Fleming, R. H., 1942. The Oceans, Prentice-Hall.

Tait, R. I., and Howe, M. R., 1968. "Some Observations on Thermo-Haline Stratification in the Deep Ocean," Deep-Sea Research, v. 15, p. 275-280.

Tolstoy, I., and Clay, C. S., 1966. Ocean Acoustics, McGraw-Hill.

Tully, J. P., 1964. "Oceanographic Regions and Assessment of Temperature Structure in the Seasonal Zone of the Pacific Ocean," J. Fish. Res. Bd. Canada, v. 21, p. 941-970.

Tully, J. P., 1964a. "Oceanographic Regions and Processes in the North Pacific Ocean," in Progress in Oceanography, v. 2, ed. by M. Sears, Pergmanon Press, p. 68-84.

Turner, J. S., 1967. "Salt Fingers Across a Density Interface," Deep-Sea Research, v. 14, p. 599-611.

Turner, J. S., and Stommel, H., 1964. "A New Case of Convection in the Presence of Combined Vertical Salinity and Temperature Gradients," Proc. Nat. Academy of Science, v. 52, p. 49-53.

Urick, R. J., 1967. Principles of Underwater Sound for Engineers, McGraw-Hill, p. 122-160.

Urick, R. J., 1967a. Observations of the Sound Field in the Deep Sea, Naval Ordnance Laboratory Technical Report 67-103.

Urick, R. J., and Searfoss, C. W., 1948. The Microthermal Structure of the Ocean Near Key West, Florida, Part I, Discussion, Naval Research Laboratory Report S-3392.

Urick, R. J., and Searfoss, C. W., 1949. The Microthermal Structure of the Ocean Near Key West, Florida, Part II, Analysis, Naval Research Laboratory Report S-3444.

Van Vliet, C. J., 1969. An Algorithm for Estimating the Isothermal Layer Depth of a Digitized Bathythermograph, NUC TN 269.

Weinberg, H., 1967. A Curve Fitting Technique for Acoustic Ray Analysis, USL Report 805.

White, R. A., 1967. "The Vertical Structure of Temperature Fluctuations within an Oceanic Thermocline," Deep-Sea Research, v. 14, p. 613-623.

Whitemarsh, D. C., Skrudzyk, D., and Urick, R. J., 1957. "Forward Scattering of Sound in the Sea and Its Correlation with the Temperature Microstructure," Journal of the Acoustical Society of America, v. 29, p. 1124-1143.

Wilson, D. F., Ricalzone, L. C., and Beckett, R. C., 1968. Some Investigations of Sound-Scattering Layers Near Key West, Florida, Naval Research Laboratory Report 6682.

Wolff, P. M., Tatro, P. R., and Megehee, L. D., 1967(?). The FNWF Sound Map Program (Unpublished manuscript).

Woods, J. D., 1968. "Wave-Induced Shear Instability in the Summer Thermocline," Journal of Fluid Mechanics, v. 32, p. 791-800.

Woods, J. D., 1968a. "An Investigation of Some Physical Processes Associated with the Vertical Flow of Heat Through the Upper Ocean," Meteorological Magazine, v. 98, p. 65-73.

Security Classification

DOCUMENT CONTROL DATA - R & D

(Security classification of title, body of abstract and indexing annotation must be entered when the overall report is classified)

1 ORIGINATING ACTIVITY (Corporate author)	2a. REPORT SECURITY CLASSIFICATION
Naval Postgraduate School Monterey, California 93940	Unclassified
	2b. GROUP

3 REPORT TITLE

Some Characteristics of Temperature Microstructure in the Ocean

4 DESCRIPTIVE NOTES (Type of report and, inclusive dates)

Master's Thesis; April 1970

5. AUTHOR(S) (First name, middle initial, last name)

Petyon Marshall Magruder, Jr.

6 REPORT DATE	7a. TOTAL NO. OF PAGES	7b. NO. OF REFS
April 1970	155	109

8a. CONTRACT OR GRANT NO	9a. ORIGINATOR'S REPORT NUMBER(S)
b. PROJECT NO	
c.	9b. OTHER REPORT NO(S) (Any other numbers that may be assigned this report)
d.	

10 DISTRIBUTION STATEMENT

This document has been approved for public release and sale; its distribution is unlimited.

11. SUPPLEMENTARY NOTES	12. SPONSORING MILITARY ACTIVITY
	Naval Postgraduate School Monterey, California 93940

13. ABSTRACT

The background of microstructure and its effects on sound propagation is reviewed. The expendable bathythermograph (XBT) system and current digitizing procedures are evaluated to determine their adequacy in investigating vertical thermal microstructure. Several methods of microthermal analysis are proposed. Temperature gradient versus depth plots are used to analyze data from several ocean regions - Atlantic Coastal, Andaman Sea, Eastern North Pacific, and the northern boundary of the Gulf Stream. Analysis of these data suggest a water mass dependence of the thermal microstructure. The significance of the small-scale structure to Naval operations is discussed.

DD FORM 1 NOV 68 1473 (PAGE 1)

S/N 0101-807-6811

Security Classification

A-31408

14. KEY WORDS	LINK A		LINK B		LINK C	
	ROLE	WT	ROLE	WT	ROLE	WT
Microstructure						
Microthermal structure						
Expendable bathythermograph						
XBT						
Digitizing						
Temperature						
Temperature gradient						
Water mass						
Underwater sound						

DD FORM 1 NOV 68 1473 (BACK)

S/N 0101-807-6821

A-31409

DISCLAIMER NOTICE

THIS DOCUMENT IS BEST QUALITY PRACTICABLE. THE COPY FURNISHED TO DTIC CONTAINED A SIGNIFICANT NUMBER OF PAGES WHICH DO NOT REPRODUCE LEGIBLY.